Spatially inhomogeneous crystal and magnetic states in strongly correlated manganese (CMR-) and copper (HTSC-) oxides.

Spatially inhomogeneous crystal and magnetic states in strongly correlated manganese (CMR[1]-) and copper (HTSC[2]-) oxides.

V.Pomjakushin

Laboratory for Neutron Scattering, ETHZ & PSI, Villigen;

I.M.Frank Laboratory of Neutron Physics, JINR, Dubna

---

[1] CMR= Colossal negative MagnetoResistance [R(H)-R(0)]/R(0)

[1] HTSC= High Temperature SuperConductivity

Most cited (>20hits) Balagurov' papers 1996-

- Aksenov, VL; **Balagurov, AM**; Sikolenko, VV; Simkin, VG; Alyoshin, VA; Antipov, EV; Gippius, AA; Mikhailova, DA; Putilin, SN; Bouree, F. 1997. Precision neutron-diffraction study of the high-T-c superconductor HgBa2CuO4+delta. *PHYSICAL REVIEW B* 55 (6): 3966-3973.*(Cited: 43)*
- **Balagurov, AM**; Pomjakushin, VY; Sheptyakov, DV; Aksenov, VL; Babushkina, NA; Belova, LM; Taldenkov, AN; Inyushkin, AV; Fischer, P; Gutmann, M; Keller, L; Gorbenko, OY; Kaul, AR. 1999. Effect of oxygen isotope substitution on tbe magnetic structure of (La0.25Pr0.75)(0.7)Ca0.3MnO3. *PHYSICAL REVIEW B* 60 (1): 383-387. *(39)*
- Lobanov, MV; **Balagurov, AM**; Pomjakushin, VJ; Fischer, P; Gutmann, M; Abakumov, AM; D'yachenko, OG; Antipov, EV; Lebedev, OI; Van Tendeloo, G. 2000. Structural and magnetic properties of the colossal magnetoresistance perovskite La0.85Ca0.15MnO3. *PHYSICAL REVIEW B* 61 (13): 8941-8949. *(27)*
- Aksenov, VL; **Balagurov, AM**; Glazkov, VP; Kozlenko, DP; Naumov, IV; Savenko, BN; Sheptyakov, DV; Somenkov, VA; Bulkin, AP; Kudryashev, VA; Trounov, VA. 1999. DN-12 time-of-flight high-pressure neutron spectrometer for investigation of microsamples. *PHYSICA B* 265 (1-4): 258-262. *(25)*
- Aksenov, VL; **Balagurov, AM**; Savenko, BN; Sheptyakov, DV; Glazkov, VP; Somenkov, VA; Shilshtein, SS; Antipov, EV; Putilin, SN. 1997. Investigation of the HgBa2CuO4+delta structure under external pressures up to 5 GPa by neutron powder diffraction. *PHYSICA C* 275 (1-2): 87-92. *(25)*
- Abakumov, AM; Aksenov, VL; Alyoshin, VA; Antipov, EV; **Balagurov, AM**; Mikhailova, DA; Putilin, SN; Rozova, MG. 1998. Effect of fluorination on the structure and superconducting properties of the Hg-1201 phase. *PHYSICAL REVIEW LETTERS* 80 (2): 385-388. *(23)*

Phase separation in high-T_c's and colossal magnetoresistance manganites

- La_2CuO_4 story: macro- and micro-phase separation, twinning, concomitance of SC & AFM.

- CMR manganites: phase separation, ordering effects, electron-phonon interactions and large (and giant) isotope effect

Phase separation scales

- Micro- or "electronic" ~10^1Å
  - HTSC[1]: striped Hubbard, t-J, SO(5), "striped" BCS…
  - CMR: FM Kondo, 1-,2-orbital DE
- Meso- or (nano-, macro) >= 10^3Å
  - "Chemical" (structural) separation: miscibility gap.
  - Intrinsic quenched (correlated) disorder + Ising, or 1-,2-orbital DE, etc[2]

e.g. [1] Arrigoni, et al PRB 2004; H-D.Chen, et al 2004; Bianconi, et al PRL 1996.

[2] Burgy, Moreo, Dagotto et al PRL,PRB 2000-2004.

Intrinsic inhomogeneities in “HTSC” and “CMR”

Competition between insulating and metallic states

$La_{2-x}Sr_xCuO_{4+y}$

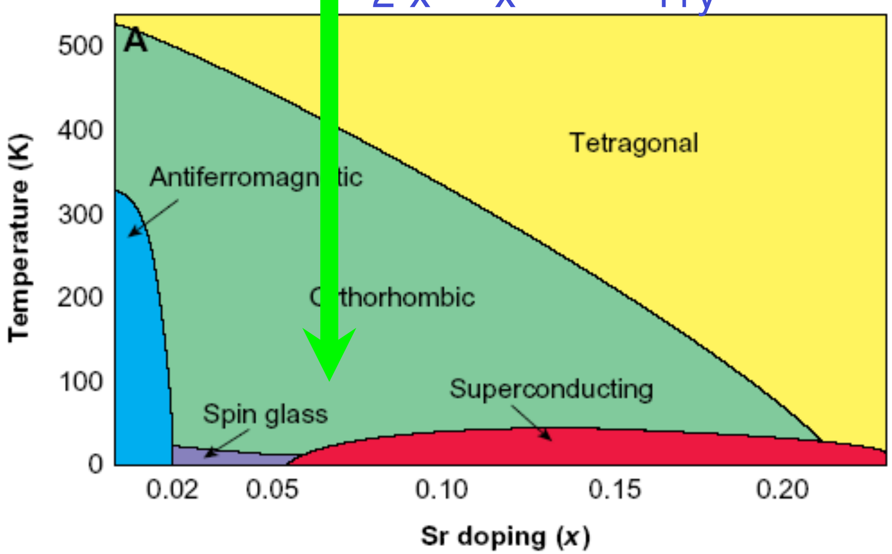

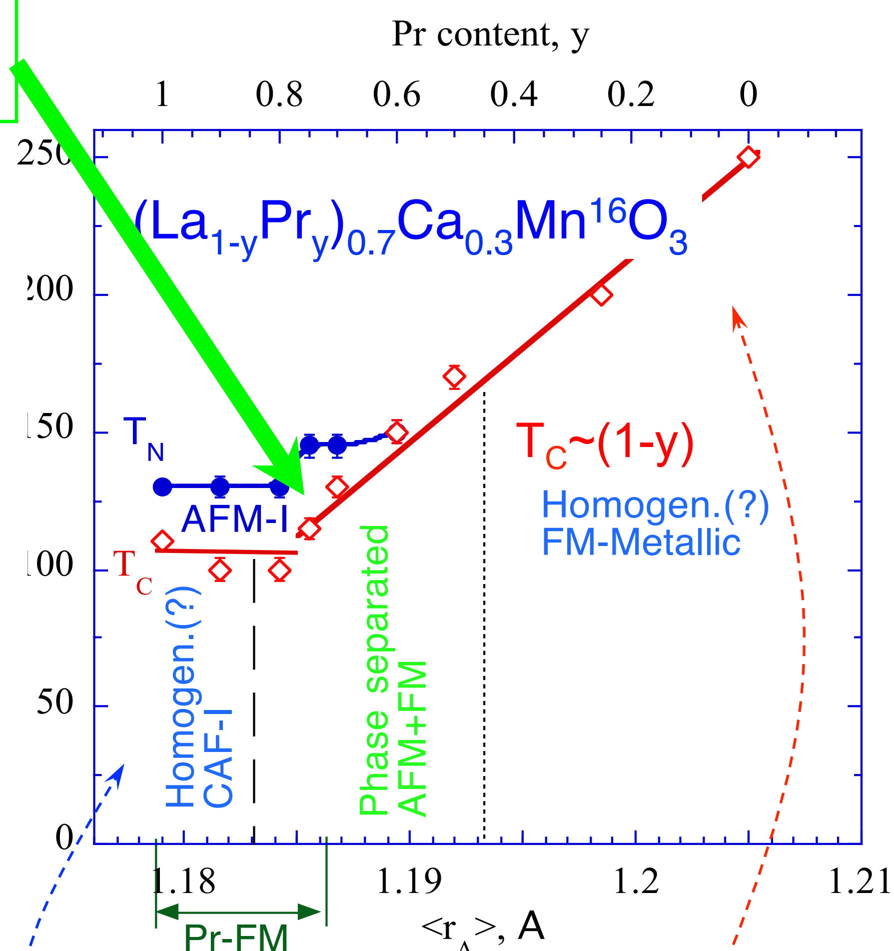

CAFM CO Mott insulattor → FM double exchange metal

Y.Imry, S.Ma (PRL 1975): random field instability

Influence of quenched disorder on the competition between ordered states separated by a first-order transition

J.Burgy, A.Moreo, M. Mayr, E.Dagotto, et al, PRL, PRB 2000-2004

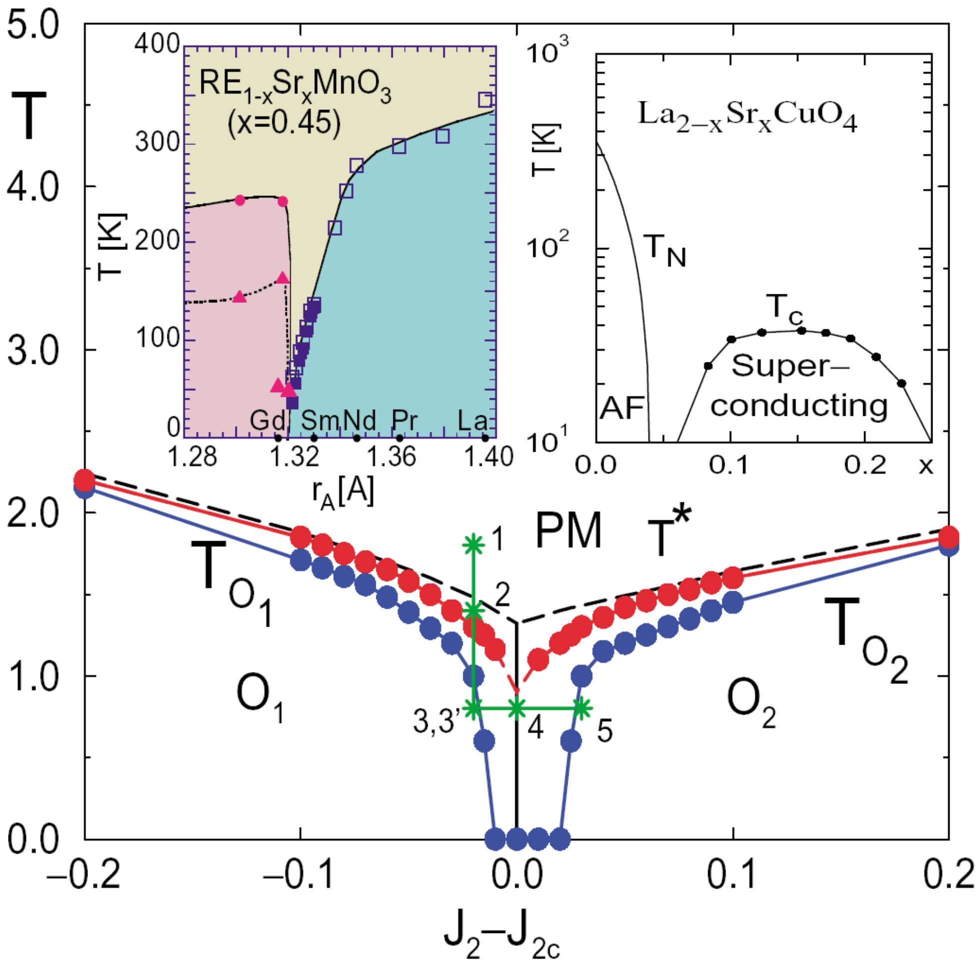

3D RFIM +correlated disorder

$$H = -J\sum_{\langle ij\rangle} s_i s_j + J'\sum_{[ik]} s_i s_k$$

$$+ \Delta \sum_{i,j} h_i s_j / d_{ij}^{\alpha},$$

α~3 elasticity mechanism of the distortion propagation (Khomskii, Kugel, 2001)

Ising spin configuration

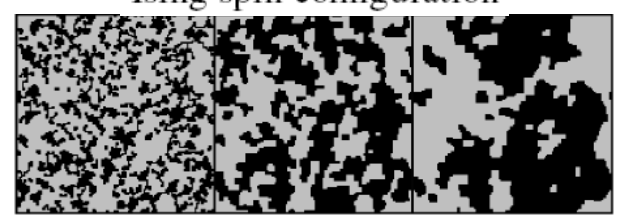

2D FM

$\alpha=\infty$ $\alpha=3$ $\alpha=1$

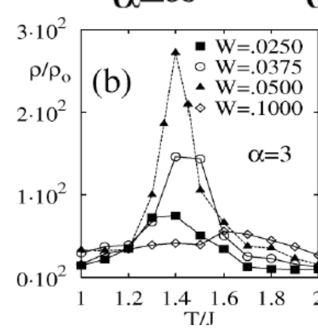

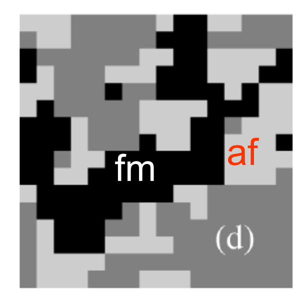

3D

Phase diagram of La_2CuO_{4+y}

Macroscopically (>10^3Å!) separated

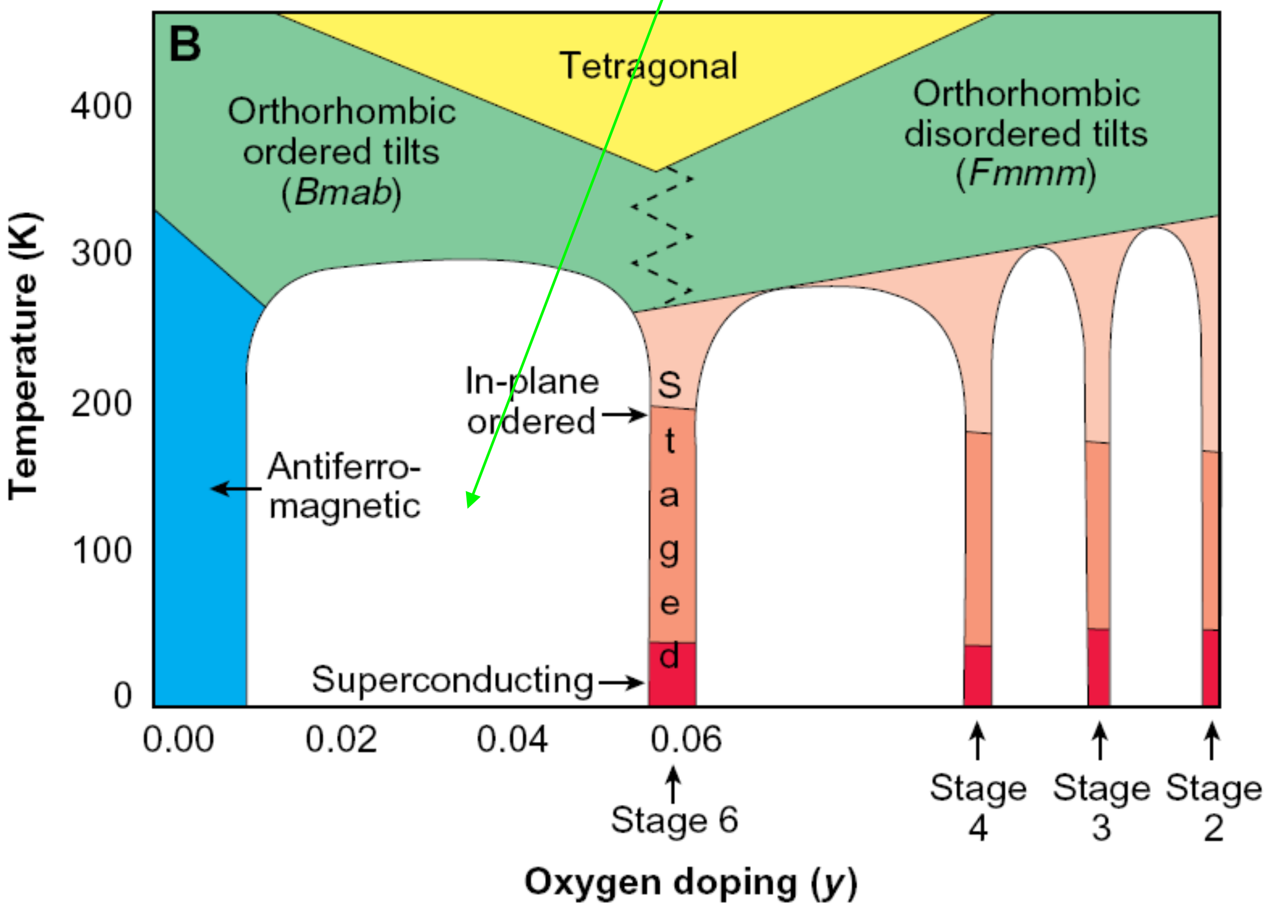

Wells et al, Science 1997

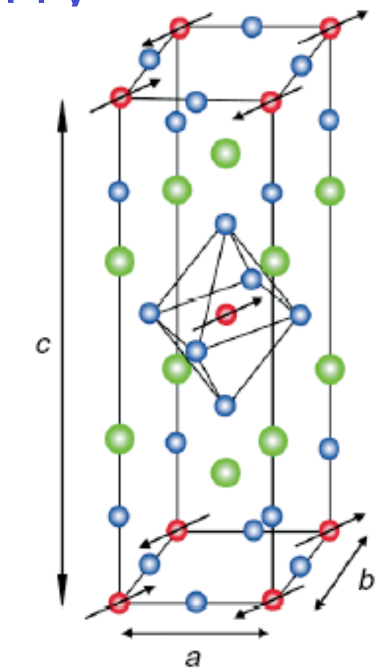

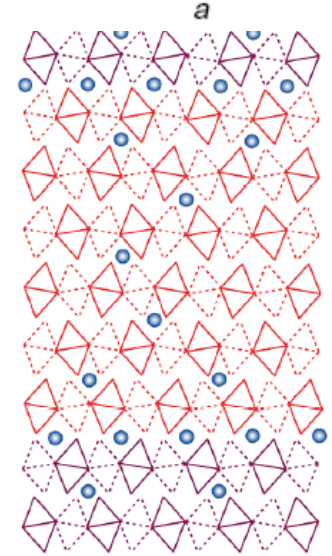

Stage 6 structure

High res ND evidence of macroscopic PS

Single crystal experiment on powder diffractometer **ФДВР**

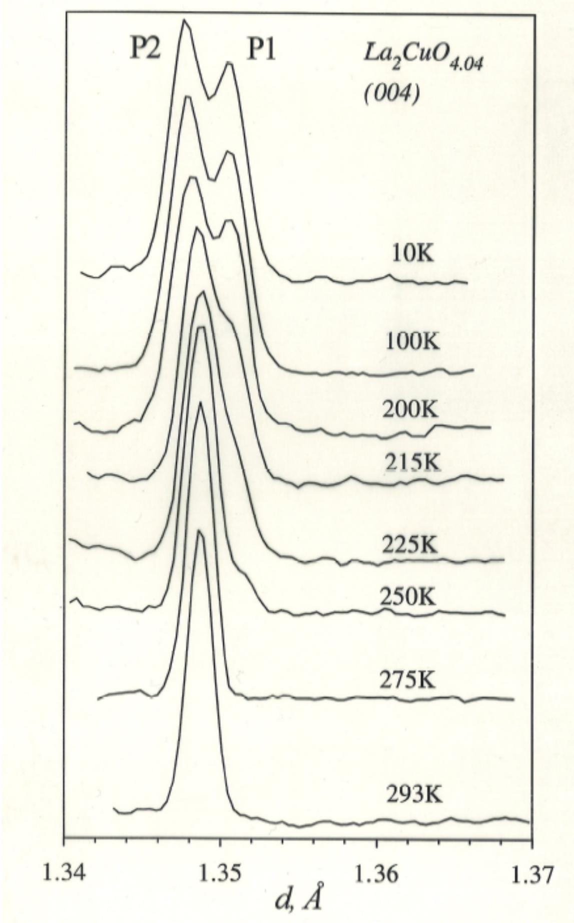

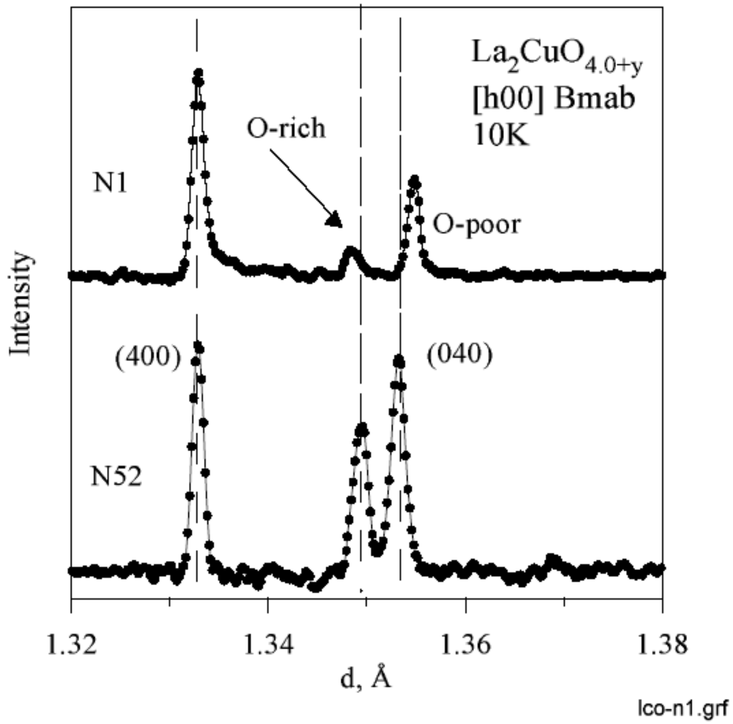

Balagurov et al, Physica C, 1997

Domain sizes from high-res neutron diffraction in La_2CuO_{4+y}

Balagurov et al, Physica C, 1997

ФДВР

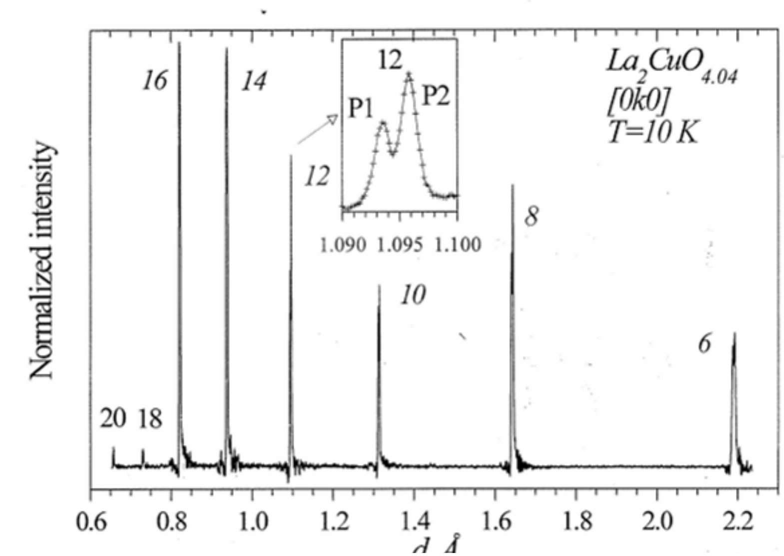

Broadening of the diffraction peaks

1. Size effect: $\Delta d^* = 1/L = const \Rightarrow \quad (\Delta d/d)^2 = (d/L)^2$
2. Strain effect: $\Delta a/a = \varepsilon = const \Rightarrow \quad (\Delta d/d)^2 = \varepsilon^2$

$$(\Delta d/d)^2_{exp} = (d/L)^2 + \varepsilon^2$$

where:

$d^* = 1/d$

$2\, d \sin\Theta = \lambda$,

L - size of coherently scattered region

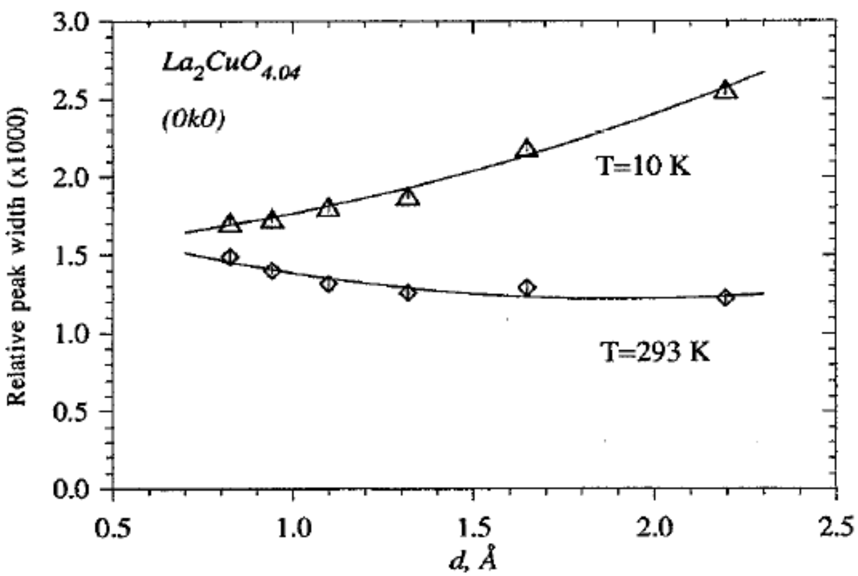

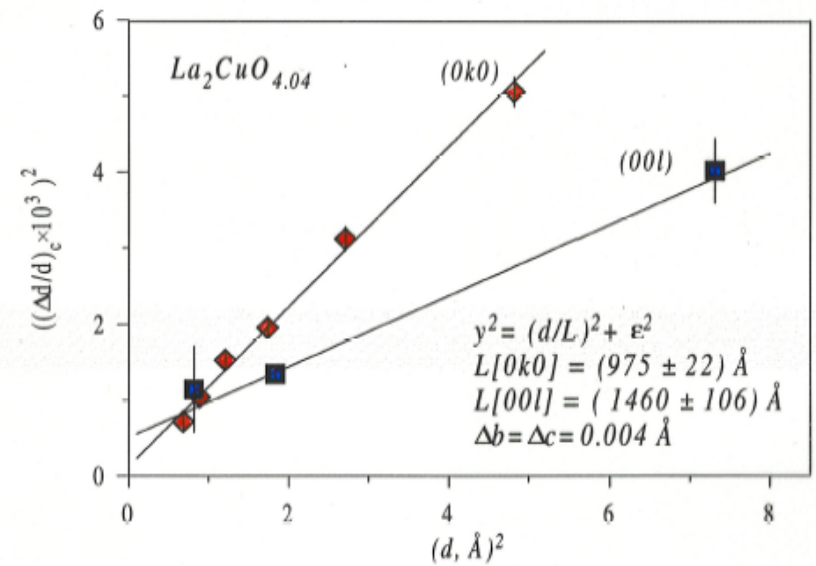

Low & high oxygen mobility in La_2CuO_{4+y}

High oxygen mobility crystals

Orthorhombic strain as a function of oxygen content

Low oxygen mobility crystals

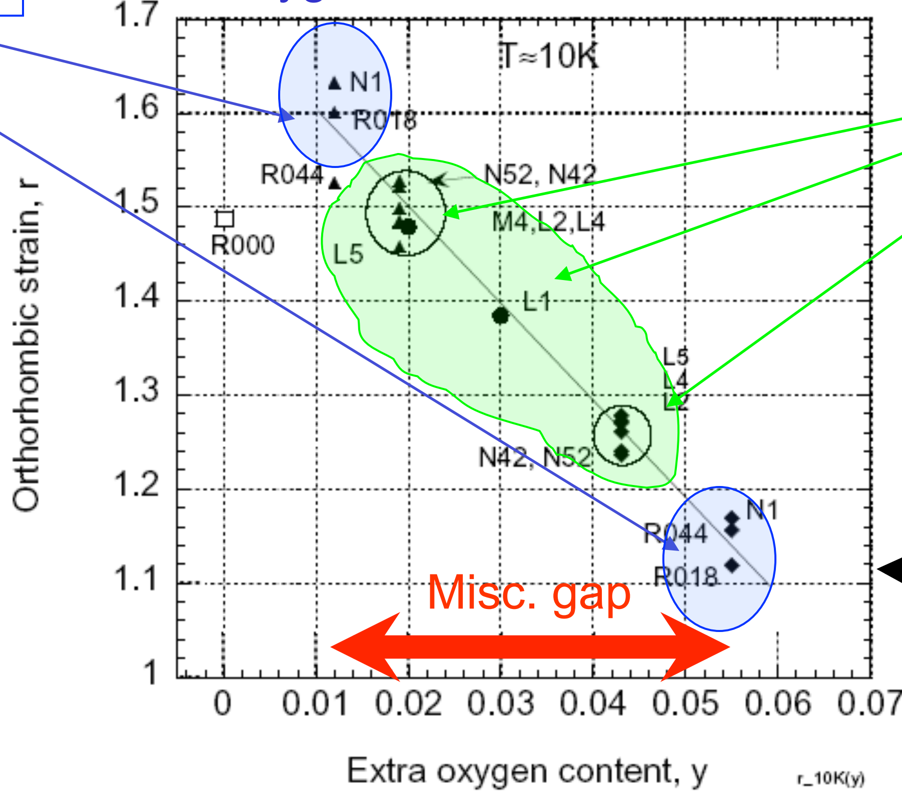

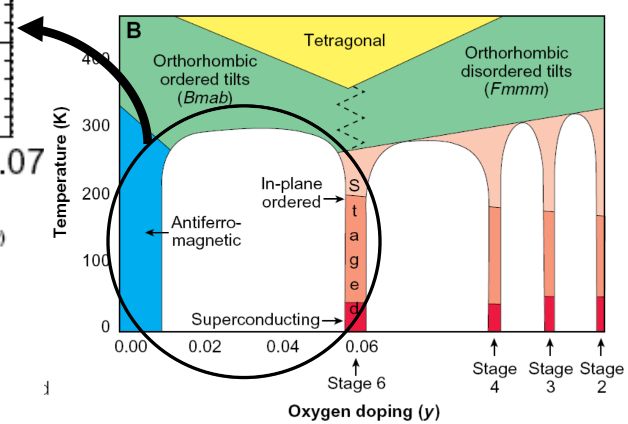

Balagurov et al, Physica C, 1997, Phys Rev **B** 1999
Pomjakushin et al, Physica C, 2000;
Sheptyakov, et al. PHYSICA C 1999

Can real crystal structure effect on oxygen mobility?

1. Single crystal structure analysis (D9) : no principal difference between PS and non-PS crystals (Sheptyakov, Pomjakushin, Balagurov, et al. PHYSICA C 1999)
2. Real crystal structure (HRFD, DN2, high-res Xray)

P4/mmm → Bmab

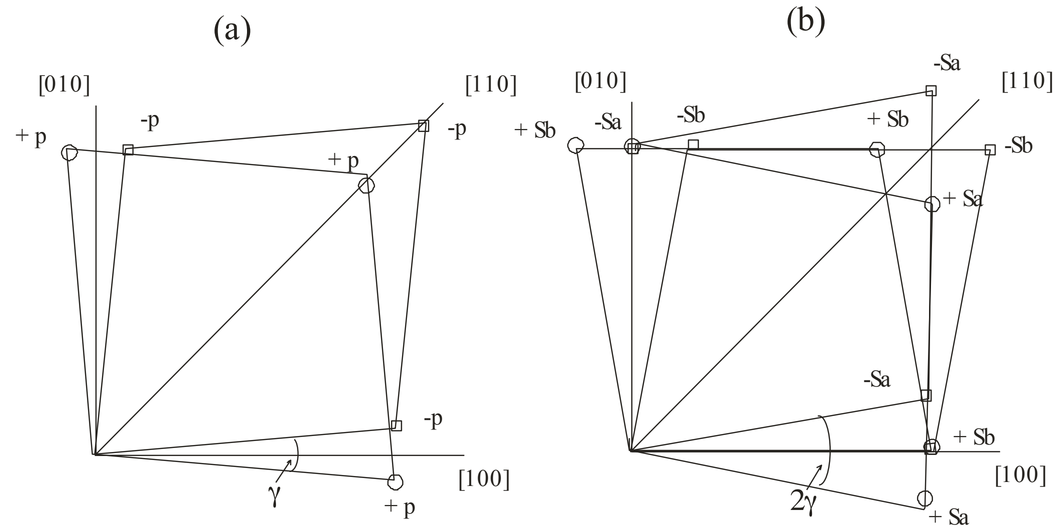

Pure shear Simple shear

Balagurov AM, et al. Twinned La2CuO4 structure
CRYSTALLOGRAPHY REPORTS 44 1999

High res. X-ray and neutron diffraction

Balagurov AM. et al. CRYSTALLOGRAPHY REPORTS (Кристаллография) 1999

DN-2

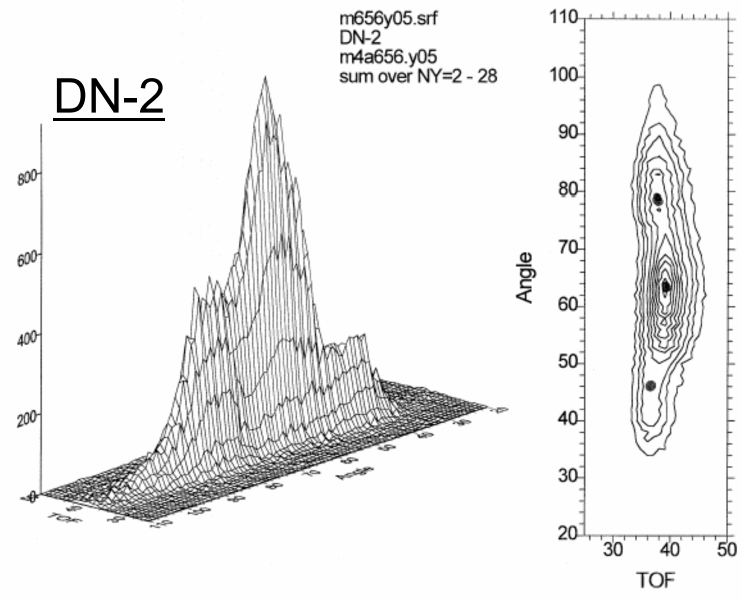

3 transformational twins:

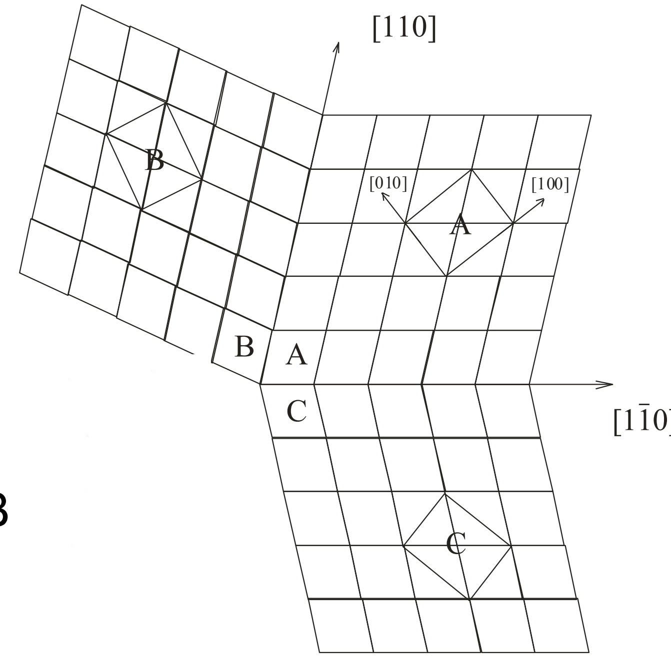

X-ray, Chernogolovka

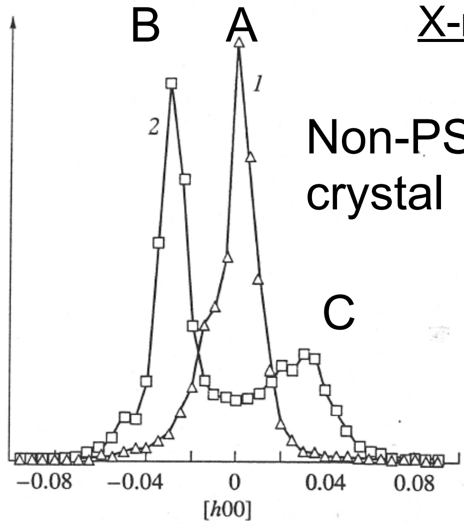

PS crystal

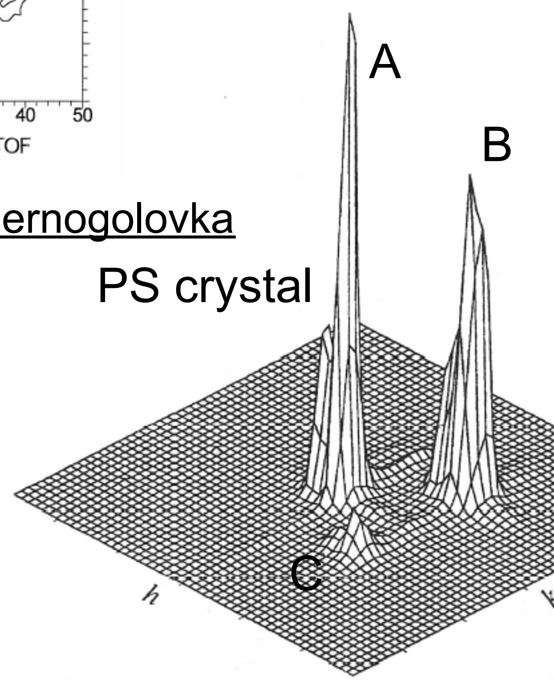

1. No incoherent boundaries in PS crystals.
2. There are extended incoherent regions in non-PS crystals

Fig. 7. Sections of two-dimensional intensity distribution

Fig. 8. Two-dimensional intensity distribution in the vicinity of the node (060) in an N1 crystal. ...

$T_{AFM}=T_c$ in low oxygen mobility La_2CuO_{4+y}

μSR zero field

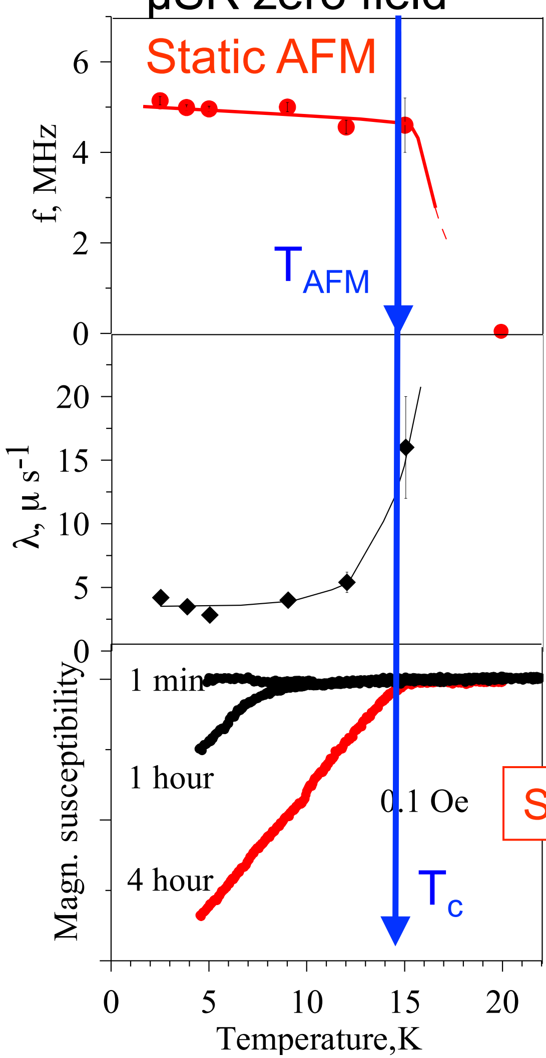

Superconductivity

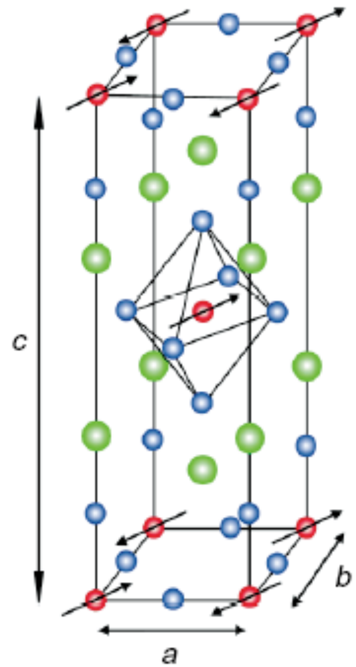

Neutron diffraction :

No long range AFM below T_c

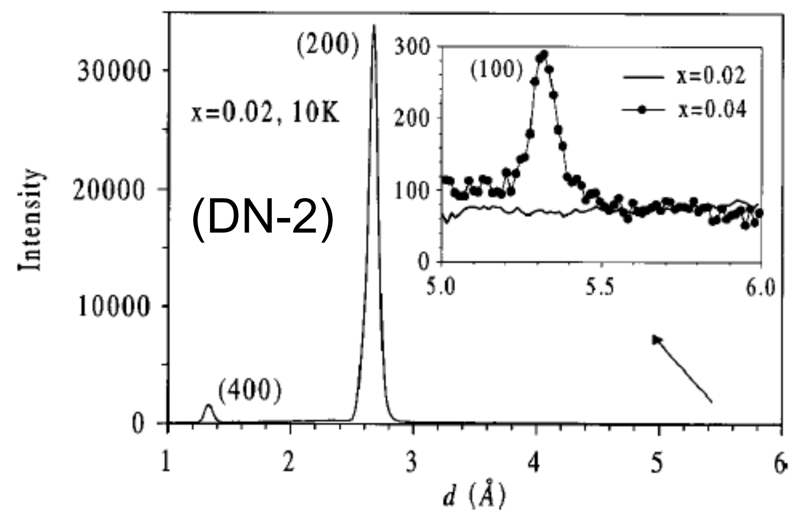

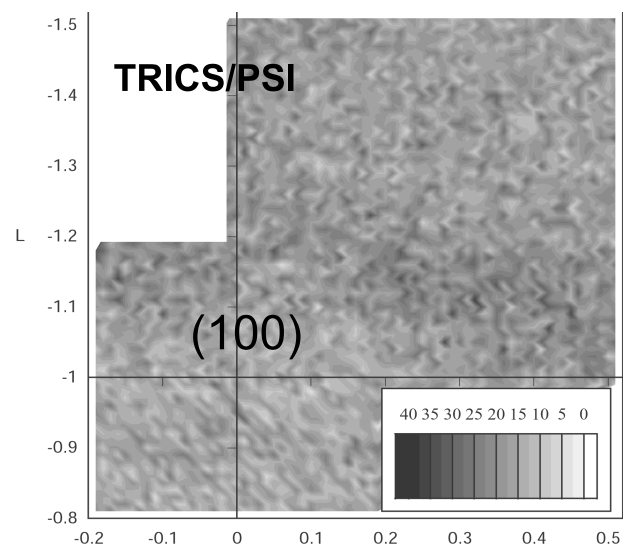

Pomjakushin et al, Phys Rev **B**, 1998;

Summary of $T_c=T_{AFM}$ in La_2CuO_{4+y}

Crystal	x	T_c	T_N	T_{LTMS}
m4[3]	0.02	15	-	15 AFM
L1 [5,6]	0.03	10	-	8 spin glass
L2 [3,5]	0.04	25	250	25 AFM
N52	0.033	25	100	$\leq$ 25 AFM
L5	$\sim$ 0.04	25	140	20 AFM
high oxygen mobility "canonical" crystal				
N1	0.02	30	250	no

5 LOM crystals with different *y* and T_c=8-25K: **All have T_c=T_{AFM}!,** No long range AFM by ND

AFM ordered fraction

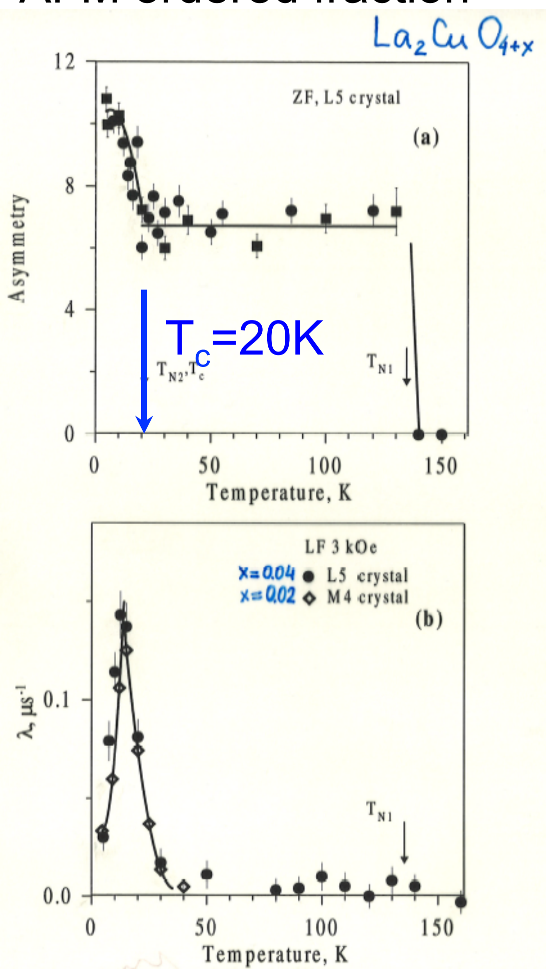

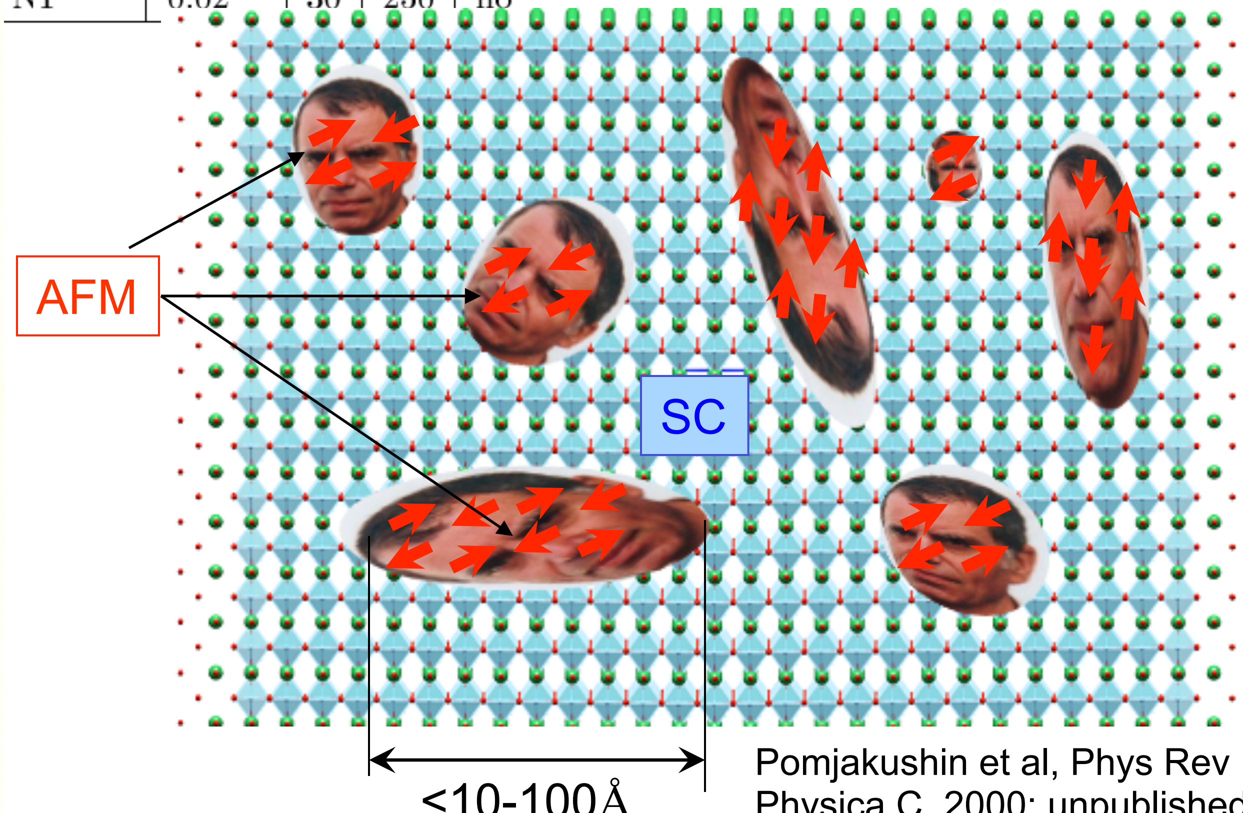

Pomjakushin et al, Phys Rev B1998; Physica C, 2000; unpublished 2002.

Later studies of PS La_2CuO_{4+y}

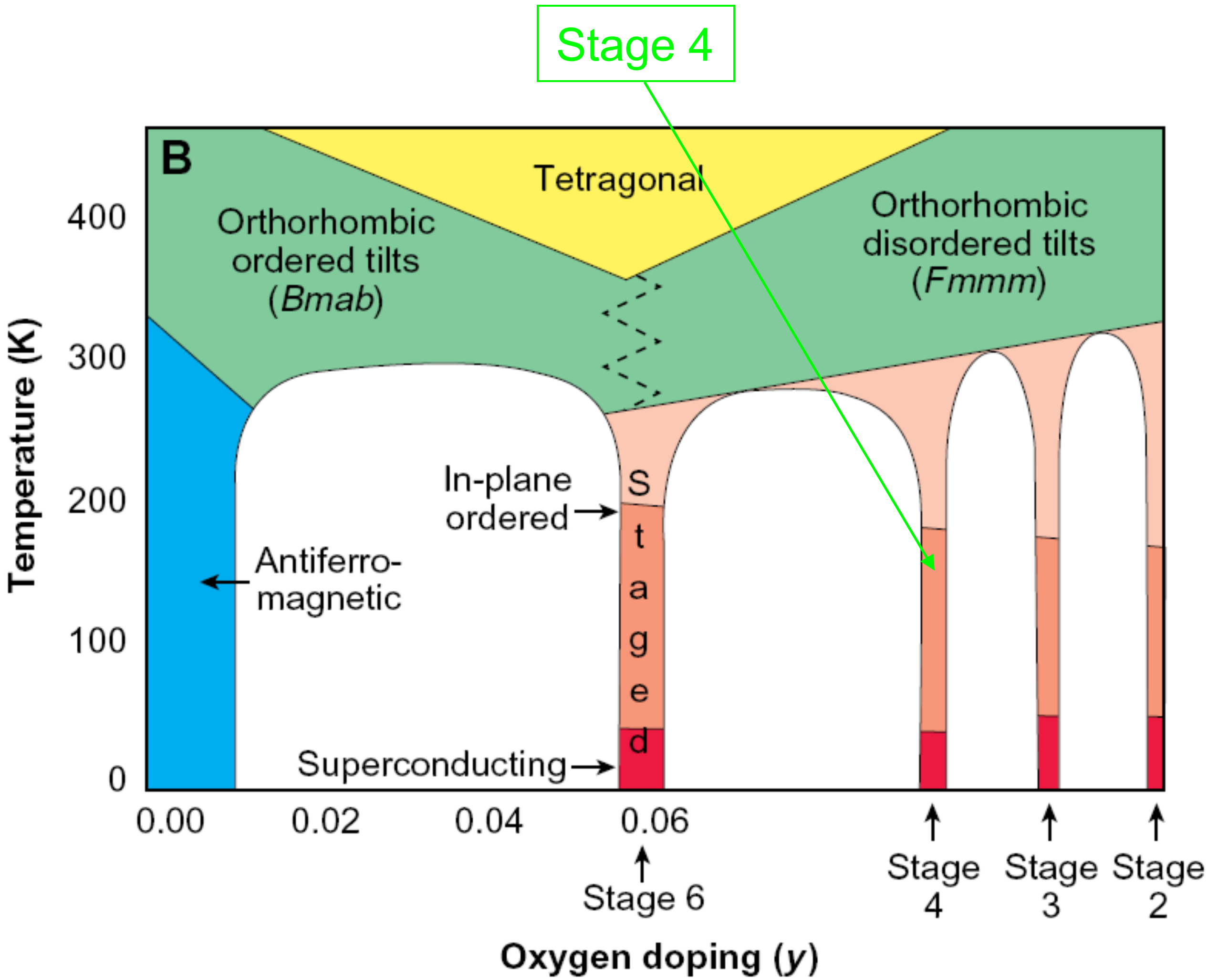

Wells et al, Science 1997

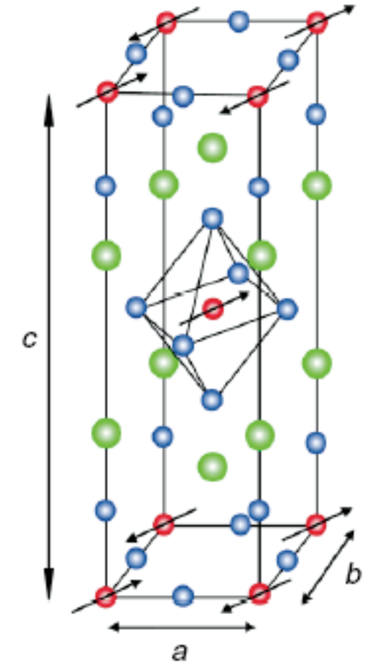

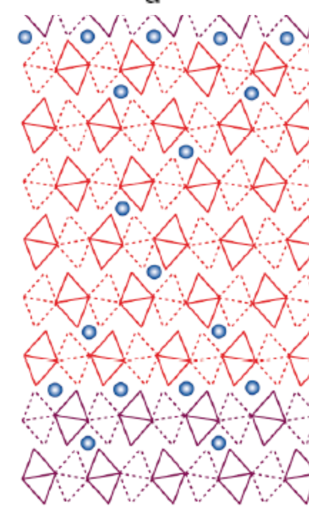

Stage 6 structure

Microscopic phase separation in stage-4 La_2CuO_{4+y}

PHYSICAL REVIEW B **66**, 014524 (2002)

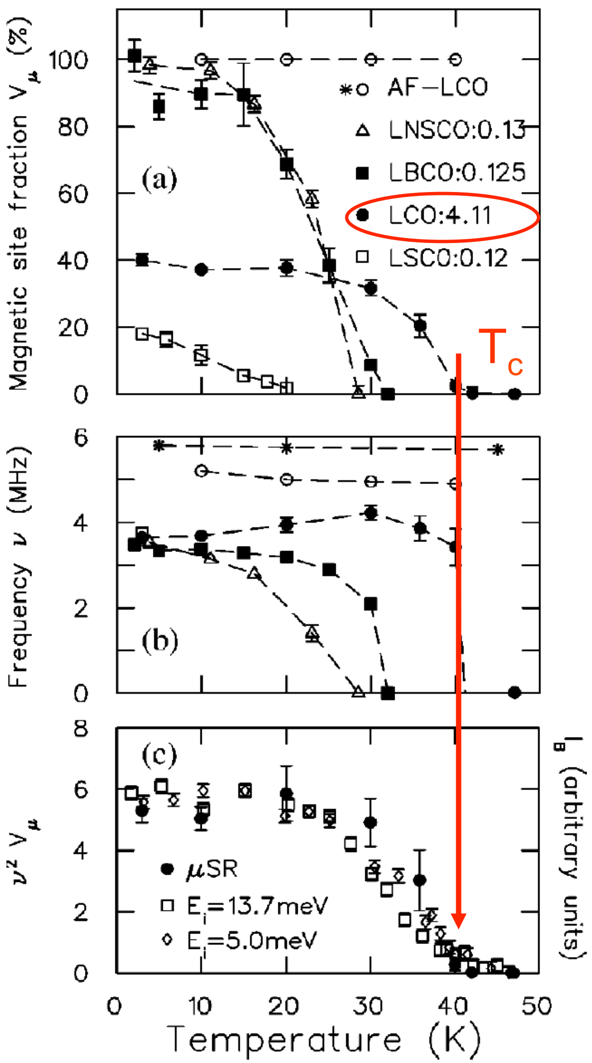

A. T. SAVICI *et al.*

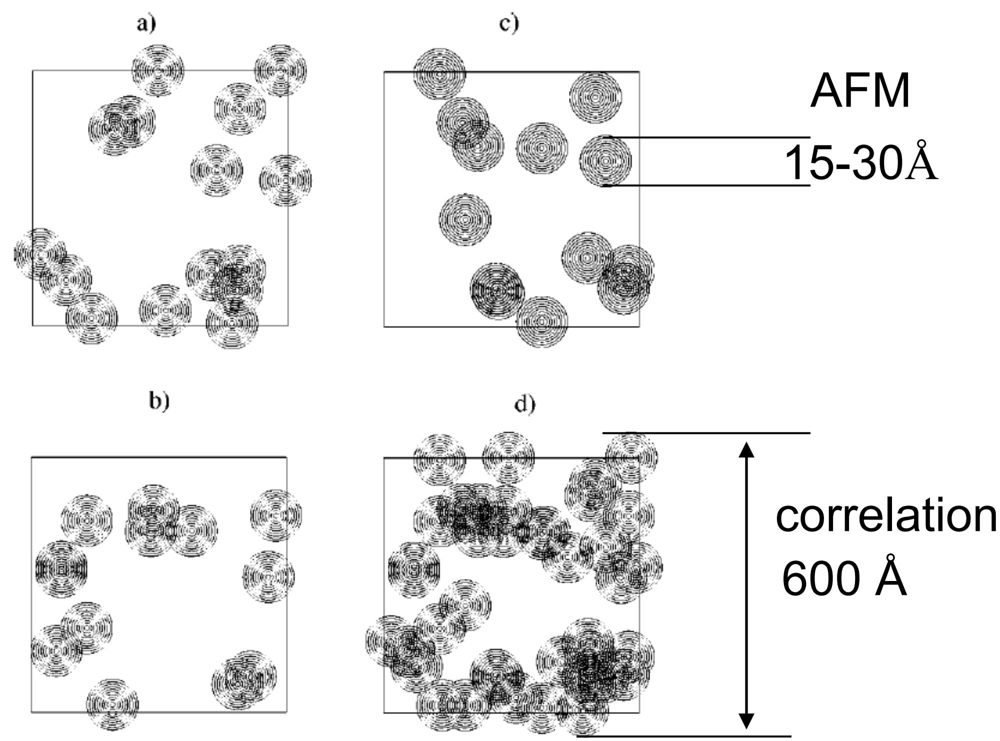

FIG. 10. Illustration of percolating cluster islands. (a)–(c) show planes with random locations of magnetic islands having integrated area fraction of 30%. (d) shows the overlap of (a)–(c). (d) demon-

FIG. 3. (a) Volume fraction V_μ of muon sites with a static mag-

Antiferromagnetic order induced by an applied magnetic feld in $La_{2-x}Sr_xCuO_{4+y}$

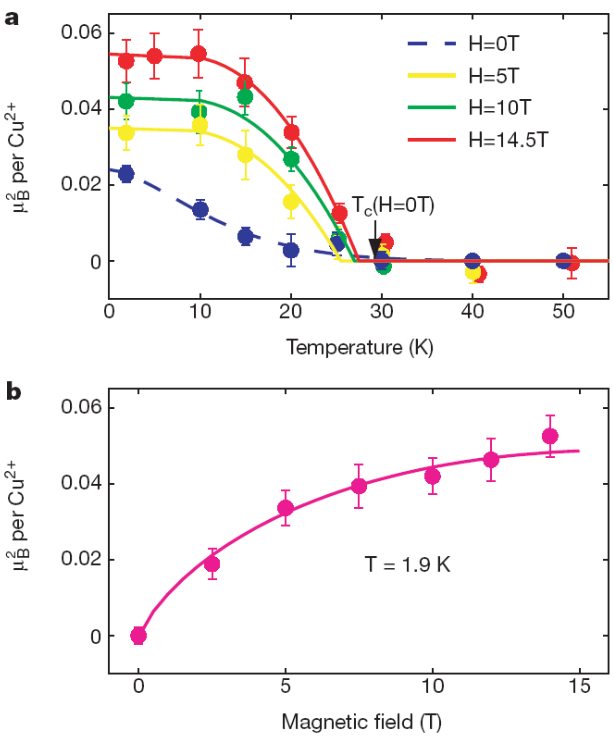

Figure 3 The dependence on temperature and field of the ordered spin moment squared. The data were calibrated using a transverse acoustic phonon measured around the (1,1) Bragg peak (energy transfer $E = 2$ meV and sound velocity = 26.9 meV Å), and are presented in units of μ_B^2 per Cu^{2+}. **a**, The temperature dependence. The zero-field signal (blue circles) increases gradually below $T_c(H = 0\,T)$, and the dashed line is a guide to the

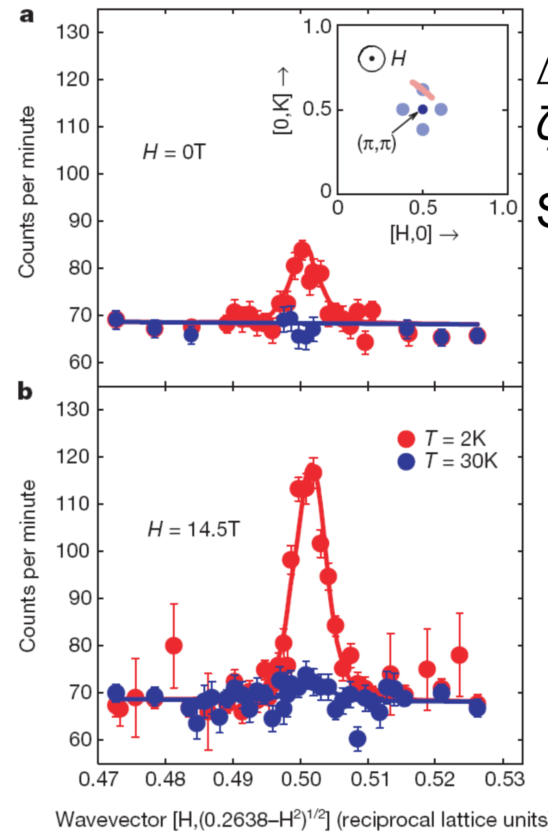

ΔE=0meV, ζ>400 Å

SO(5): ξ~20 Å

Figure 2 Magnetic neutron diffraction data for $La_{2-x}Sr_xCuO_4$ with $x = 0.10$. The inset shows the relevant reciprocal space, labelled using the two-dimensional notation appropriate for the superconducting CuO_2 planes. The black dot at (0.5,0.5) represents

B. Lake, et al, NATURE |VOL 415 | 17 JANUARY 2002, “Antiferromagnetic order induced by an applied magnetic feld in ahigh-temperature superconductor”

Coexistence of static AFM & SC in $La_{2-x}Sr_xCuO_{4+y}$

- Macro-PS (>1000Å) related to chemical miscibility gap (e.g. phase separation in oxygen -rich and –poor phases)
- Micro (<100Å) or meso-PS (>400Å) into SC and AFM phases in chemically single phase single crystals.
- Fact of $T_N = T_C$ is present in many cases.
- Theories: SO(5), quenched disorder near I-order phase transition

CMR[1] manganites

[1] CMR= Colossal negative MagnetoResistance [R(H)-R(0)]/R(0)

The present status of "CMR manganites"

- One of the best studied transition metal oxide system. (another best known example is high-T_C copper oxides)
- Spectacular different kinds of extraordinary phenomena and ordering effects
  - M-I transitions induced by T,P,H,…
  - Charge, Orbital, Magnetic Ordering. Charge/orbital stripes.
  - Electron-lattice interaction. Polaron formation
  - Intrinsic Phase Separation: microscopic (10-100Å) electronic and/or macroscopic one (>1000Å)
- Allows one to verify/develop theoretical approaches to strongly correlated electron systems[1].
  - Based on DE, + el.phonon + orbital d.f. + inter-site V, + elastic.

[1] Yu.A. Izymov, Yu. N. Skryabin, Phys. Usp., 44, 109 (2001)

Magnetoresistance in metals and semimetals

$\Delta R/R(0) > 0$ in **nonmagnetic** metals.
Orbital, quantum magnetoresistance
$\Delta\rho = +\rho_0(eH/mc\,\tau)^2$, or $\sim +N_iH/\pi n^2_e ec$
$\Delta\rho = +\rho_0$ for $H \gg \Omega$

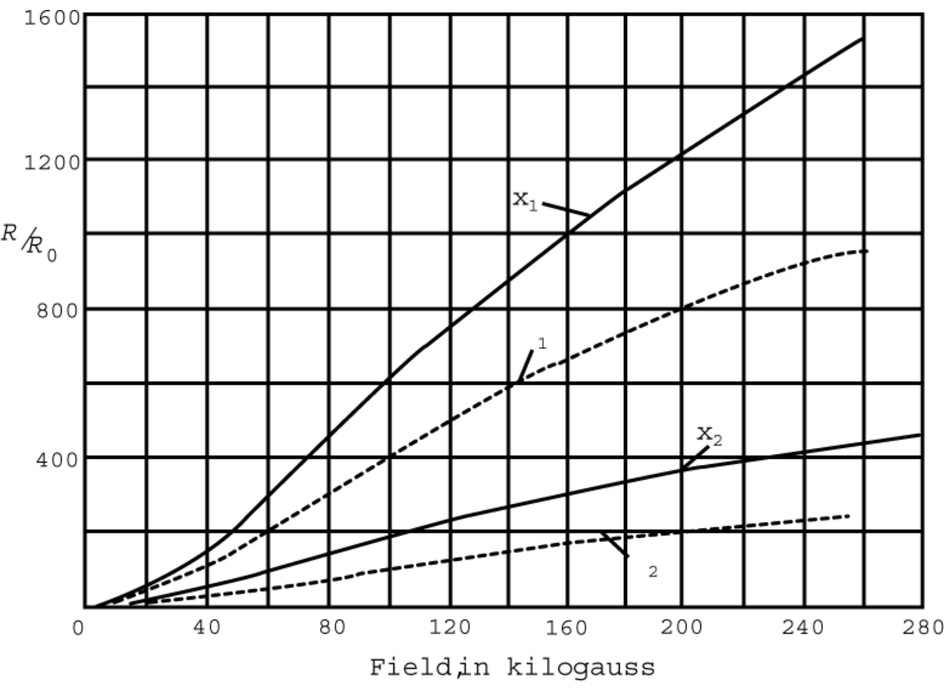

Bi single crystal. T=77K [Kapiza P.L. 1928]

$\Delta R/R(0) < 0$ in **ferromagnetic** metals.
Spin-disorder scattering
$\Delta\rho = -\rho_J \sim J^2S(S+1)$

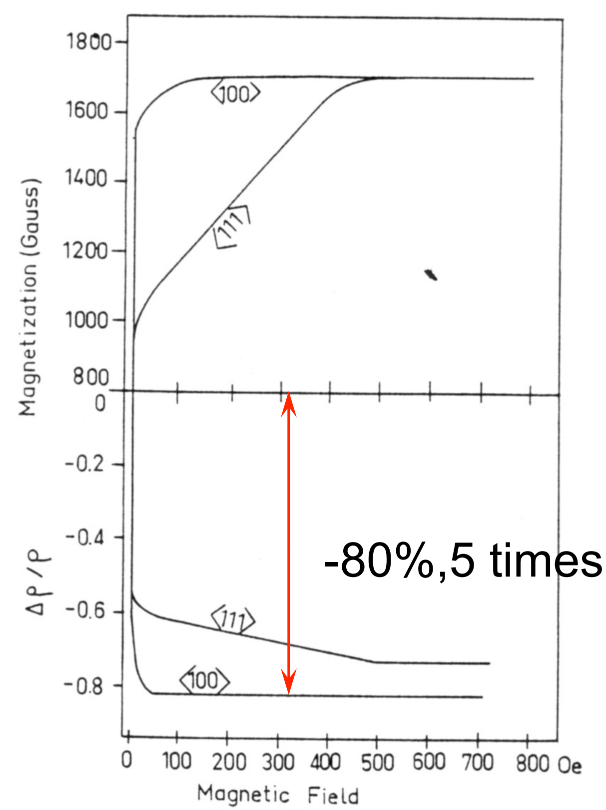

Iron whiskers T=4.2K [Taylor et al. 1968]

Transition metal 3d perovskite-like oxides AMO_3

M=

Sc	$Ti^{4+/3+}$	$V^{4+/3+}$	$Cr^{4+/3+}$	$Mn^{4+/3+}$	$Fe^{4+/3+}$	$Co^{4+/3+}$	Ni^{3+}	Cu^{3+}	Zn
$3d^14s^2$	$3d^{0/1}$	$3d^{1/2}$	$3d^{2/3}$	$3d^{3/4}$	$3d^{4/5}$	$3d^{5/6}$	$3d^7$	$3d^8$	$3d^{10}4s^2$

A=Sr,Ba,Y,La,Pr,…

$$H = -\sum b_{ij} c^+_{i\sigma} c_{j\sigma} + U \sum n_j n_j$$

$W < U_{eff}$: Mott insulator

$W > U_{eff}$: metal

Bandwidth
π,σ transf. int. b_{ij}

On-site Coulomb

$3d^n3d^n \rightarrow 3d^{n+1}3d^{n-1}$

$3d^n2p^6 \rightarrow 3d^{n+1}2p^5$

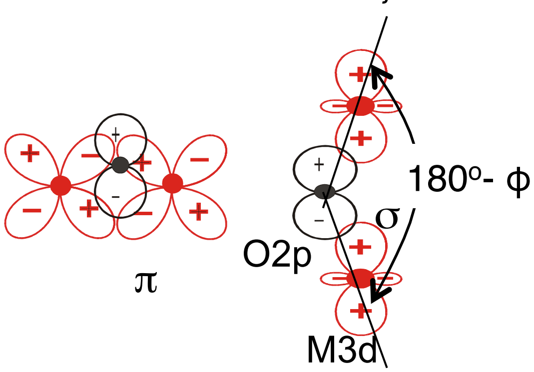

VOLUME 71, NUMBER 14 PHYSICAL REVIEW LETTERS 4 OCTOBER 1993

Giant Negative Magnetoresistance in Perovskitelike $La_{2/3}Ba_{1/3}MnO_x$ Ferromagnetic Films

R. von Helmolt,[1,2] J. Wecker,[1] B. Holzapfel,[1] L. Schultz,[1] and K. Samwer[2]
[1]*Siemens AG, Research Laboratories, D-8520 Erlangen, Germany*
[2]*Institute of Physics, University of Augsburg, D-8900 Augsburg, Germany*
(Received 14 May 1993)

At room temperature a large magnetoresistance, $\Delta R/R(H=0)$, of 60% has been observed in thi magnetic films of perovskitelike La-Ba-Mn-O. The films were grown epitaxially on $SrTiO_3$ substrates b off-axis laser deposition. In the as-deposited state, the Curie temperature and the saturation magnetiza tion were considerably lower compared to bulk samples, but were increased by a subsequent heat trea ment. The samples show a drop in the resistivity at the magnetic transition, and the existence of mag

Small-bandwidth manganites (PrCa)MnO_3

Large bandwidth manganites

Double exchange (Mn^{3+}-O-Mn^{4+}) metal: $La_{2/3}Sr_{1/3}MnO_3$

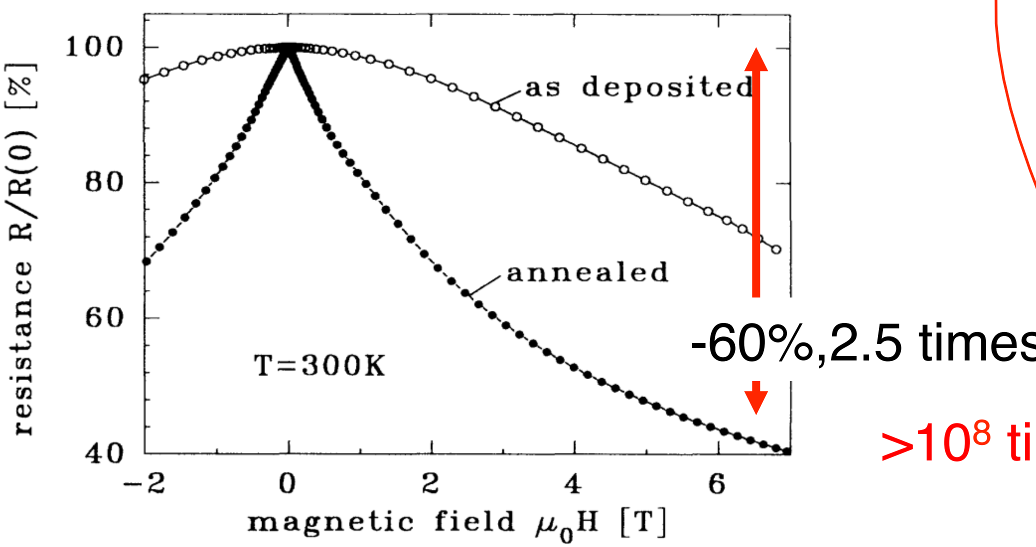

FIG. 3. Resistivity versus field curves for the as-deposited sample (T_S=600 °C) and after annealing at T_A=900 °C for 12 h, measured at T=300 K.

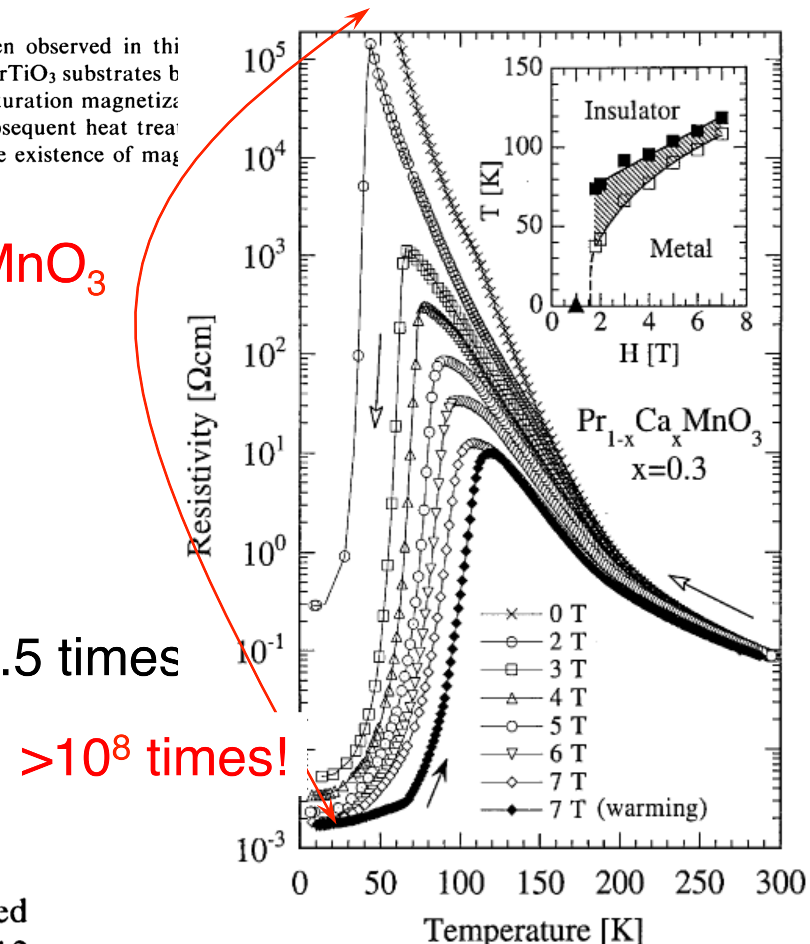

From Tomioka, Tokura 1999

Essential interactions in manganites/cobaltites

Intraatomic interactions

J_H~2 eV, 10Dq~1-2 eV, U_{eff}~3-5eV

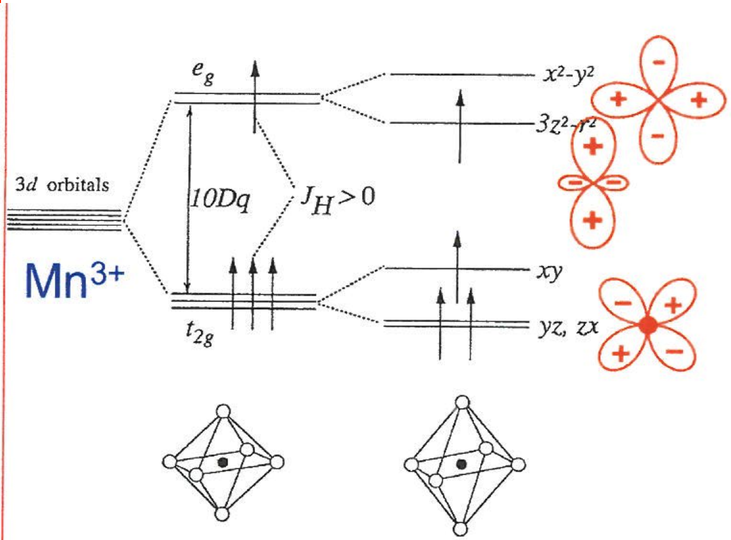

Electron-lattice interactions

J/T split of e_g provides strong el.-lattice coupling

$$t^* = t\exp(-\frac{\gamma E_{JT}}{\hbar\omega})$$

Orbital ordering, effective spin-orbit

Interatomic interactions

1. Superexchange

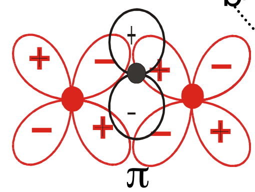

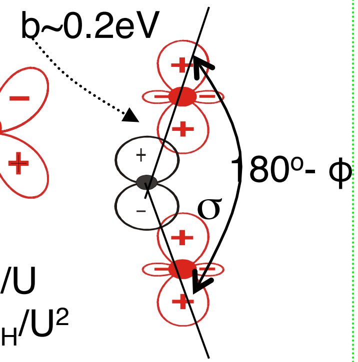

J_{AF} ~ $-b^2/U$
J_{FM}~ b^2J_H/U^2

AF,F ordering

2. Double exchange

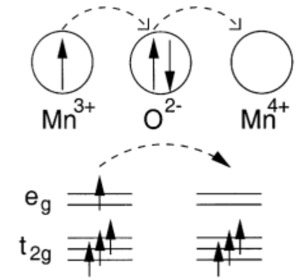

t ~ b cos(θ/2)
J_{FM}~ zt

FM ordering
real charge transfer

3. Intersite Coulomb V

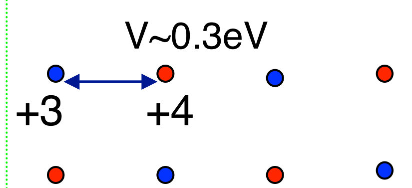

$$H = +V\sum_{ij} n_i n_j - t\sum_{ij} c_i^+ c_j$$

charge ordering

4. Elastic interactions

- Long range strain ~$1/R^3$
- Short range optical phonons

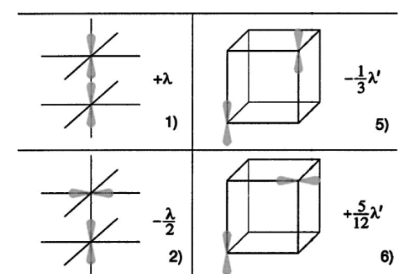

orbital ordering

M-I transition in $(La_{1-y}Pr_y)_{0.7}Ca_{0.3}MnO_3$

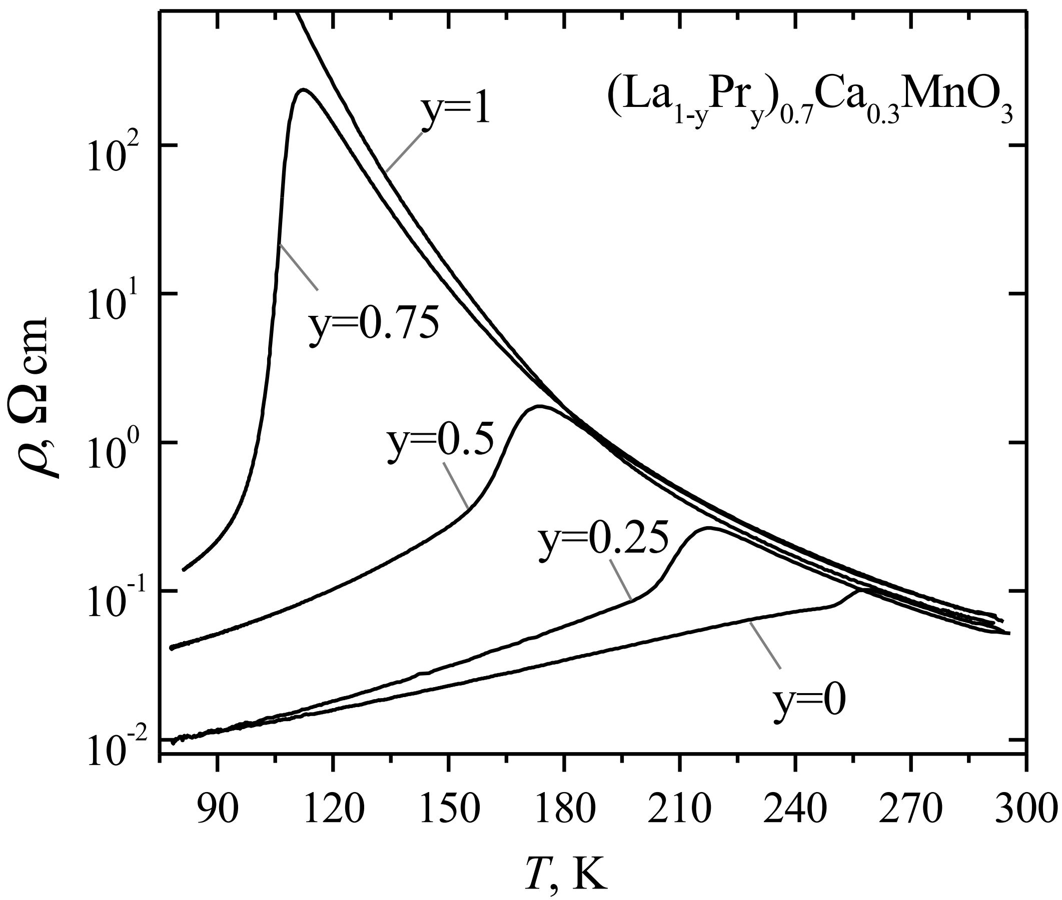

Babushkina et al, 2000

$(La_{1-y}Pr_y)_{0.7}Ca_{0.3}Mn^{16}O_3$ phase diagram

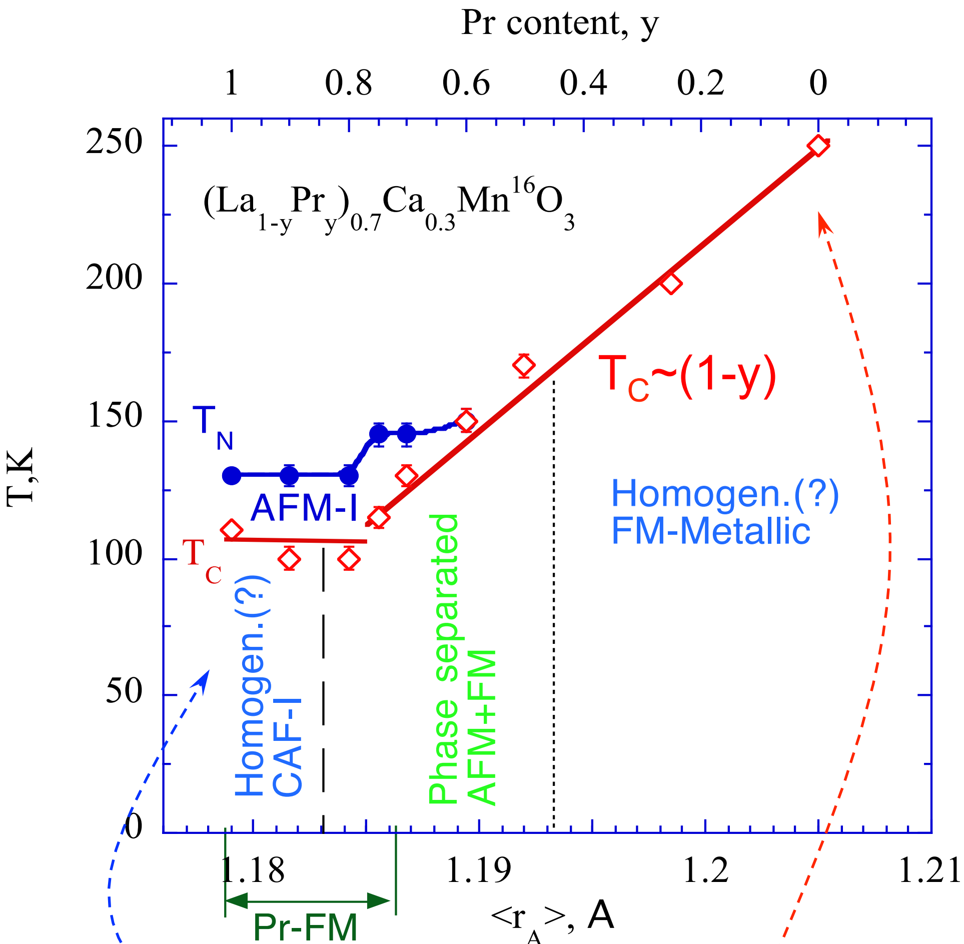

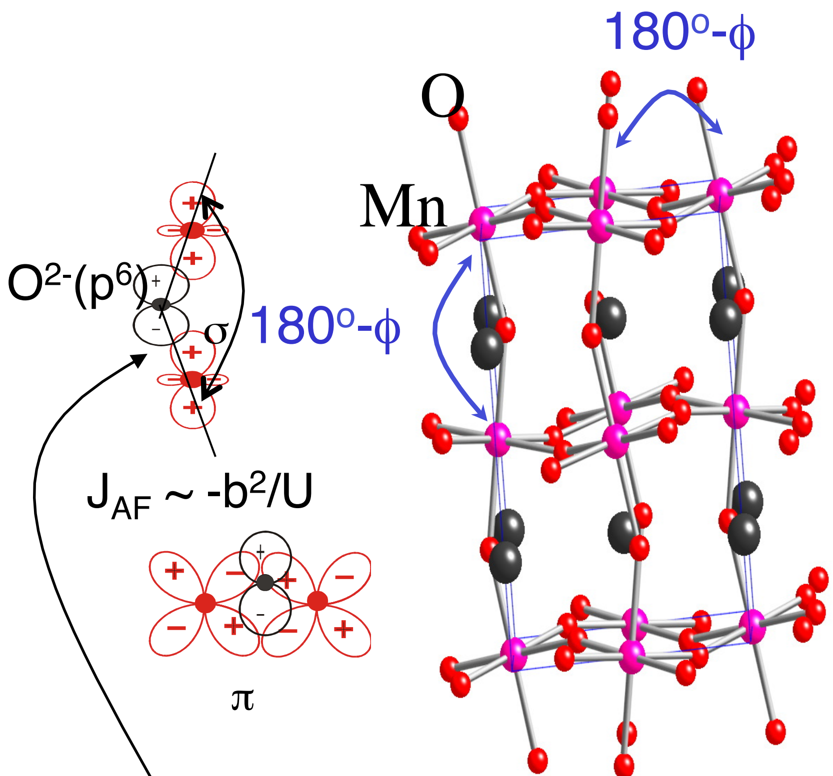

CAFM Mott insulattor → FM double exchange metal

(Mn-O) electron transfer integral
$b_\sigma \sim \cos(\phi) \sim \langle r_A \rangle \sim (1-y)$
is increased with *y* resulting in the insulator-metal transition

Balagurov *Phys. Rev. B* **64**, 024420-1 (2001).

$(La_{1-y}Pr_y)_{0.7}Ca_{0.3}Mn^{16}O_3$ phase diagram

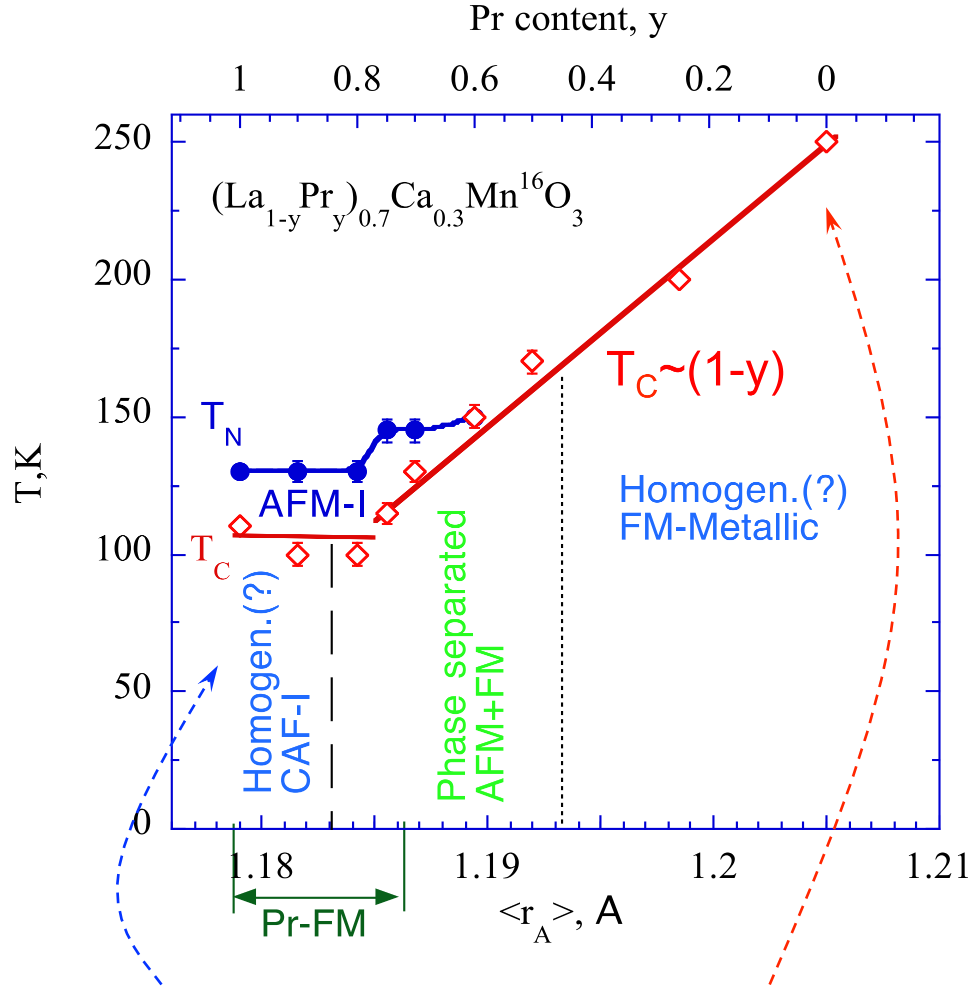

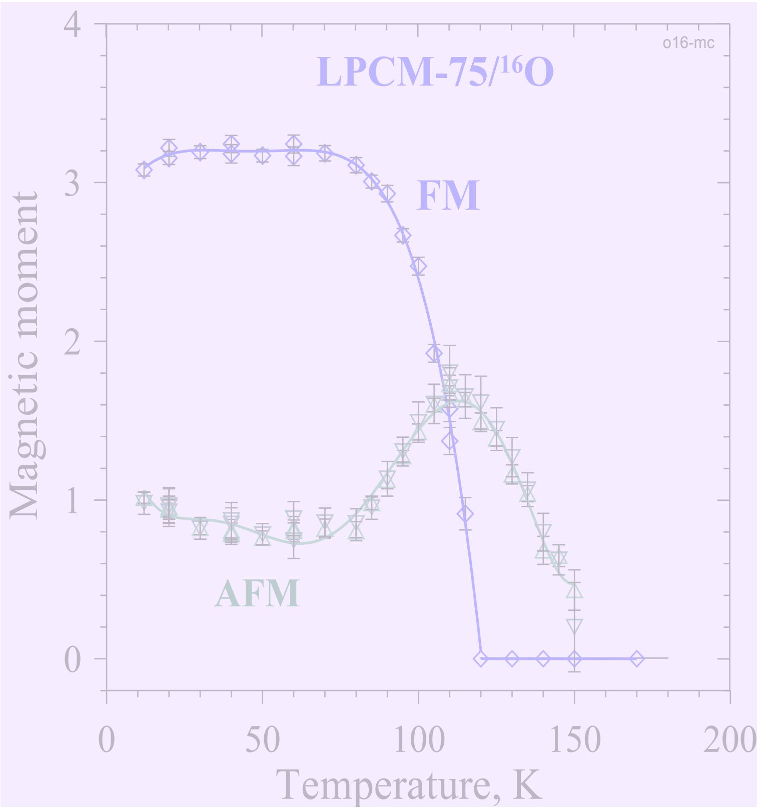

CAFM Mott insulattor → FM double exchange metal

Balagurov *Phys. Rev. B* **64**, 024420-1 (2001).

$(La_{1-y}Pr_y)_{0.7}Ca_{0.3}Mn^{16}O_3$ magnetic structure

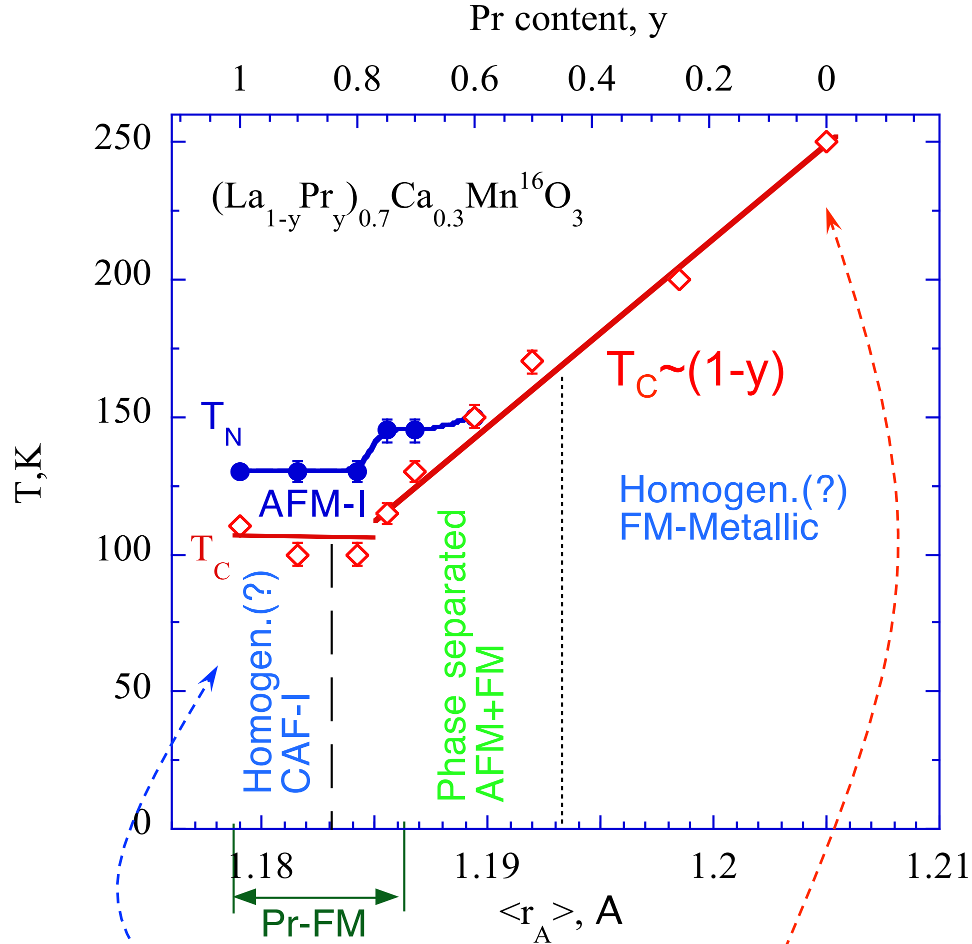

Pseudo CE=PCE: [½ 0 0] and [½ ½ 0]

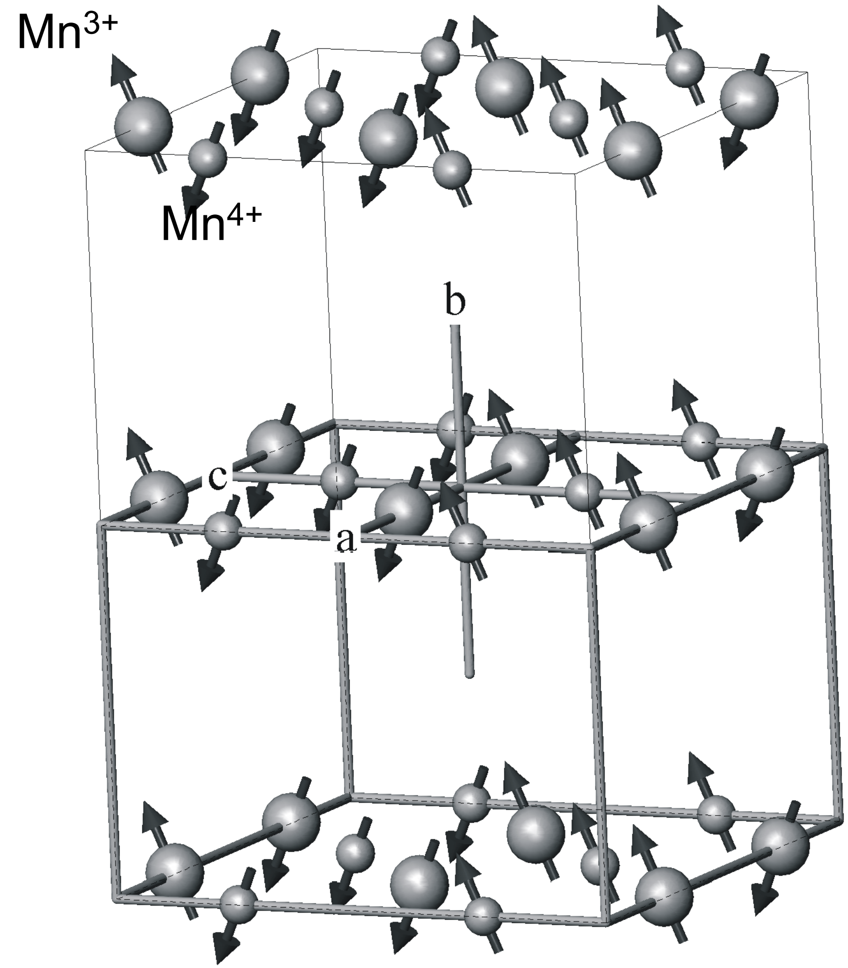

CAFM Mott insulattor → FM double exchange ı

Balagurov *Phys. Rev. B* **64**, 024420-1 (2001).

Diffraction in external magnetic field $\mathbf{H}_{ext} \perp \mathbf{Q}$

Homogeneous

$I_{Bragg} \sim M^2(1-(\mathbf{qm})^2)$

$\mathbf{m}=\mathbf{M}/M$, $\mathbf{q}=\mathbf{Q}/Q$

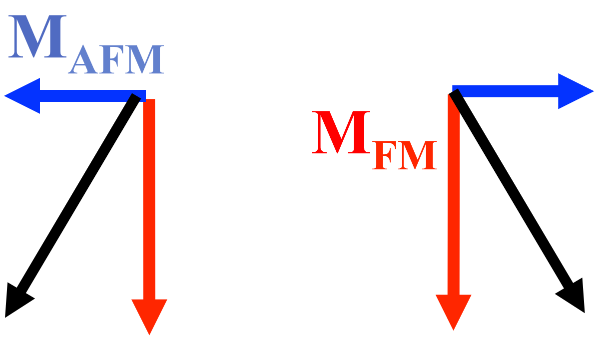

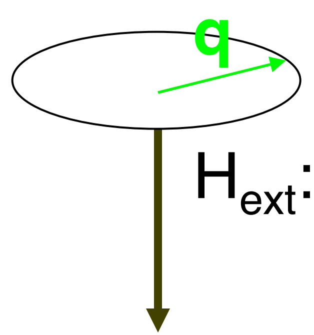

I_{AFM} is decreased

I_{FM} is increased

Spatially separated

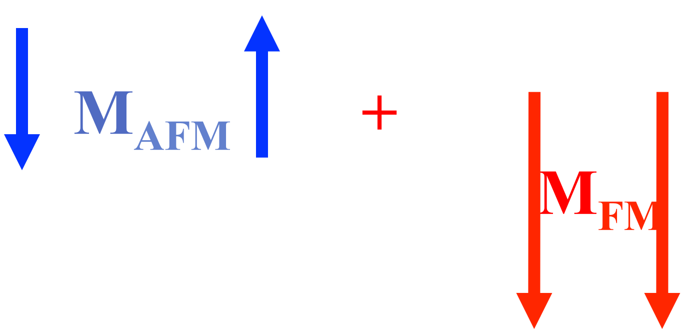

I_{AFM} ~const ($H<H_c$)

I_{FM} is increased

$(La_{1-y}Pr_y)_{0.7}Ca_{0.3}MnO_3$: Bragg peak intensities as a function of H_{ext}

Balagurov *Phys. Rev. B* **64**, 024420-1 (2001).

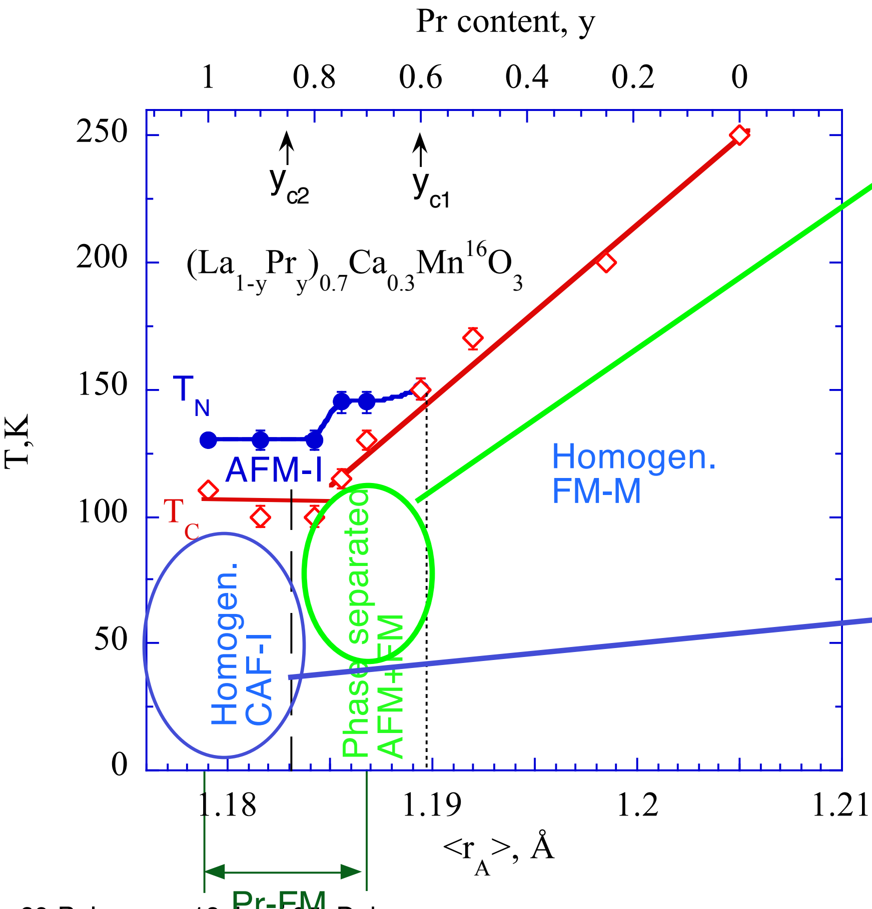

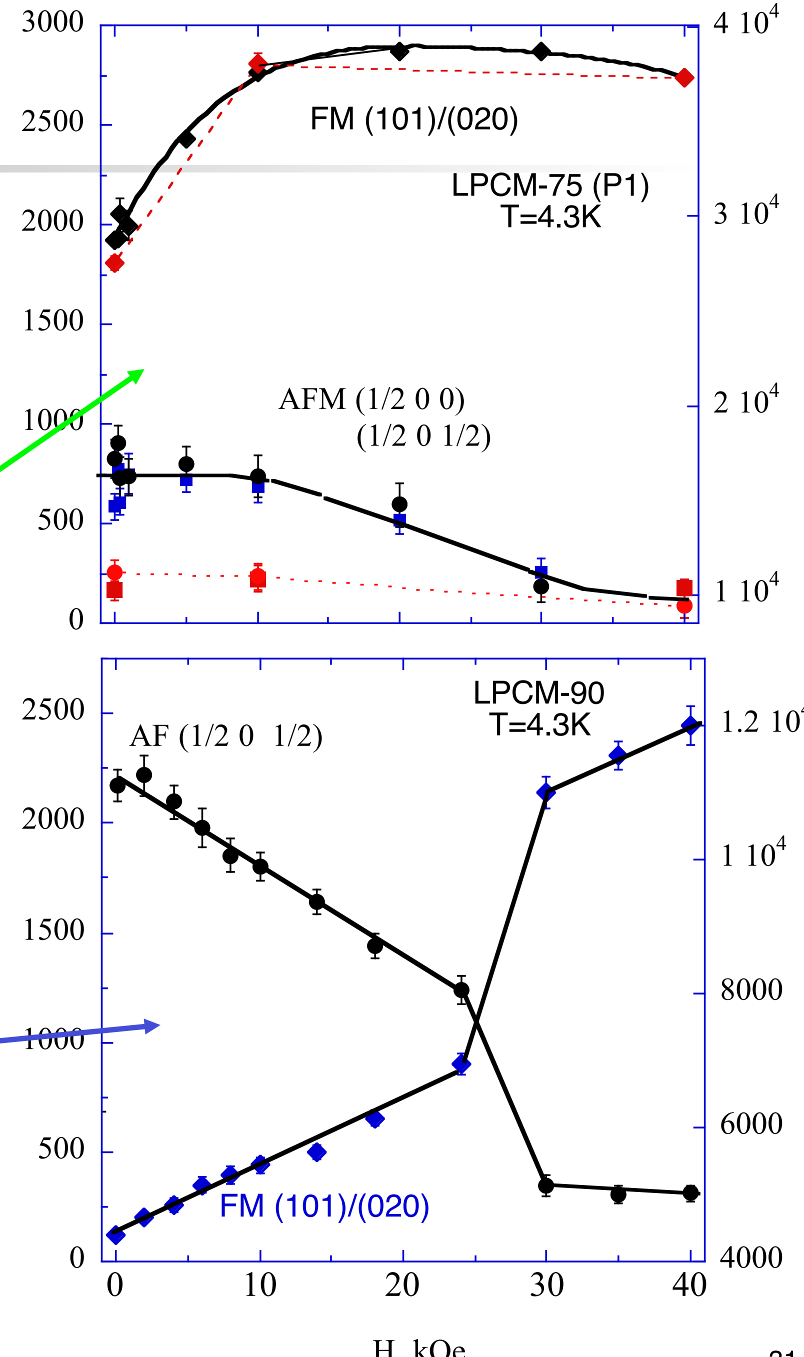

Size effect: What are the domain sizes?

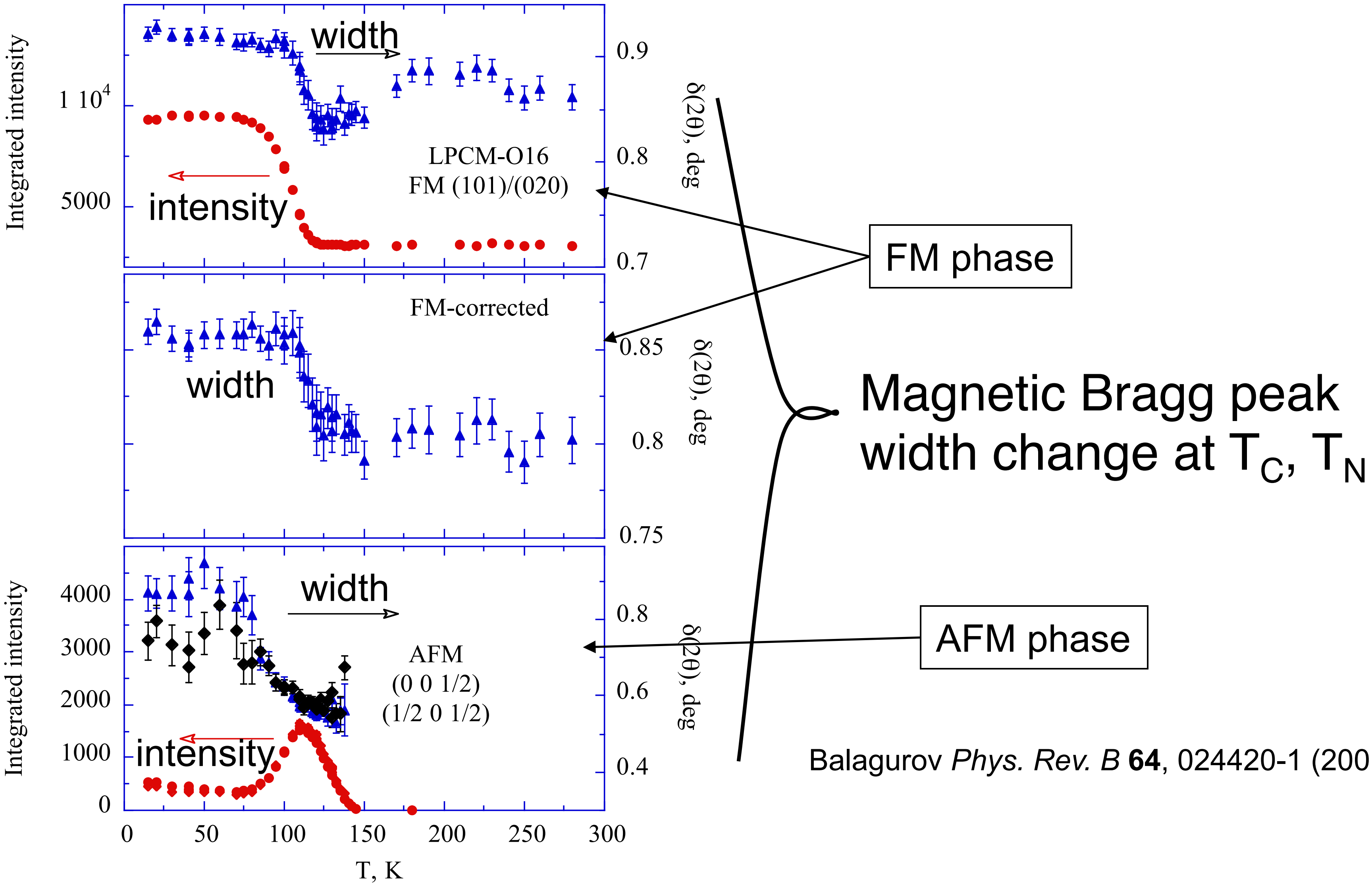

Balagurov *Phys. Rev. B* **64**, 024420-1 (2001).

Size effect

1. Size effect: $\Delta d^* = 1/L = const \Rightarrow$ $(\Delta d/d)^2 = (d/L)^2$
2. Strain effect: $\Delta d/d = \varepsilon = const \Rightarrow$ $(\Delta d/d)^2 = \varepsilon^2$

Total: $(\Delta d/d)^2_{exp} = (d/L)^2 + \varepsilon^2$

$d^* = 1/d$, $\Delta d/d = \Delta\Theta/\mathrm{tg}\Theta$

Crude estimation of the low limit of the magnetic domain sizes, assuming zero strain contri-bution gives L>10^3 Å

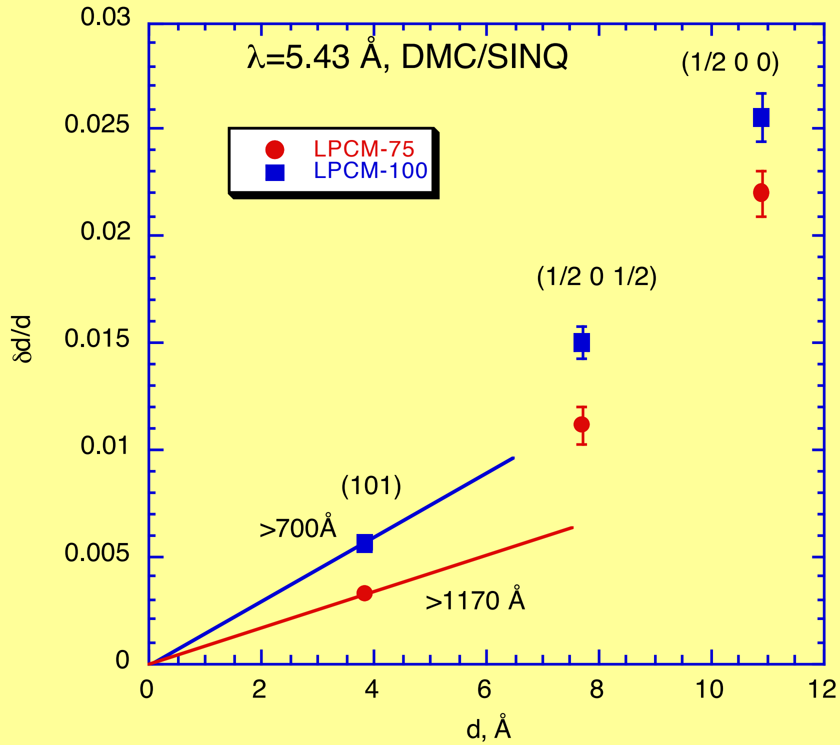

MO Imaging of Percolative Conduction Paths and Their Breakdown in Phase-Separated $(La_{0.3}Pr_{0.7})_{0.7}Ca_{0.3}MnO_3$

Tokunaga, et al Phys Rev Letters 2004.
(Faraday effect)

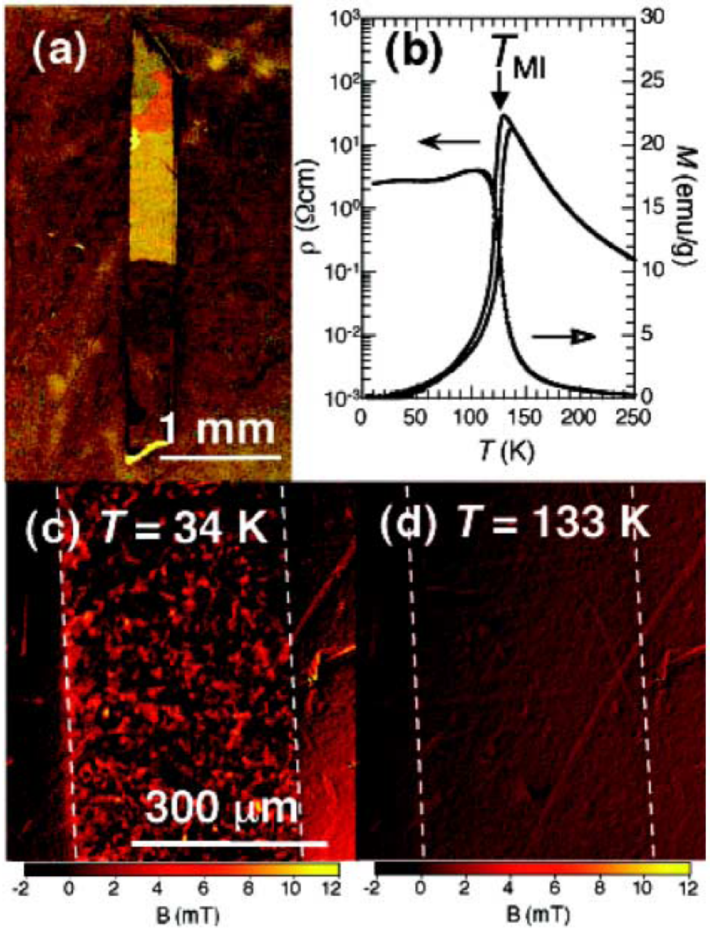

magnetization

Current distribution

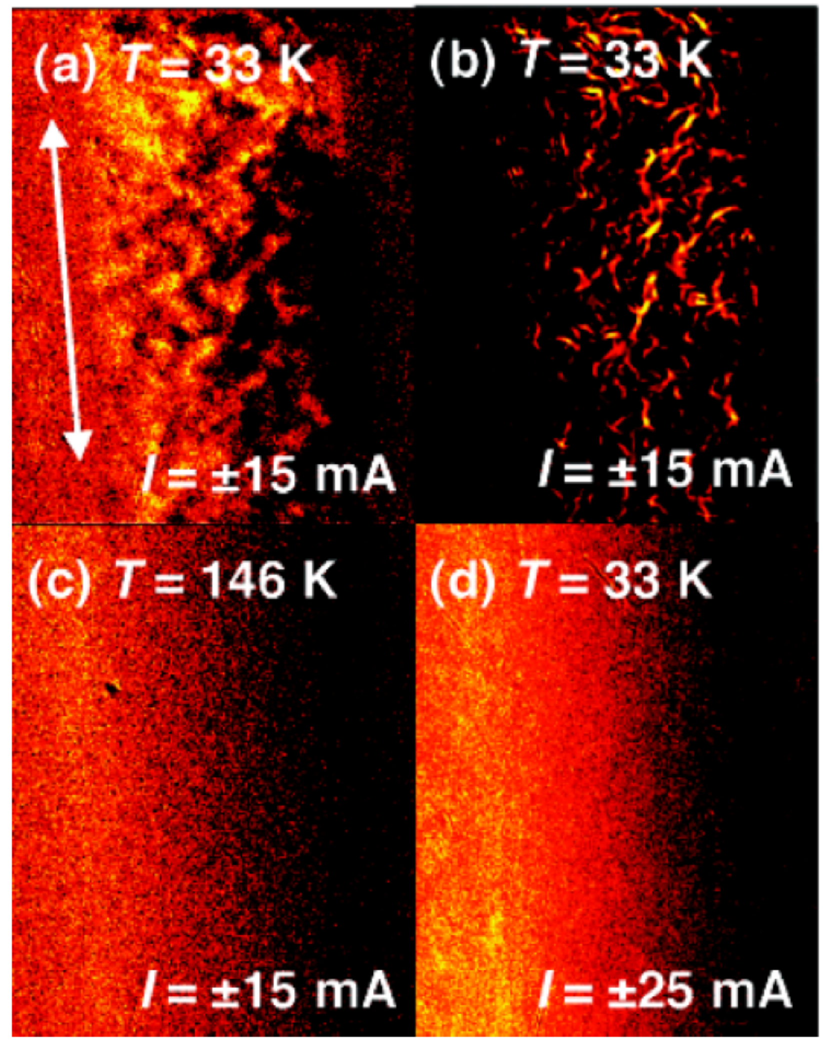

avr. 450 sets

Phase separation caused by the effect of disorder near MI-order transition

From: Moreo, Dagotto, PRL (2000)

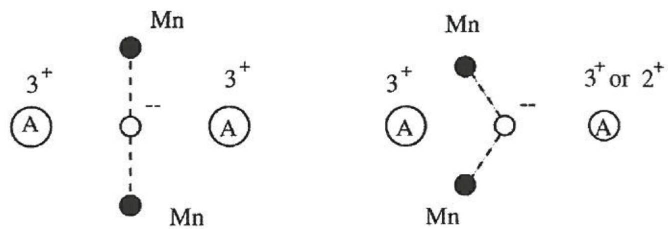

$$H = -t\sum_{i} c^{+}_{i\sigma} c_{j\sigma} + J\sum_{ij} S_i S_j + H_{el-ph}$$

t is locally reduced due to smaller Pr-cation radius in $(La_{1-y}Pr_y)_{0.7}Ca_{0.3}MnO_3$

1.216 Å

1.216 Å

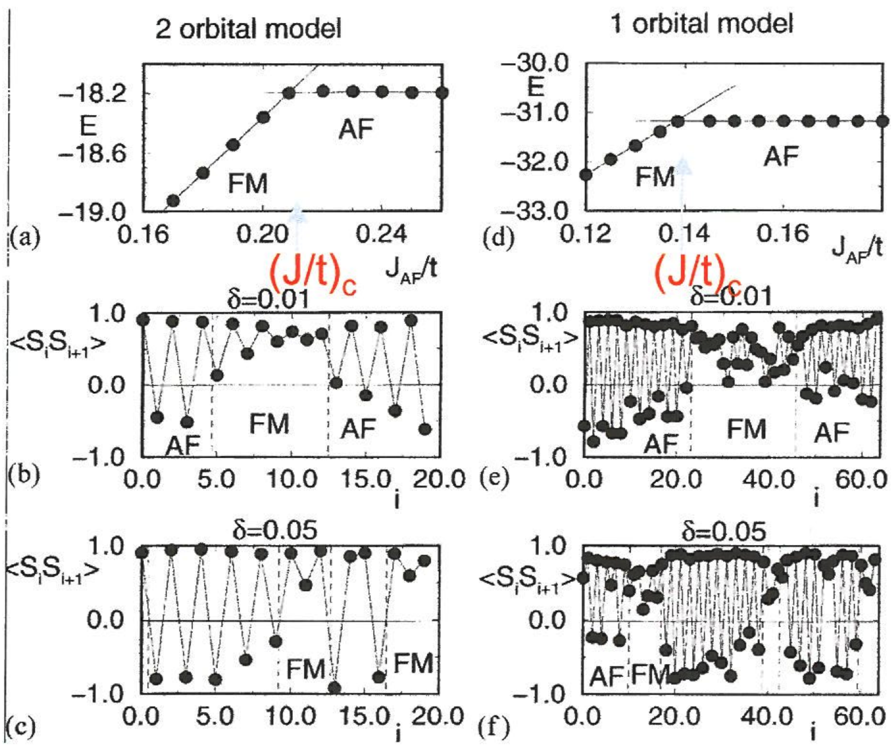

Generation of "giant" coexisting clusters

Energy per site vs. J/t for antiferro- and ferromagnetic state

MC averaged nearest-neighbor t_{2g}-spin correlations vs position along the chain.
J/t varies between $(J/t)_c$-δ and $(J/t)_c$+δ

Influence of quenched disorder on the competition between ordered states separated by a first-order transition

J.Burgy, A.Moreo, M. Mayr, E.Dagotto, et al, PRL, PRB 2000-2004

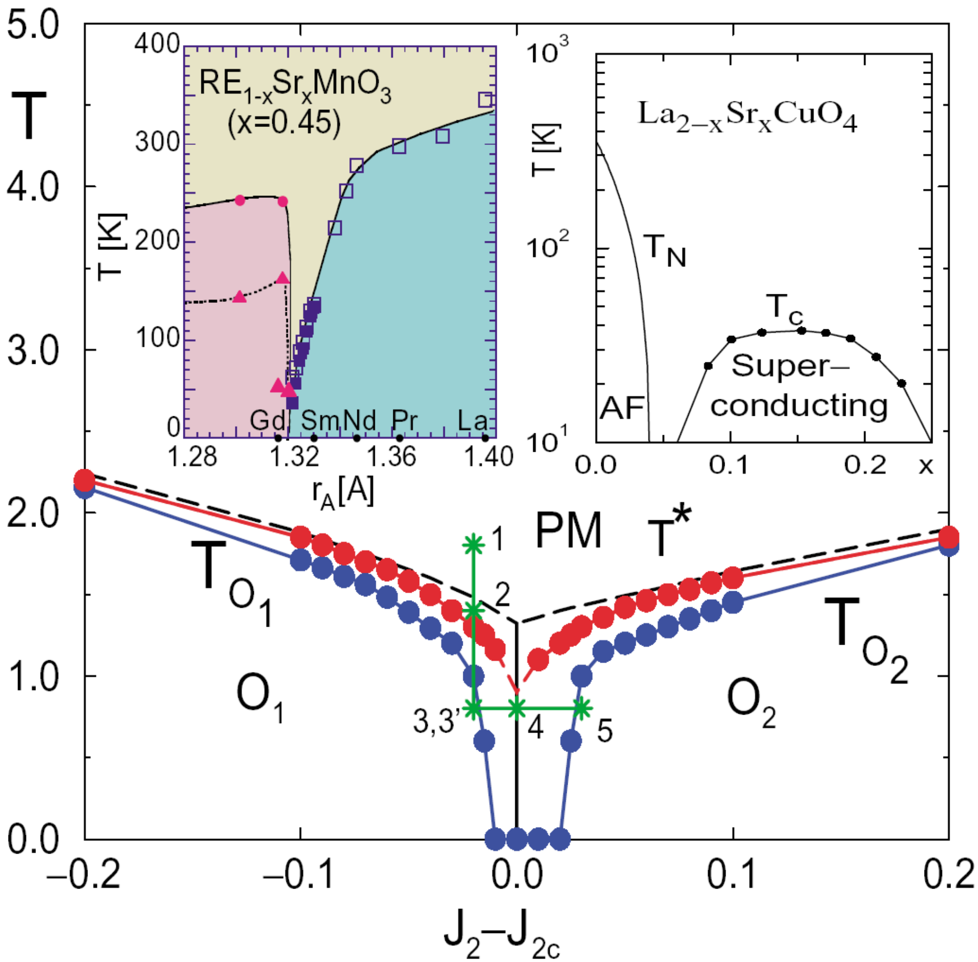

3D RFIM +correlated disorder

$$H = -J\sum_{\langle ij\rangle} s_i s_j + J'\sum_{[ik]} s_i s_k$$

$$+ \; \Delta\sum_{i,j} h_i s_j / d_{ij}^{\alpha},$$

α~3 elasticity mechanism of the distortion propagation (Khomskii, Kugel, 2001)

Ising spin configuration

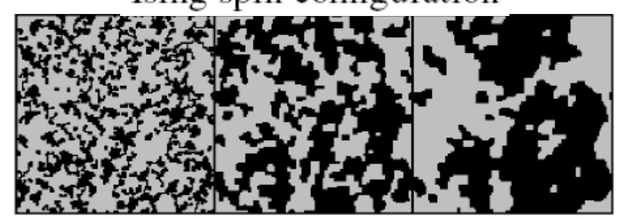

$\alpha=\infty$ $\alpha=3$ $\alpha=1$

2D FM

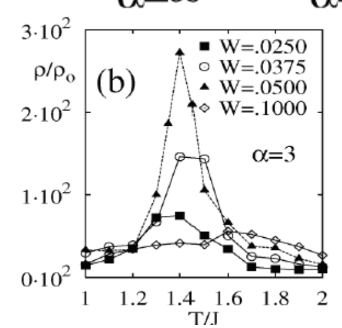

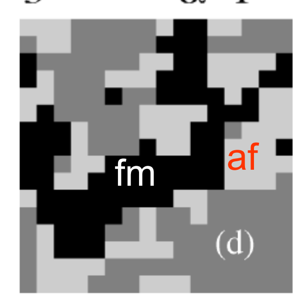

3D

Large isotope effect in metallic manganites

Decrease in T_C by $^{16}O \rightarrow {}^{18}O$ exchange

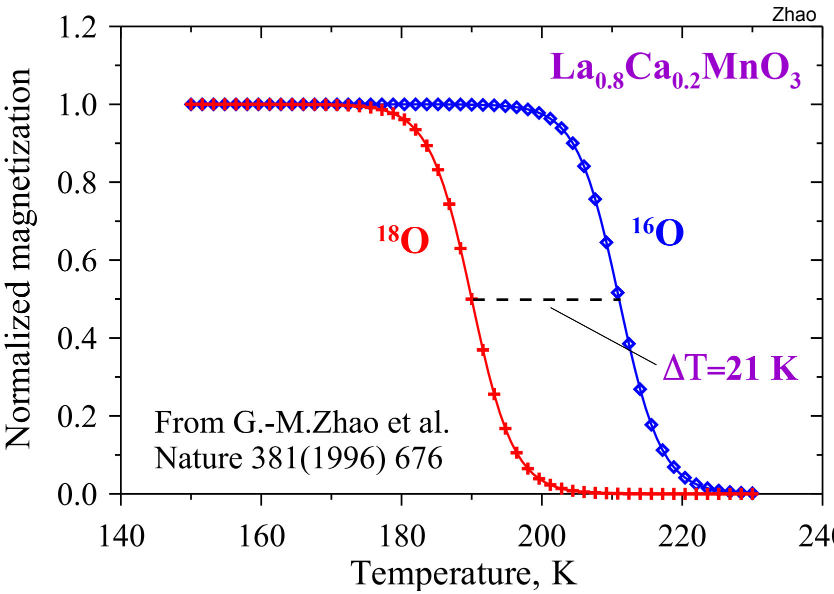

Oxygen isotope exponent

$$\alpha_0 = -\Delta \ln T_C / \Delta \ln M = 0.5\gamma E_{JT} / \hbar\omega$$

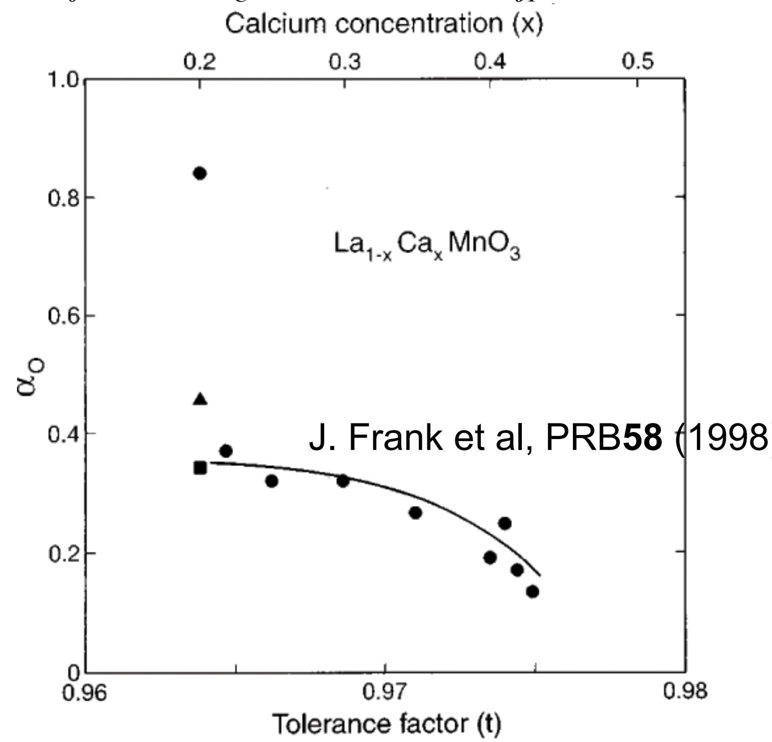

Small polaron[1]

$$t^* = te^{-g^2} = t\exp\left(-\frac{\gamma E_{polaron}}{\hbar\omega}\right) \sim t\exp(-k\sqrt{M})$$

$$\gamma = \gamma(E/t) \sim 1$$

J/T-polaron Mn^{3+}/ Mn^{4+}

$t^3_{2g}e_g^{\,1}$ / $t^3_{2g}e_g^{\,0}$

double exchange: $T_C \sim t$

<u>One-orbit DE + small polaron model</u>

U.Yu, et al PRB **61**, 8938 (2000)

C.A. Perroni et al, PRB **66**, 184409 (2002)

S.W. Biernacki PRB **61**, 184409 (2002)

α_0=0.3-0.65

[1]A.S.Alexandrov, N.F.Mott Int. J. mod. Phys **8,** 2075 (1994)

$(La_{1-y}Pr_y)_{0.7}Ca_{0.3}MnO_3$: $\chi_{ac}(T)=\chi'(T)+i\chi''(T)$

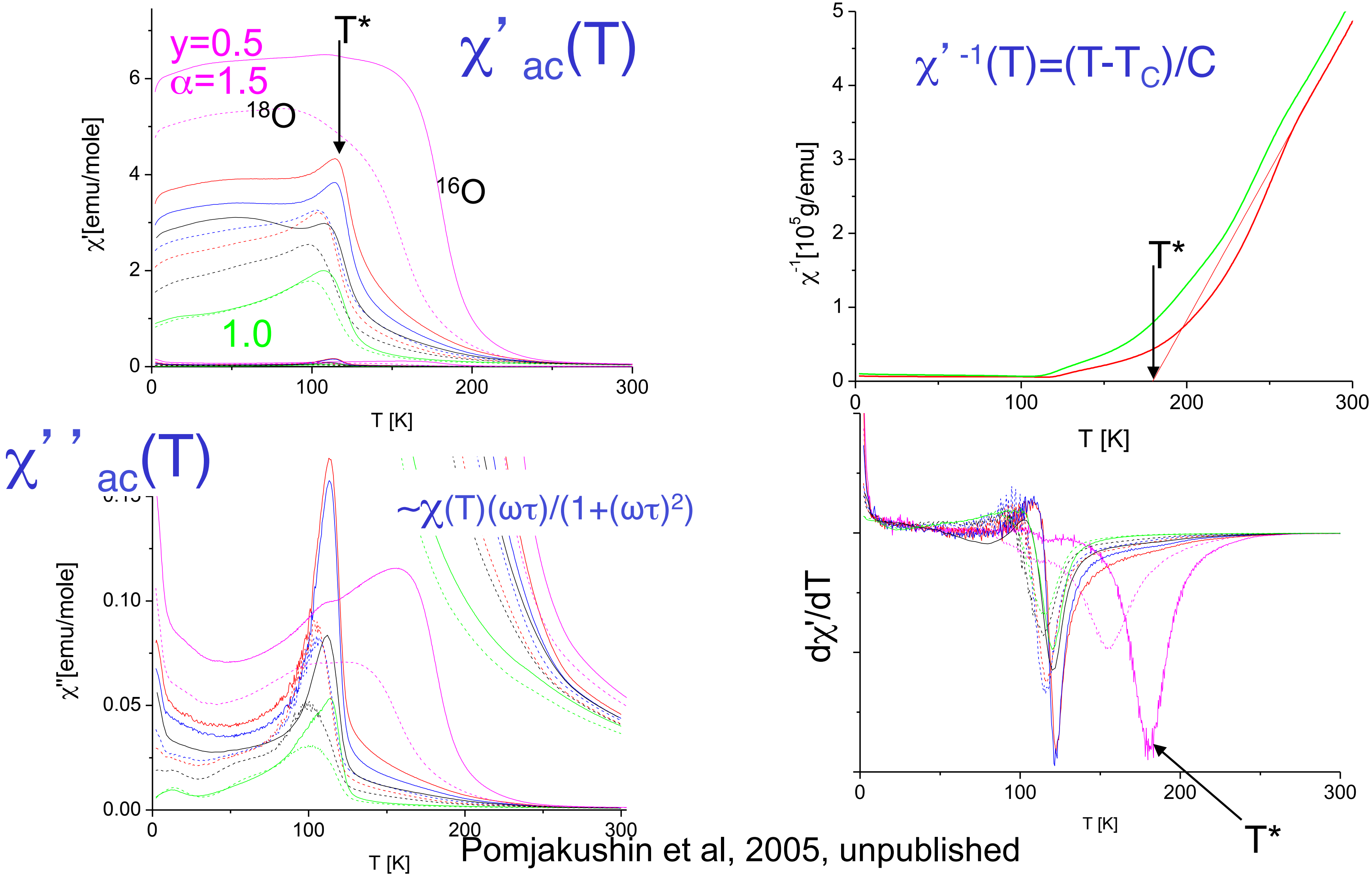

Pomjakushin et al, 2005, unpublished

Giant isotope effect in intermediate-bandwidth manganites

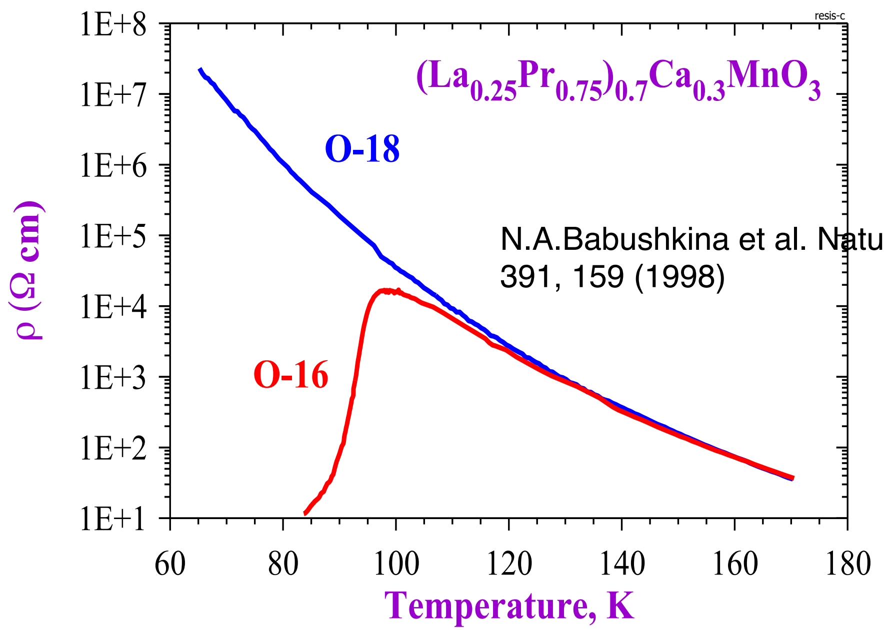

N.A.Babushkina et al. Nature 391, 159 (1998)

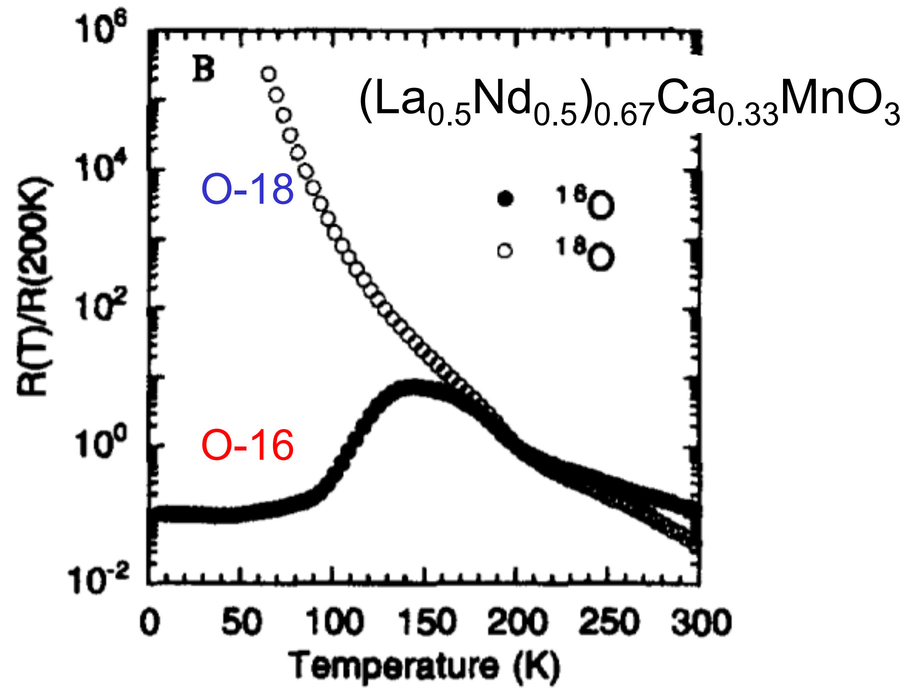

Guo-meng Zhao et al, Solid State Comm. **104**, 57 (1997)

$$t^* = t\exp(-\frac{E_{pol}}{\varpi})$$ is not enough!

M-I is a percolative transition in phase separated state

Giant isotope effect: magnetic structure

$(La_{1-y}Pr_y)_{0.7}Ca_{0.3}MnO_3$, y=0.75

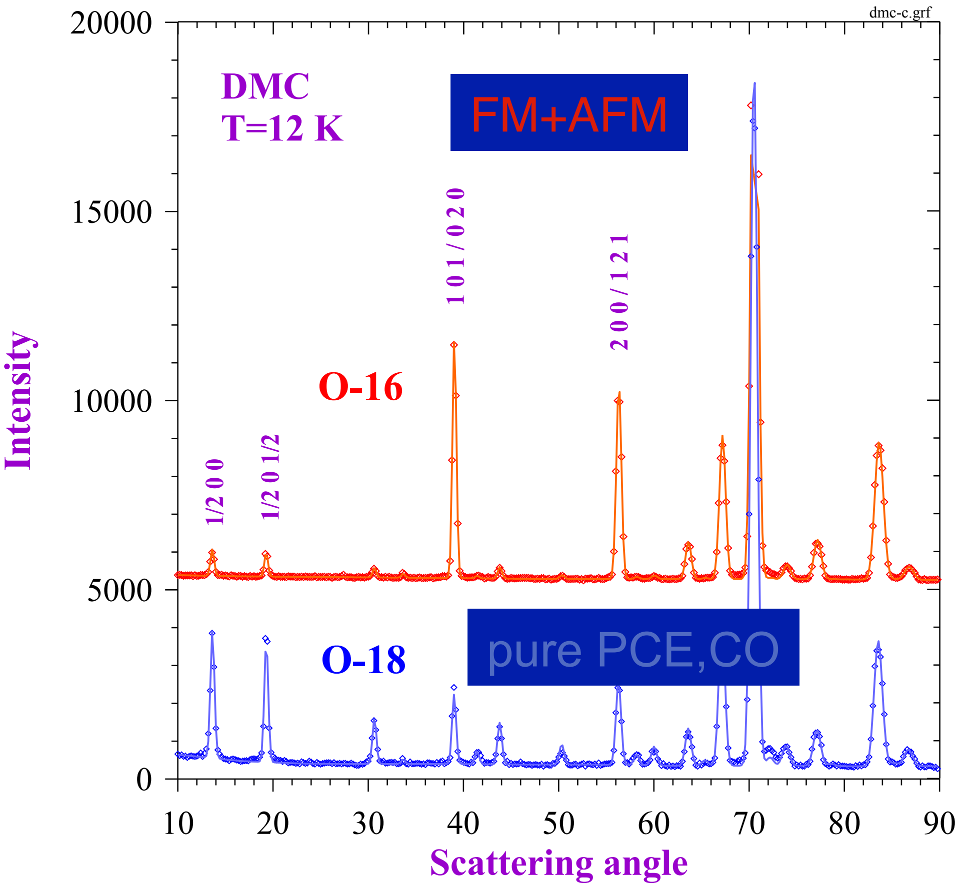

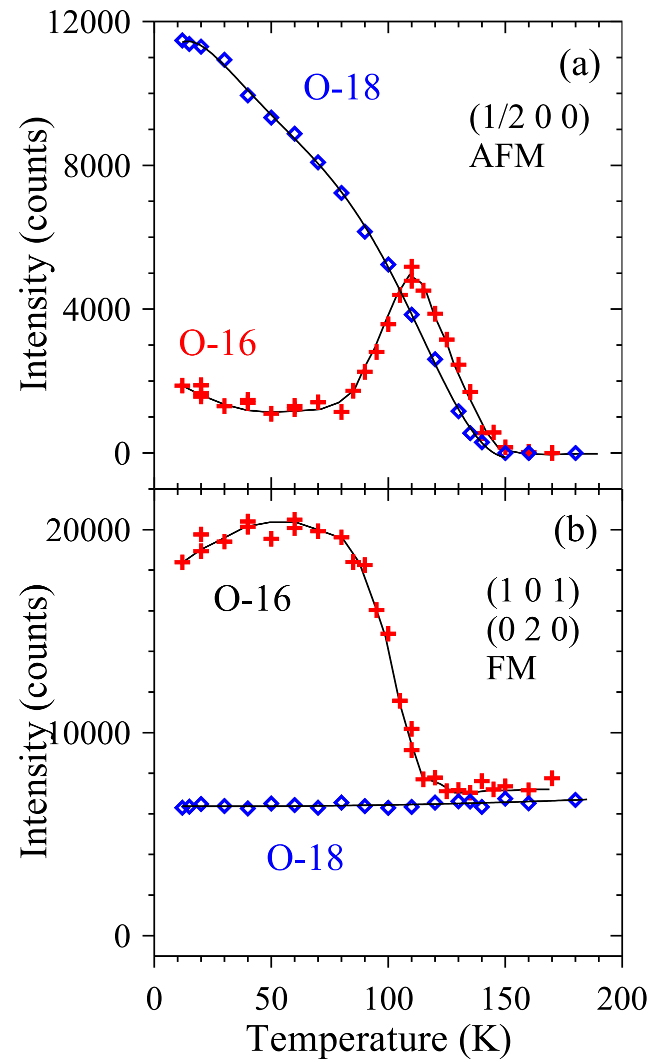

Balagurov et al, *Phys. Rev. B* **60**, 383 (1999)

Natural continuation: Isotope effect in the vicinity of M-I transition @ y=0.8

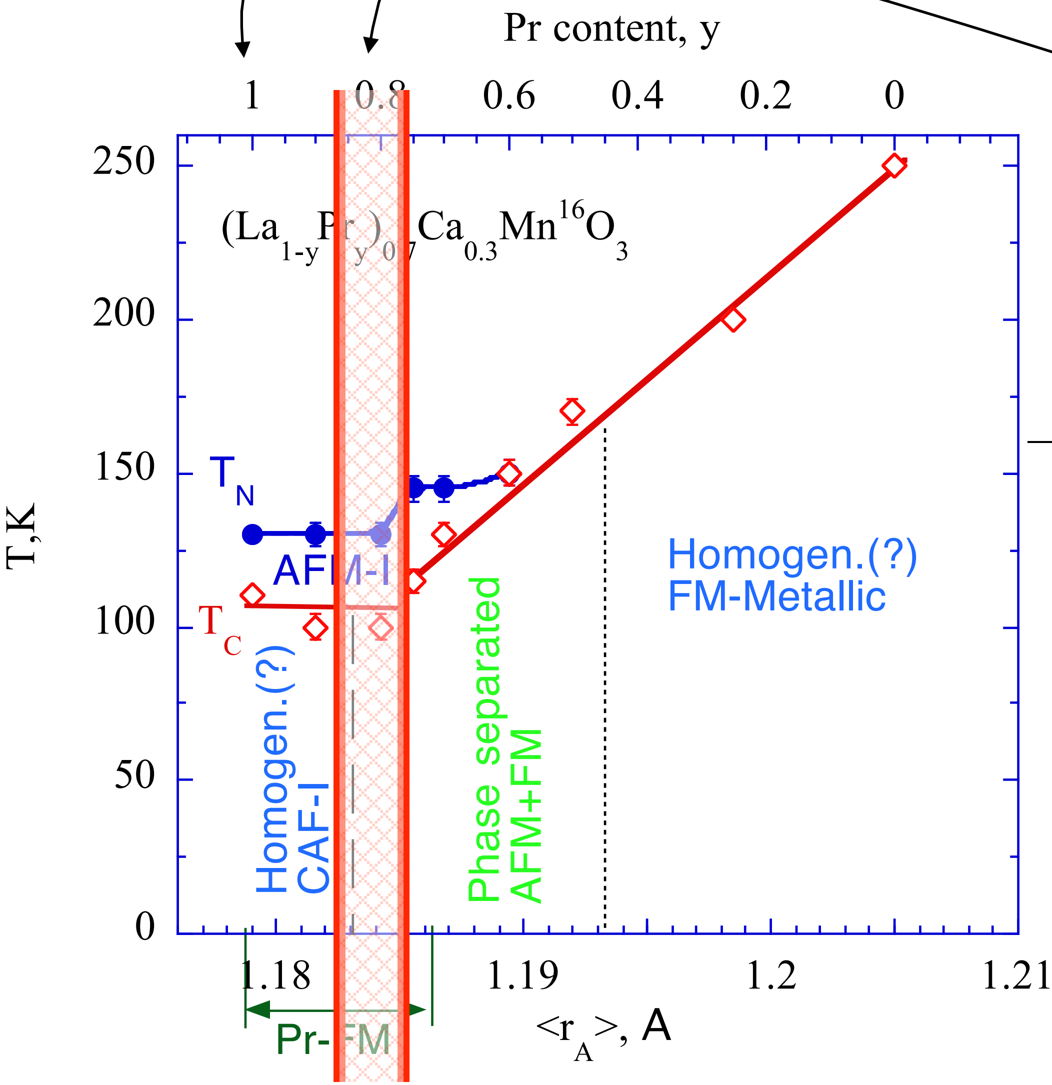

y=0.7, 0.8 and 1.0

HR diffraction and $\chi_{ac}(T)$:

➢the y-range of the giant isotope effect.

➢detailed T-scans: the interplay magnetic, orbital and charge ordering

---

Polaronic narrowing works if:

e-hopping time	$\tau \sim 1/\omega$	opt. phonon ~20 meV

Isotope effect expected?

NO	YES
superexchange $J_{AF} \sim -b^2/U$ $\tau = \hbar/U$, U=5eV	doble-exchange charge ordering $T_C \sim zt$ $T_{CO} \sim t/V$, V~0.2

Magnetic state. Bragg I(T)

x=0.8. 0.75. “New” O-series

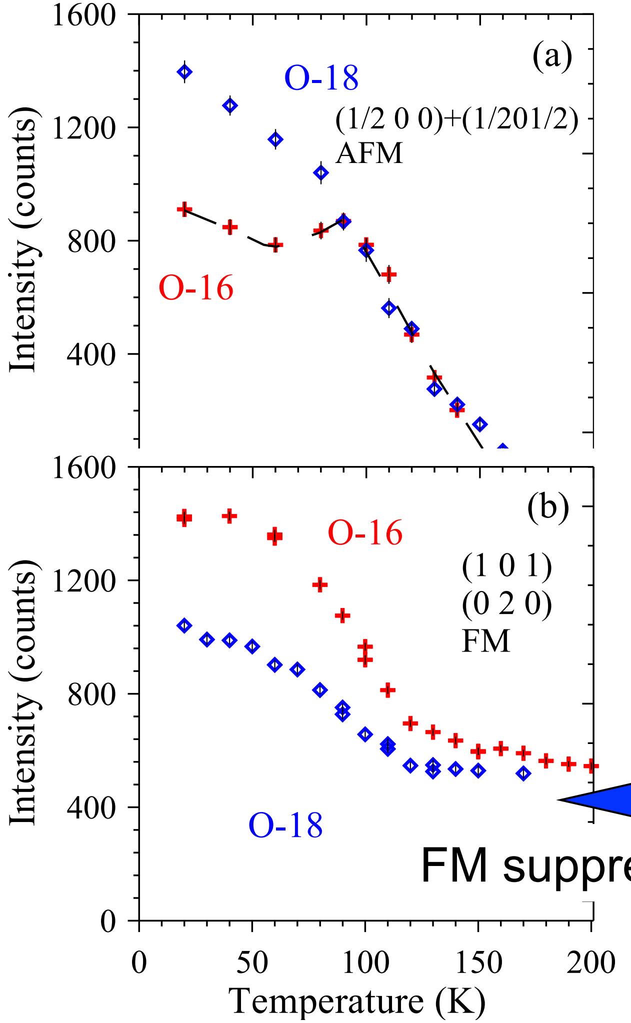

x=0.75. “Old” N-series

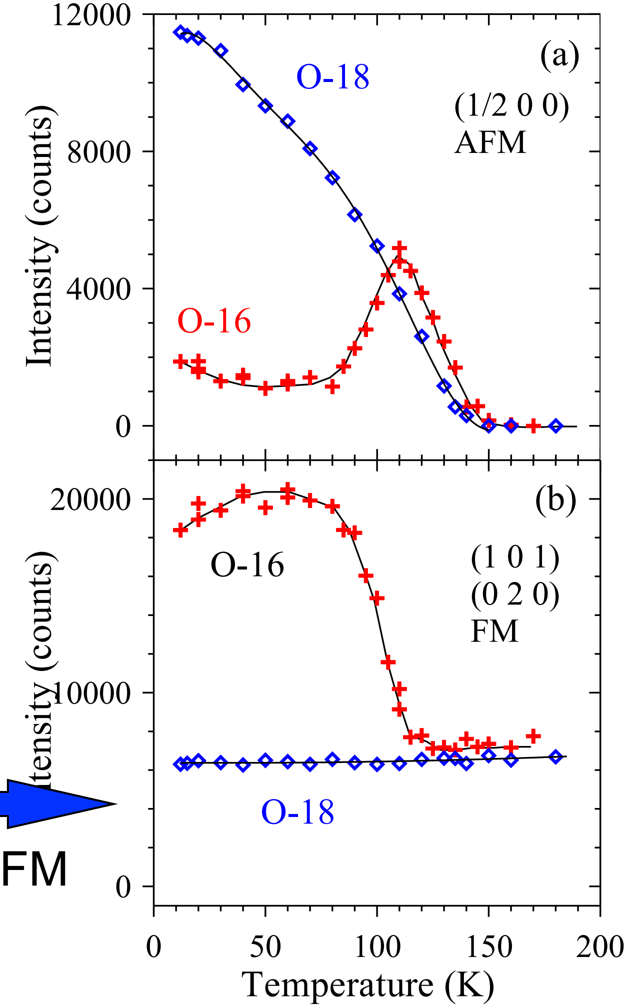

FM suppressed

No FM

What is the difference between the samples

$(La_{1-y}Pr_y)_{0.7}Ca_{0.3}MnO_3$

- **O-series (y=0.2, 0.5, 0.8, 0.75, 0.7, 1.0):** by the solid state synthesis from oxides and carbonates of respective metals. The ^{18}O (>85%) samples as well as the final ^{16}O samples were obtained via respective oxygen isotope exchange at the same conditions

- **N-series**[1]: by the "paper" synthesis starting from aqueous solutions of nitrates of the respective metals (N-series) with the final thermal treatment similar to the O-series

[1] Balagurov et al, *Phys. Rev. B* **60**, 383 (1999); *Phys. Rev. B* **64**, 024420-1 (2001); *Eur. Phys. J. B* **19**, 215 (2001)

Saturated effective magnetic moments in $(La_{1-y}Pr_y)_{0.7}Ca_{0.3}MnO_3$

"New" O-series

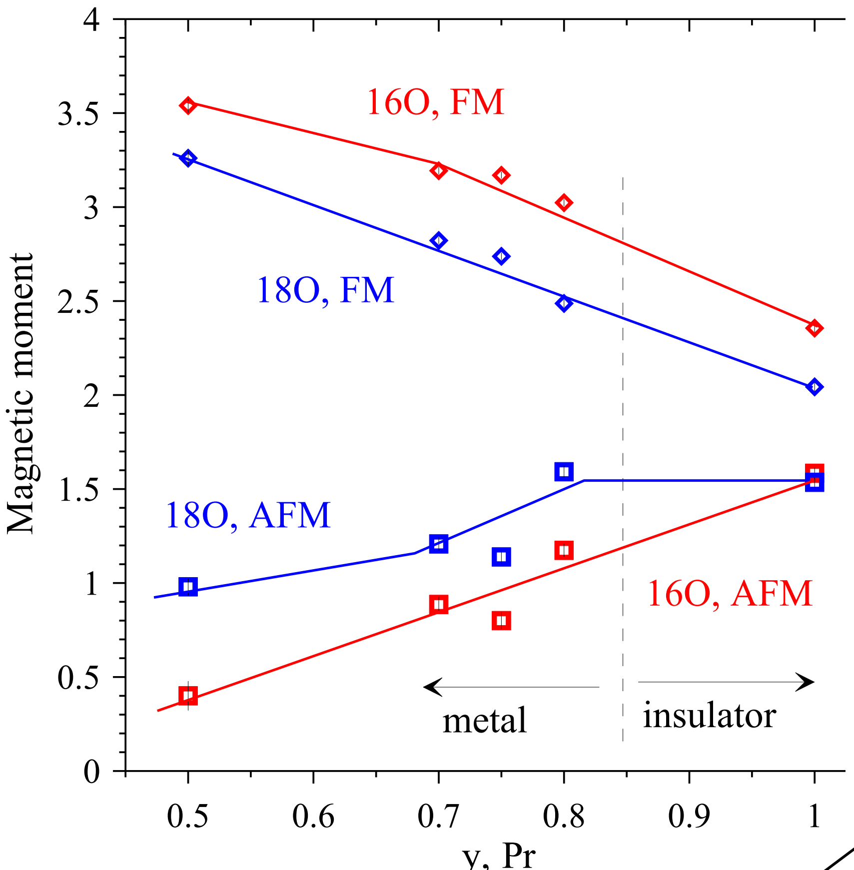

Metallic FM+AFM separated state

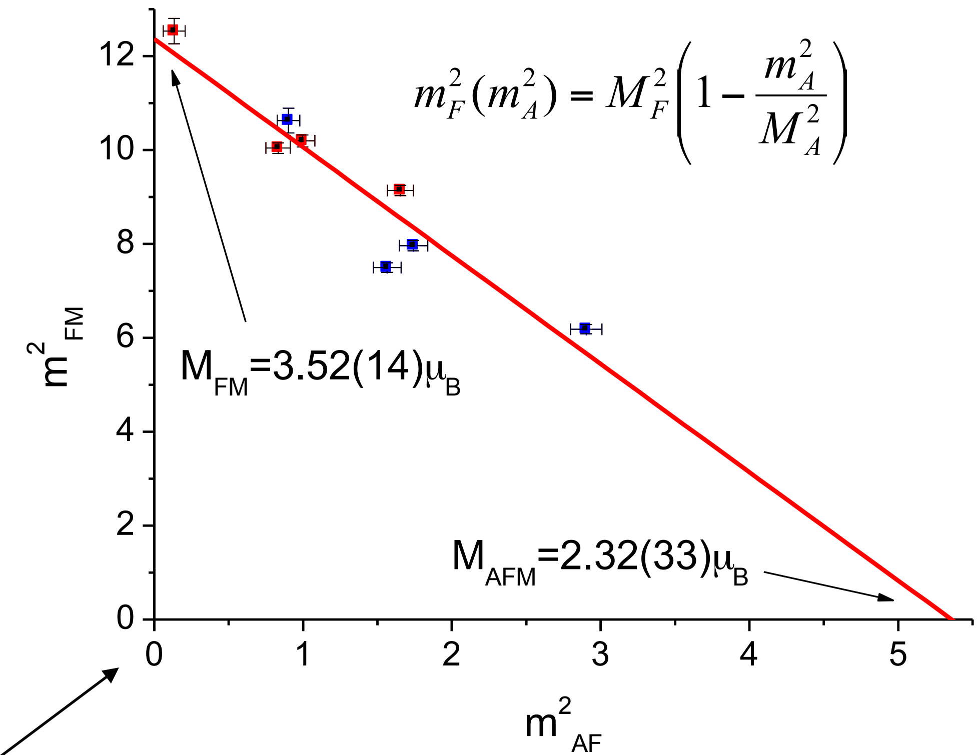

Effective moments

$m_{AF} = \nu^{1/2} M_{AF}$
$m_F = (1-\nu)^{1/2} M_F$

Volume fraction

Saturated effective magnetic moments in $(La_{1-y}Pr_y)_{0.7}Ca_{0.3}MnO_3$

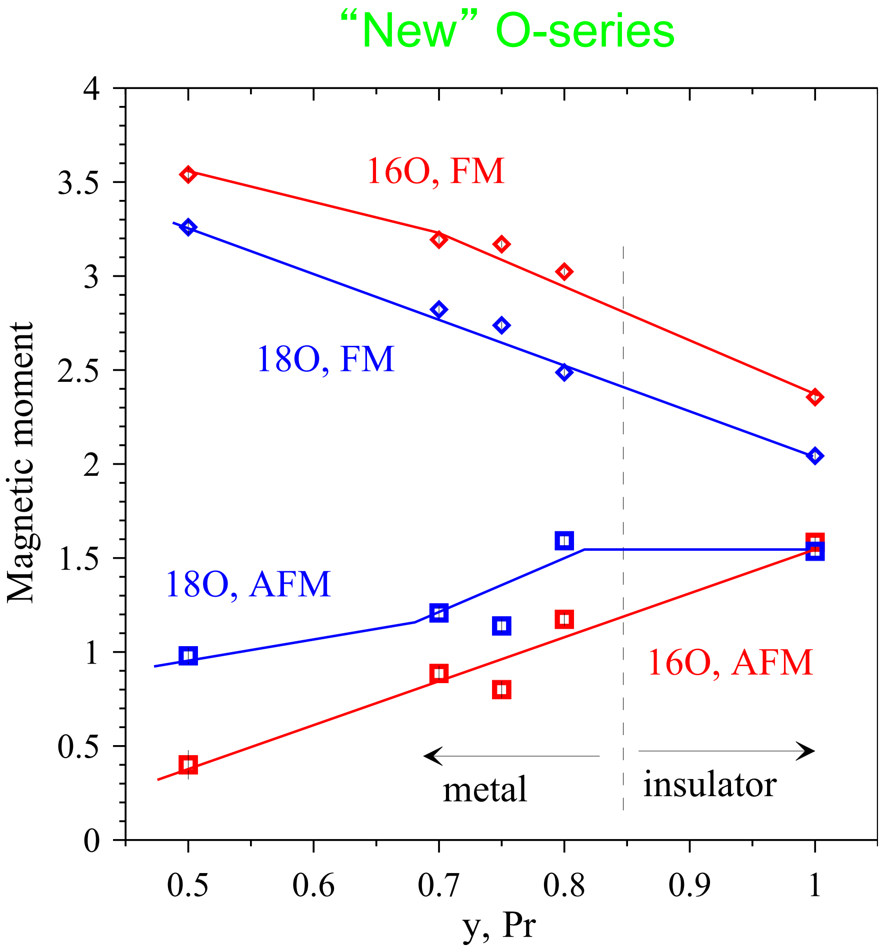

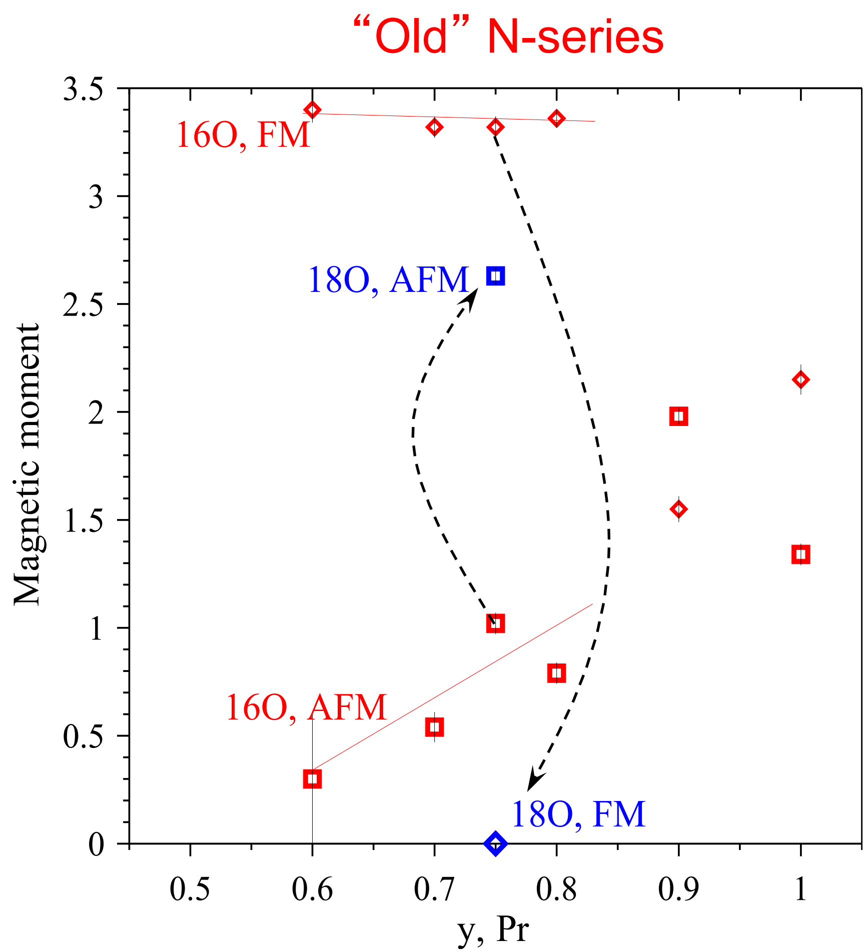

Effective moments

$$\begin{cases} m_{AF} = \nu^{1/2} M_{AF} \\ m_F = (1-\nu)^{1/2} M_F \end{cases}$$

Volume fraction

What is the difference between two series? Crystal structure?

$(La_{1-y}Pr_y)_{0.7}Ca_{0.3}MnO_3$, y=0.75 from both N- and O-series
Pnma, single phase at 290K

SLS X-ray material beamline.
Ultra-high resolution. λ=0.9A

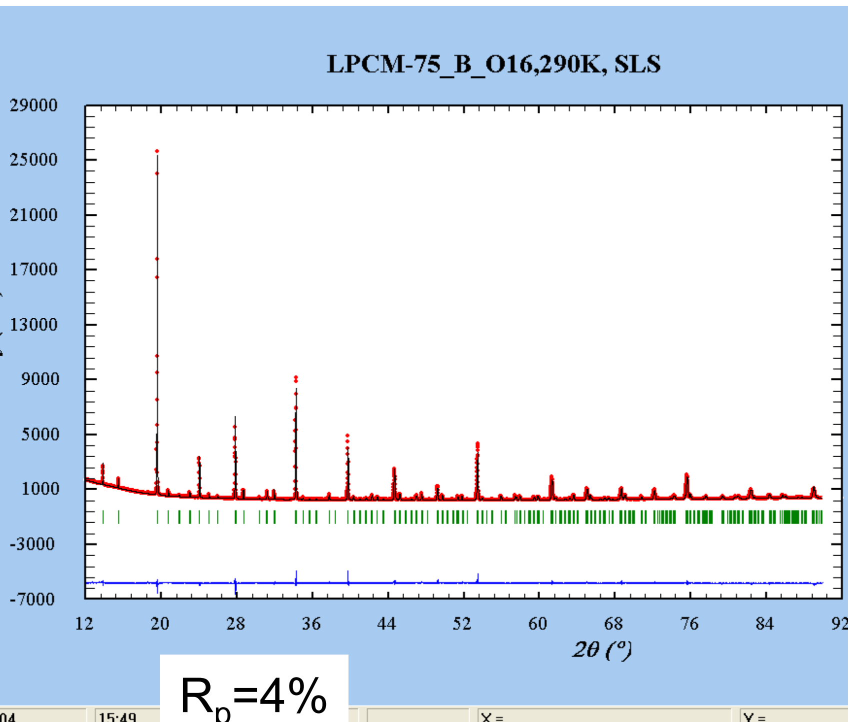

R_p=4%

HRPT/SINQ diffraction pattern.
λ=1.9A, HI-mode

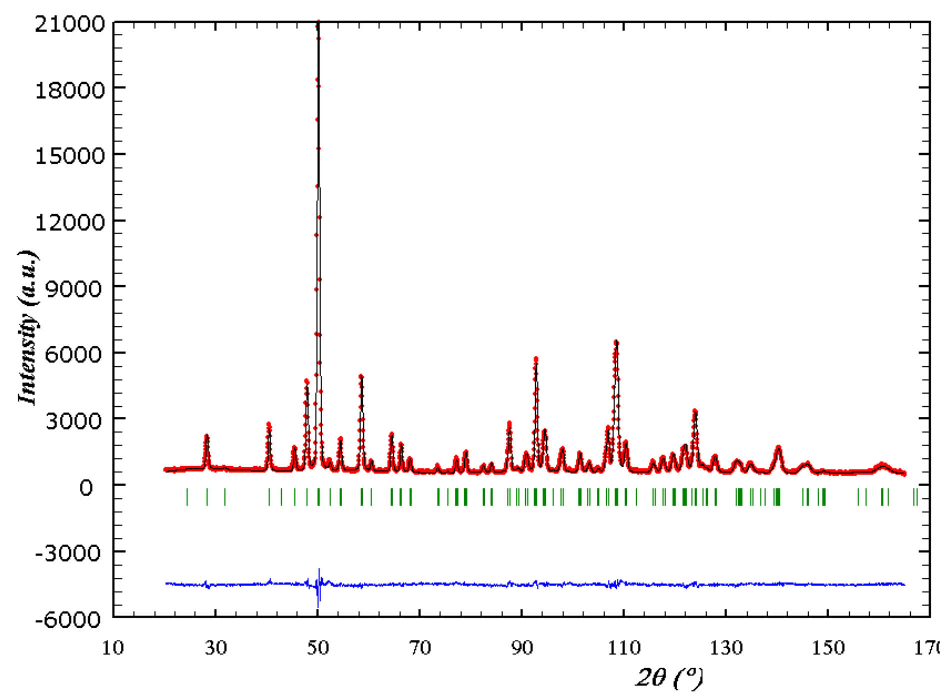

R_p=3.4%, χ^2=3

Comparison of lattice parameters

Pnma

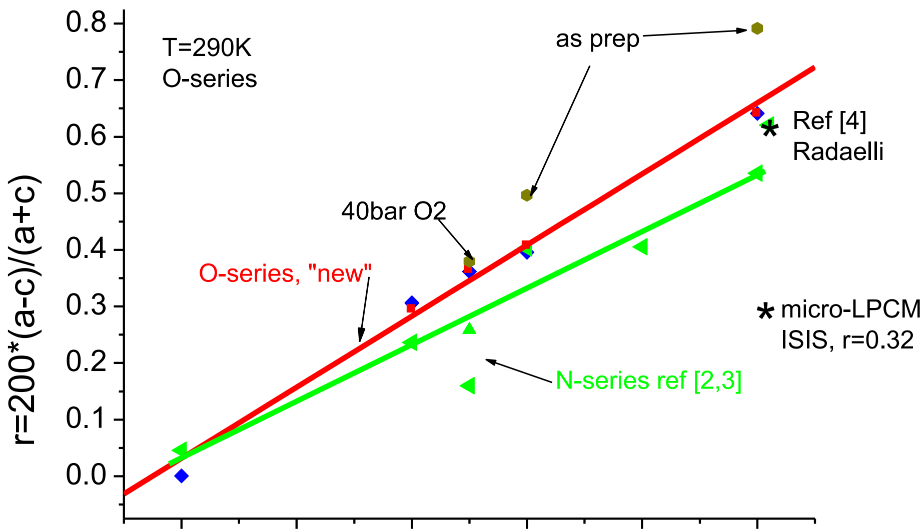

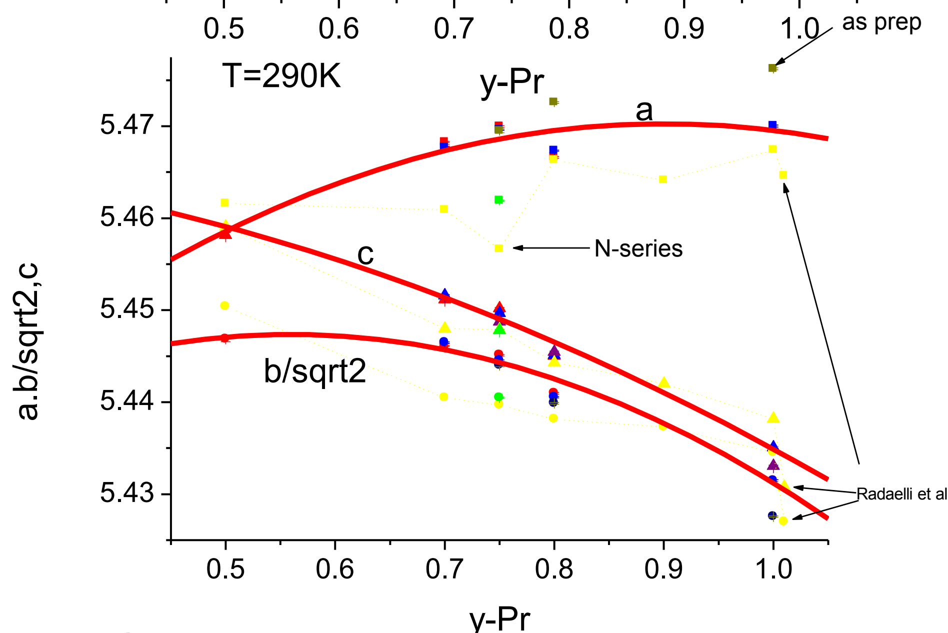

$(La_{1-y}Pr_y)_{0.7}Ca_{0.3}MnO_3$,

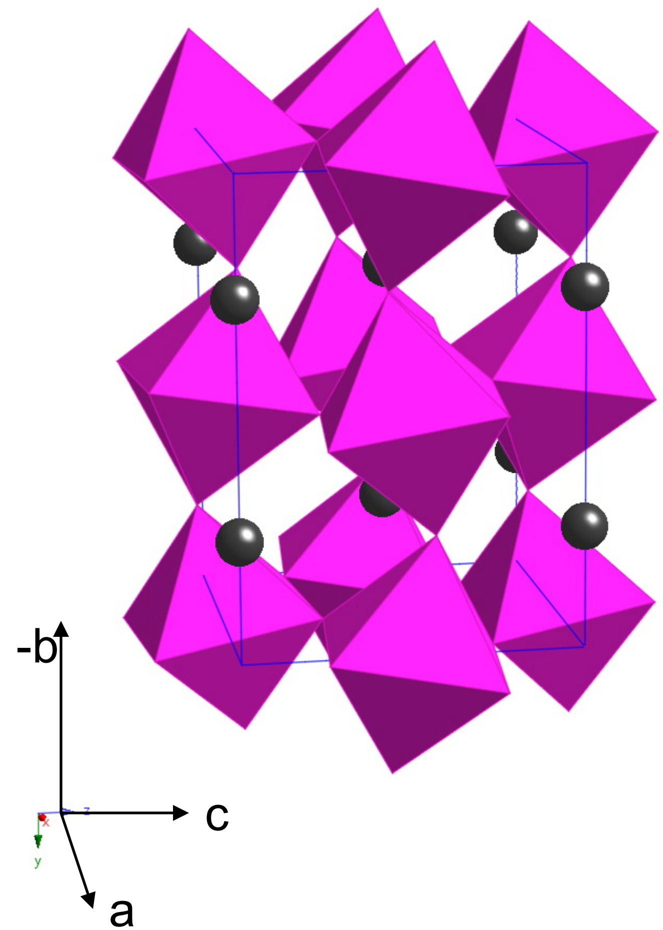

Bragg peak widths. Synchrotron X-ray, HRPT

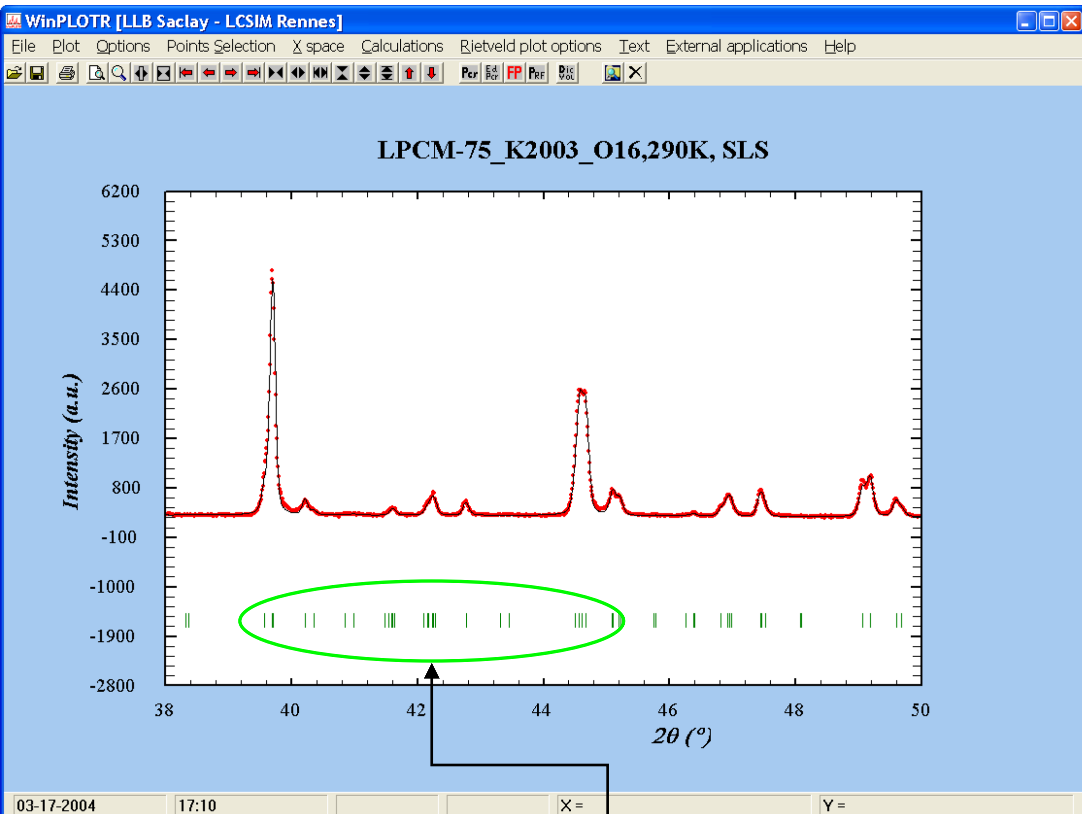

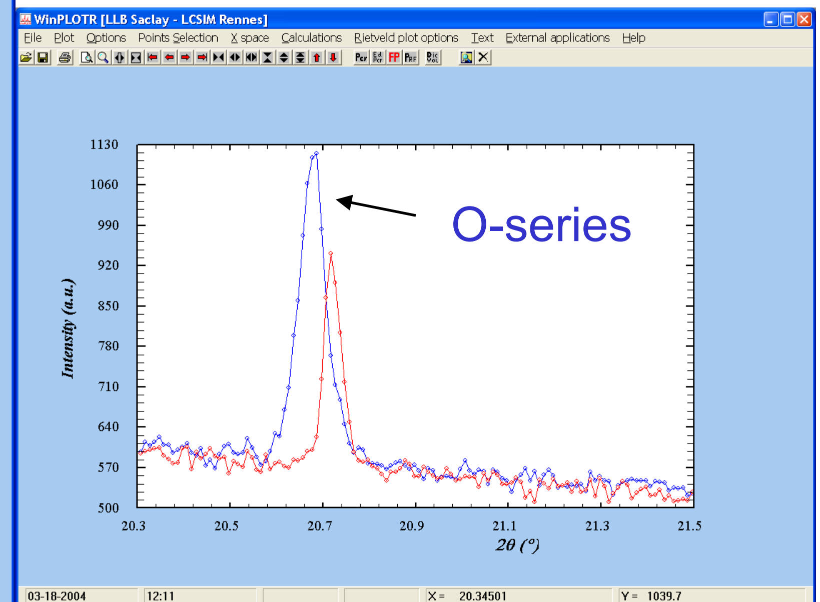

Pseudo-cubic metrics:
Strong peak overlap

Deconvolution of the Bragg-peak widths

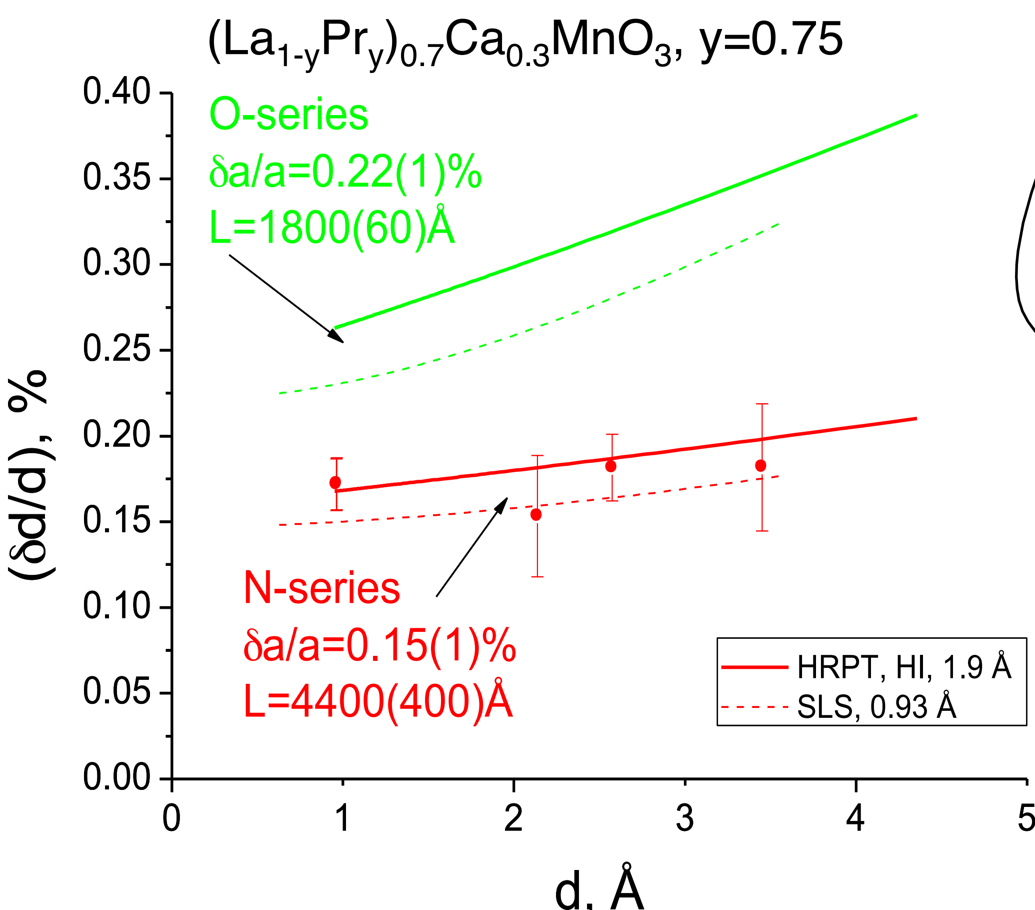

Deconvolution of the pseudo-Voigt Bragg peaks width δ(2θ)="*Cagliotti*" with the instrument resolution function.

<u>Bragg peak width</u>

δd/d= δa/a ⊗ d/L

strain size

PV=Pseudo-Voigt

Gaussian ⊗ Lorenzian

$$\int_{-\infty}^{\infty} G(2\theta-\xi)L(\xi)d\xi$$

$$I_{exp} = \int_{-\infty}^{\infty} PV_{sample}(2\theta-\xi)PV_{instrument}(\xi)d\xi$$

Deconvolution of the Bragg-peak widths. Comparison of HRPT and synchrotron

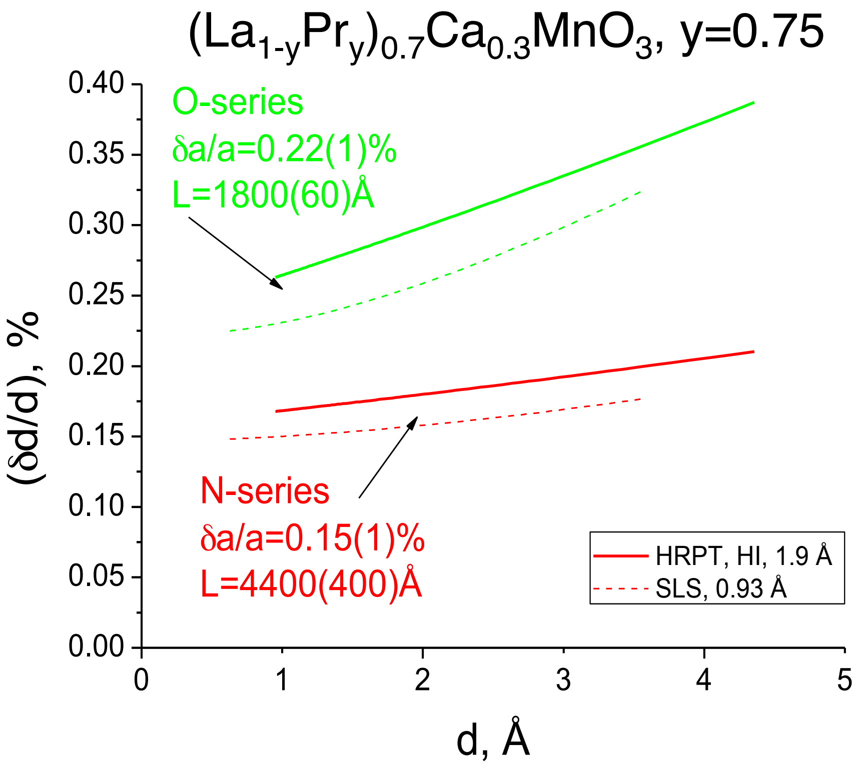

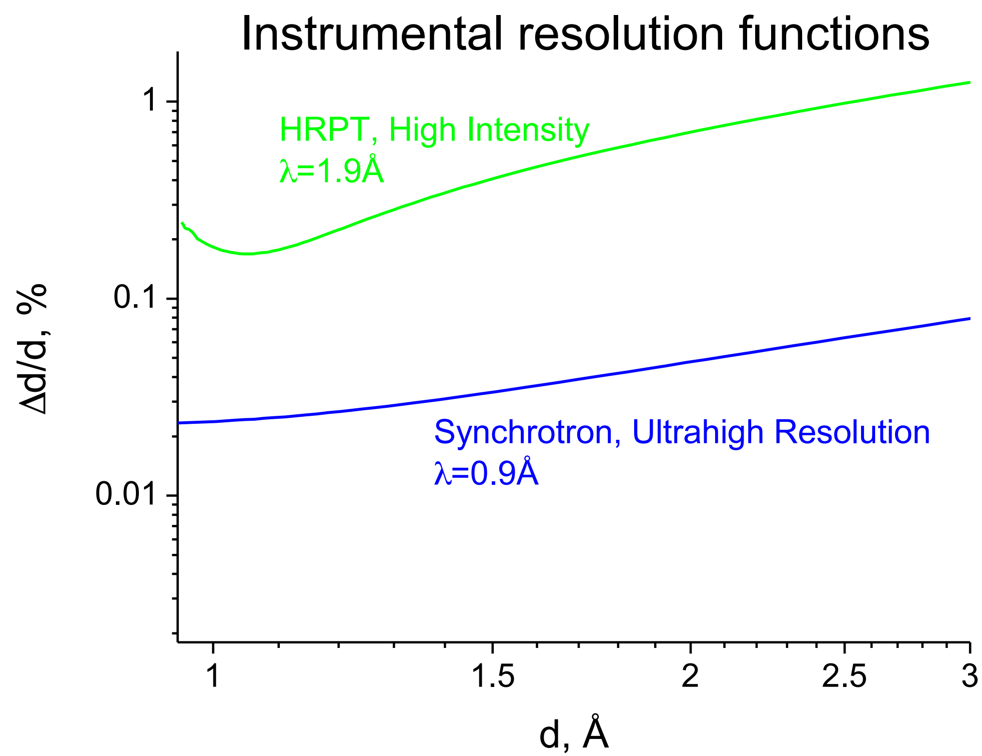

$$I_{\exp}(2\theta) = \int_{-\infty}^{\infty} PV_{sample}(2\theta - \xi) PV_{instrument}(\xi) d\xi$$

Lorenzian ⊗ Gaussian

Isotope effect: conclusions

$(La_{1-y}Pr_y)_{0.7}Ca_{0.3}MnO_3$ (y=0.2-1.0) with ^{16}O/ ^{18}O

1. the $^{16}O \rightarrow ^{18}O$ results in an increase in AFMI fraction at the expense of the decrease in FMM fraction in the phase separated state (y=0.2-0.8).
2. elastic interactions are important for the formation of CO-AFM or/and FM metallic states: the redistribution is suppressed by lattice micro-strains.
3. the FM magnetic moment and T_C are decreased by $^{16}O \rightarrow ^{18}O$ in the ***insulating*** CO state: DE should be involved!

…work in progress…: how do T_C, T_N, T_{CO}, OO, low-T two-phase state are changed by $^{16}O \rightarrow ^{18}O$

Acknowledgements

V.L. Aksenov, A.M. Balagurov, A.I. Beskrovny, Y.V. Obukhov, V.G.Simkin
Frank Laboratory of Neutron Physics, JINR, Dubna

V.N. Duginov
Laboratory of Nuclear Problems, JINR, Dubna

N.A Babushkina, L.M. Belova, A.V. Inyushkin, A.N. Ponomarev, A.N. Taldenkov, A.A. Zakharov
RSC Kurchatov Institute, Moscow

K.Conder, P. Fischer, L. Keller, E. Pomjakushina, D. Sheptyakov
Laboratory for Neutron Scattering, ETH Zurich and PSI, Villigen

O.Y. Gorbenko, A.R. Kaul
Chemistry Department, Moscow State University, Moscow

B. Sh. Bagautdinov, V.Sh. Shekhtman
Institute of Solid State Physics, RAS, Chernogolovka

S. N. Barilo
Belorussian Institute of Semiconductors and Solid State Physics, Minsk

A.Amato, F.Gygax, M. Gutmann, D.Herlach, A.Schenck
PSI, Villigen

The End

Thermal cycling through T_C

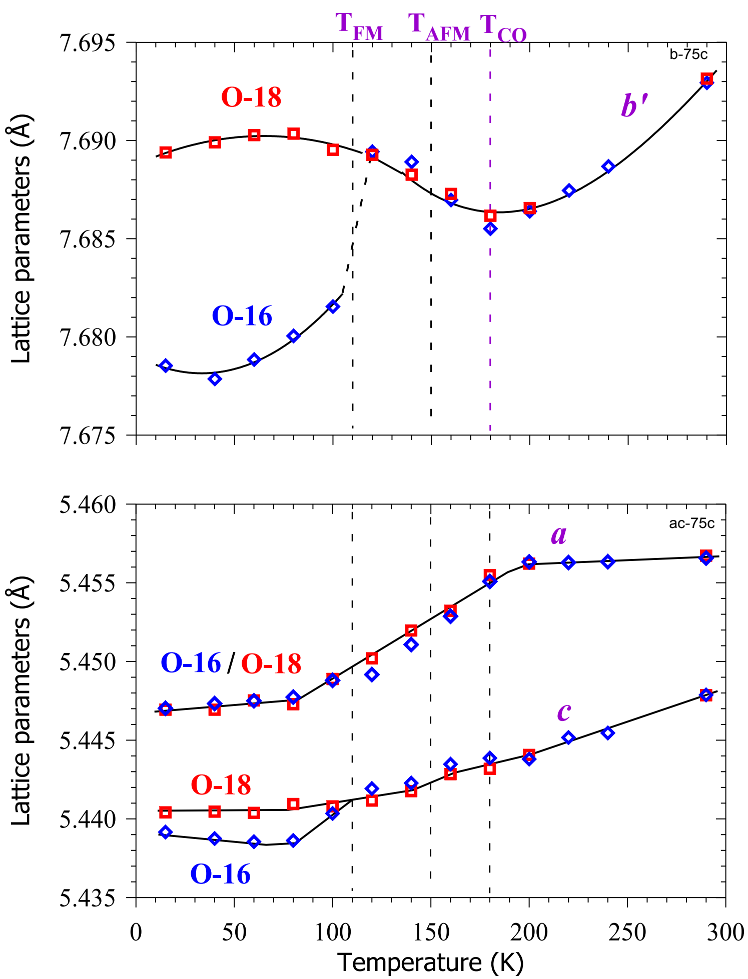

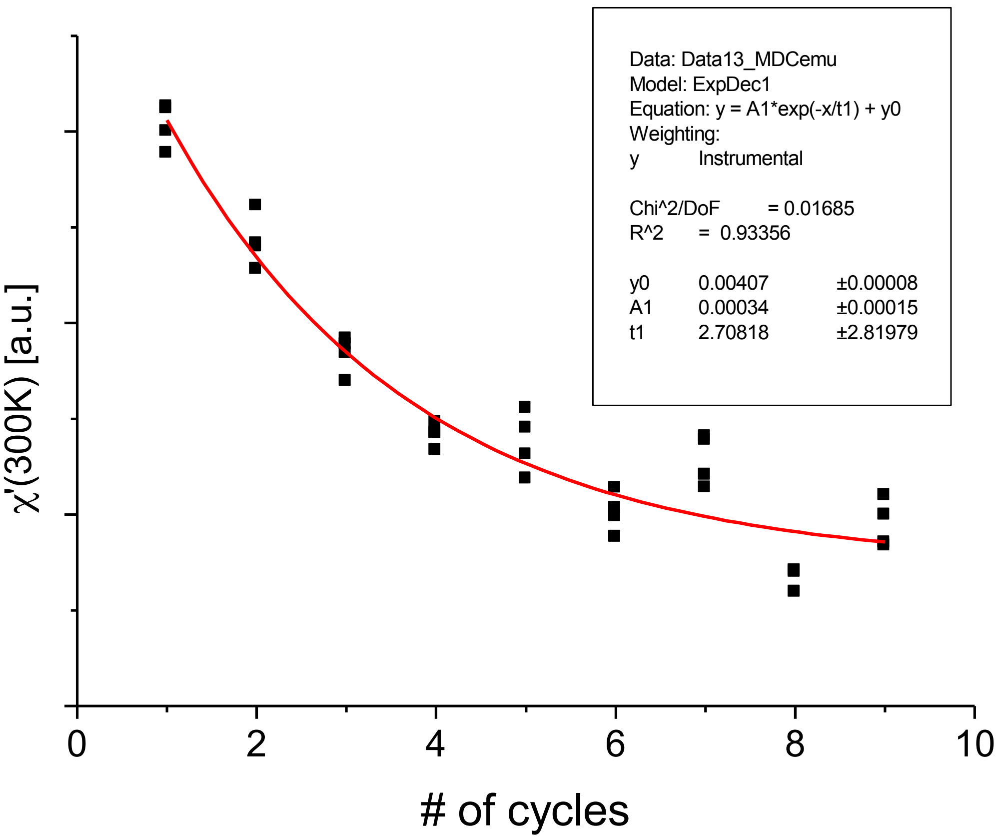

What next?

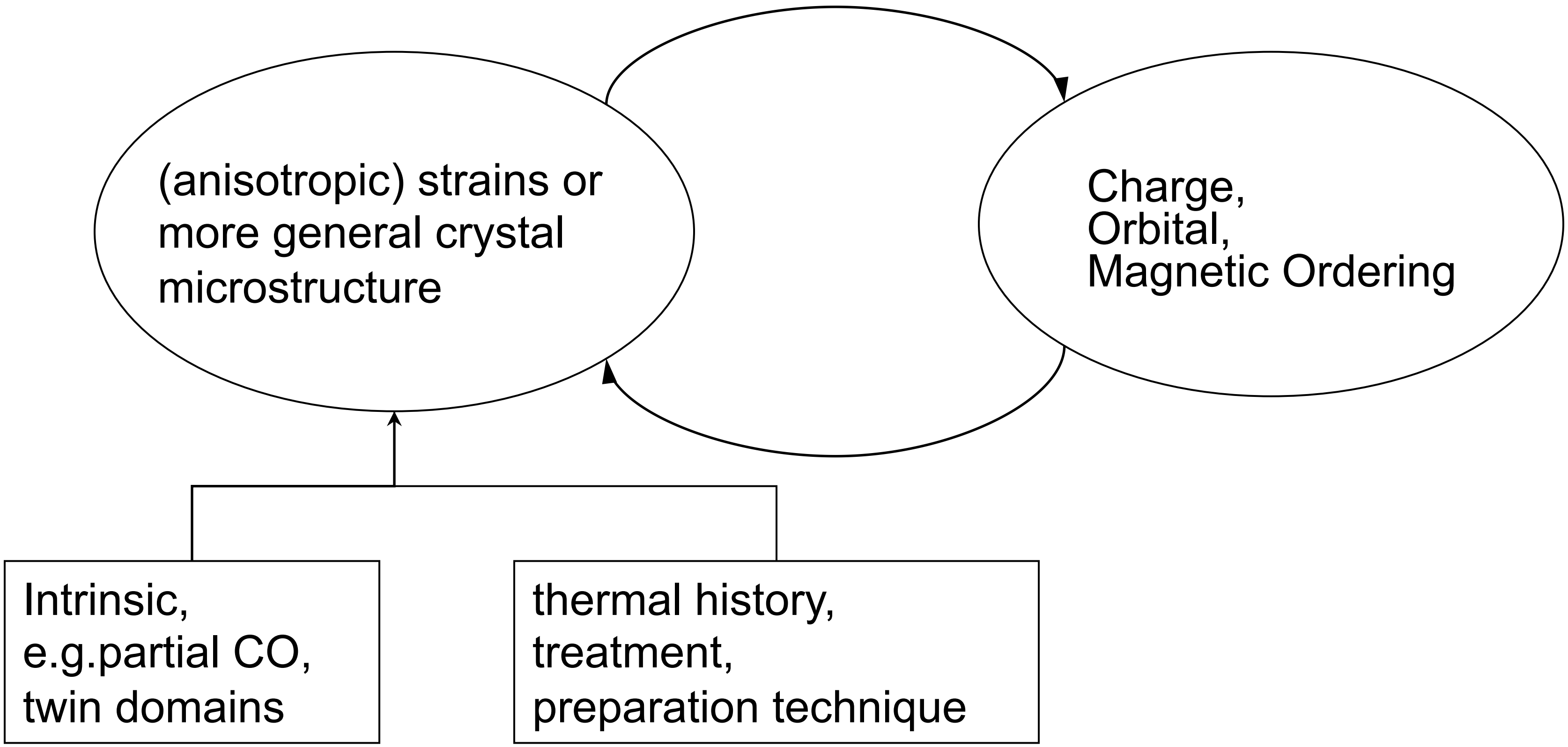
(anisotropic) strains or more general crystal microstructure
Charge,
Orbital,
Magnetic Ordering
Intrinsic,
e.g.partial CO,
twin domains
thermal history,
treatment,
preparation technique

Lattice parameters. *Pnma*

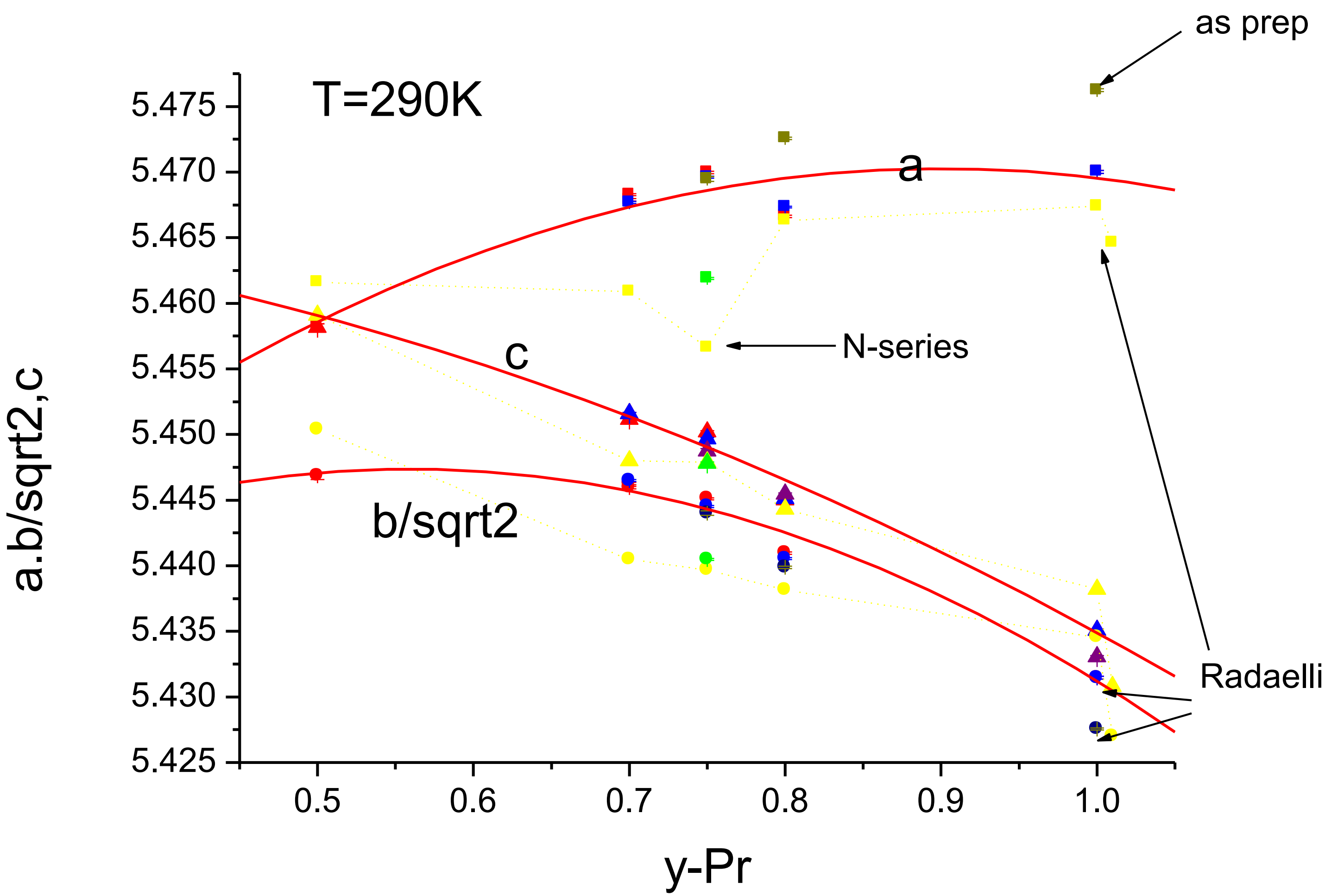

T_C, isotope exponent

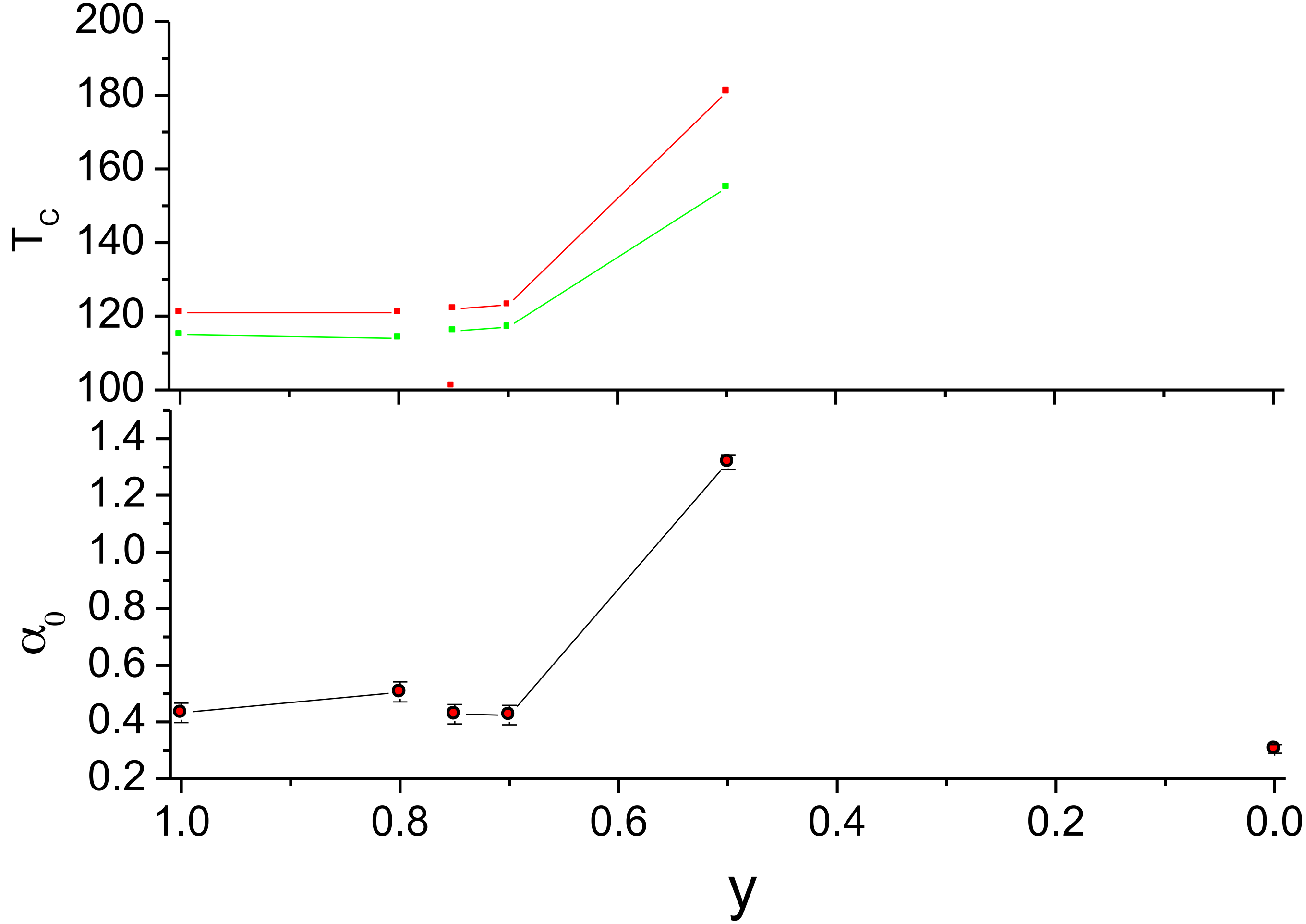

y=0.75

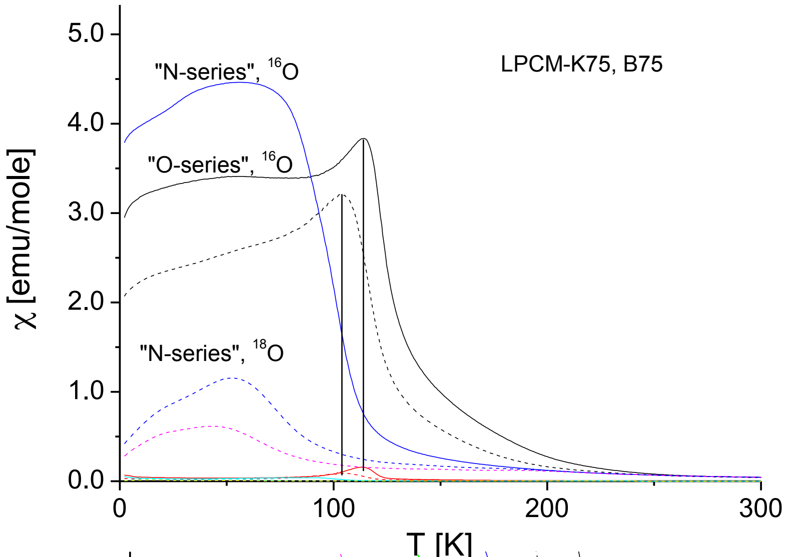

χ [emu/mole]
5.0
4.0
3.0
2.0
1.0
0.0
0
100
200
300
T [K]
"N-series", 16O
"O-series", 16O
"N-series", 18O
LPCM-K75, B75

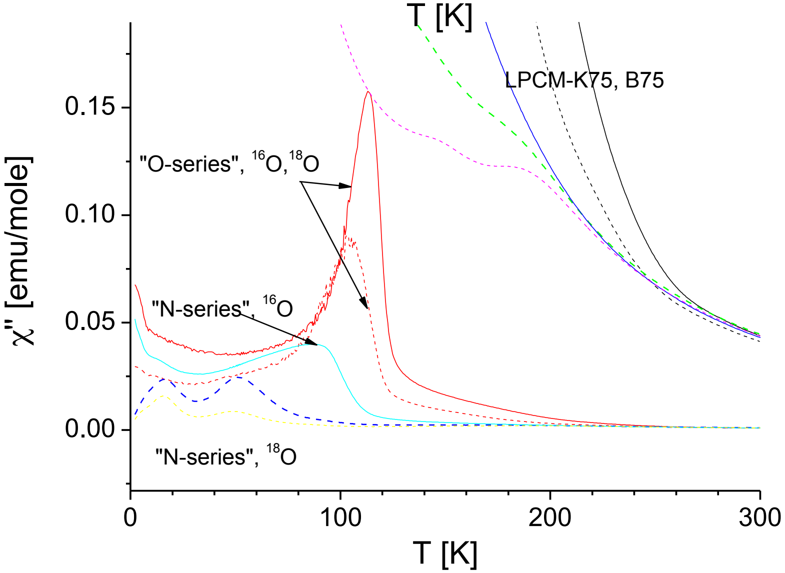

χ" [emu/mole]
0.15
0.10
0.05
0.00
0
100
200
300
T [K]
LPCM-K75, B75
"O-series", 16O,18O
"N-series", 16O
"N-series", 18O

Giant isotope effect in $(La_{1-y}Pr_y)_{0.7}Ca_{0.3}MnO_3$: further studies

- Partial $^{16}O \rightarrow {}^{18}O$ isotope substitution in LPCM-75.
- ^{18}O isotope effect in the whole range of doping y=0.25 – 1.0

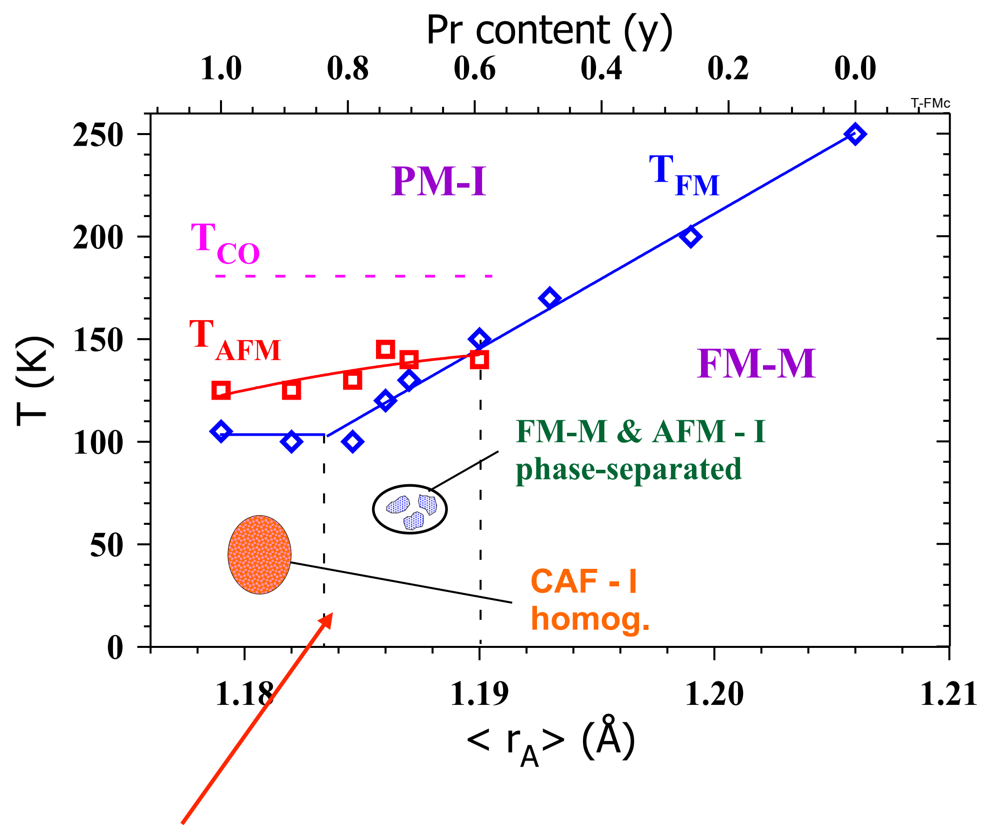

O = ^{16}O (99.7%)

Giant isotope effect near MI-transition @ y=0.8

DMC diffraction pattern. sample=100mg, time=6h

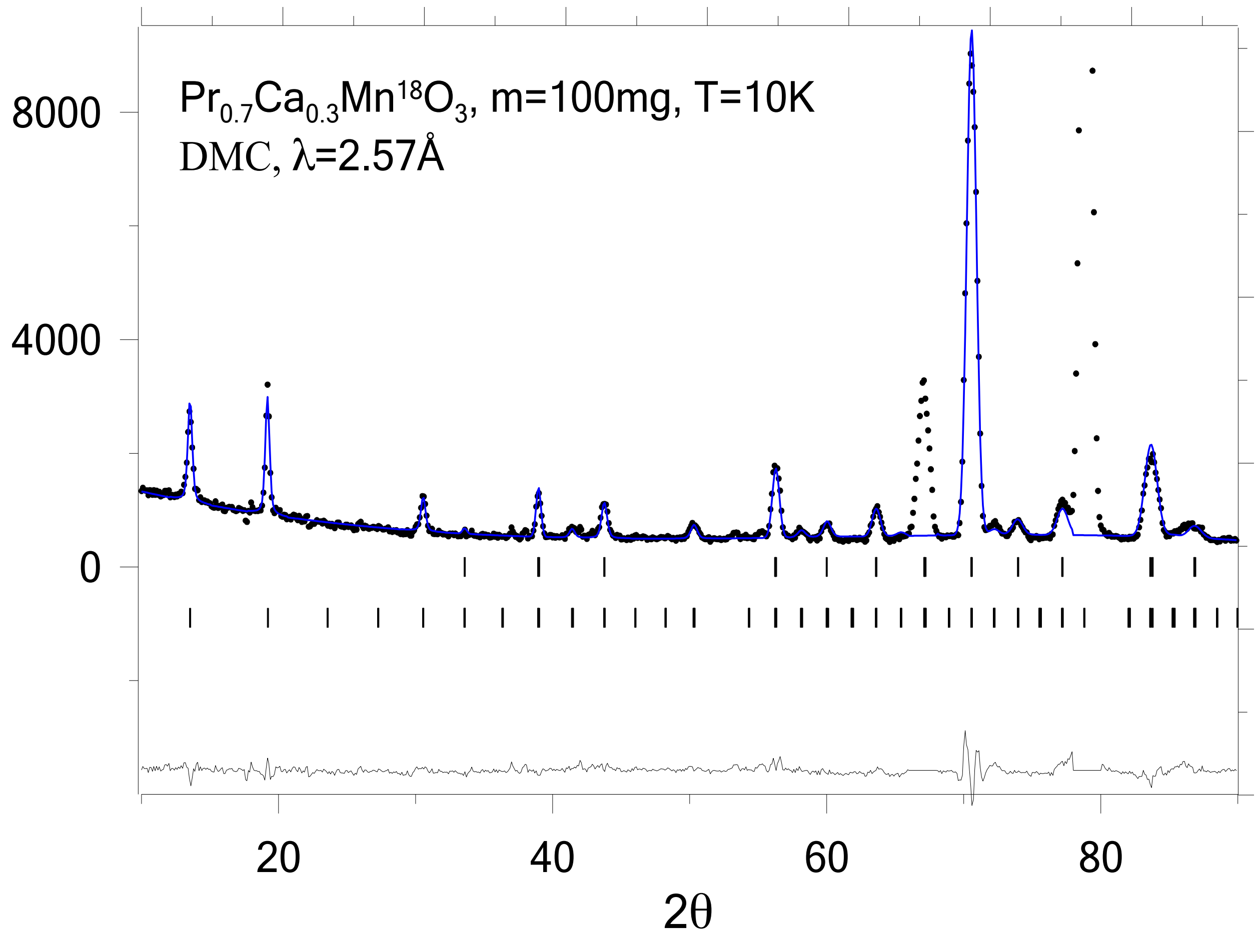

Figure 1: An example of the Rietveld refinement pattern and difference plot of neutron diffraction data (DMC/SINQ) for the ^{18}O-enriched sample of $Pr_{0.7}Ca_{0.3}MnO_3$. The sample mass is about 100 mg. The rows of indexing show nuclear and magnetic phases respectively. Two peaks at $2\theta \approx 66^o$ and 79^o are from Al container, which was used to minimize the background.

$(La_{1-y}Pr_y)_{0.7}Ca_{0.3}MnO_3$ phase diagrams

$O = {}^{16}O$ (99.7%)

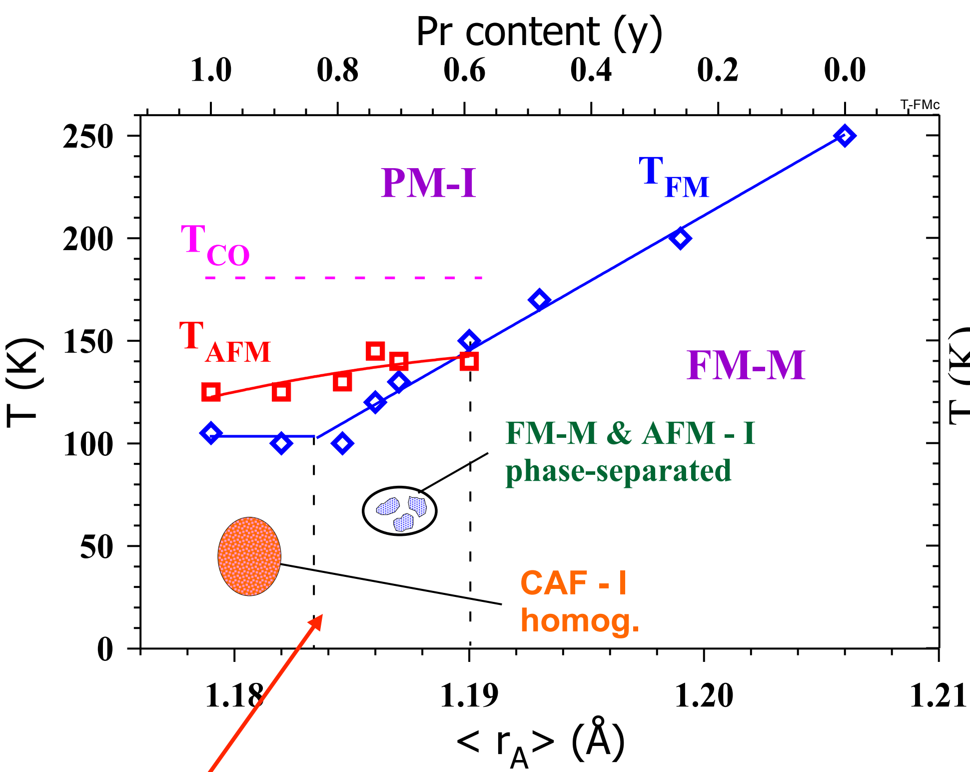

MI-transition @ y=0.8

$O = {}^{18}O$ (75%)

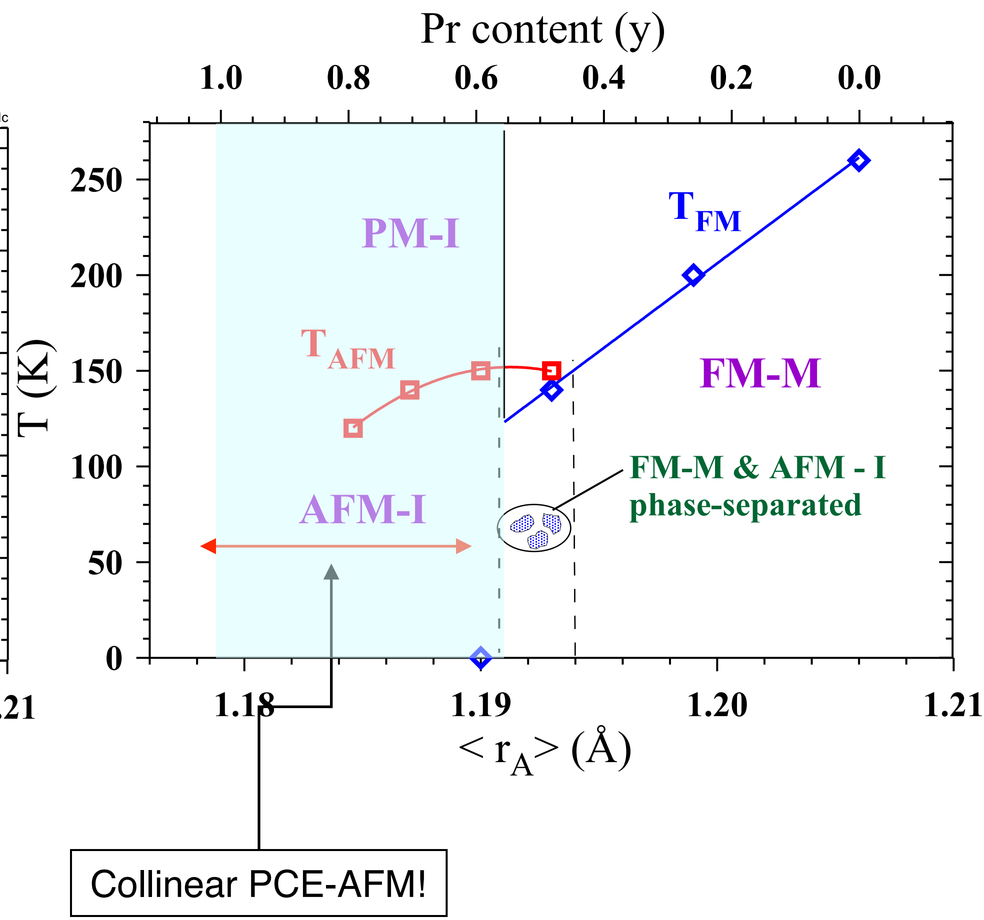

Continuation…

- Isotope effect both in LPCM and in new "giant isotope effect" manganites, e.g. $Sm_{0.45}Sr_{0.55}MnO_3$ and $Sm_{0.50}Sr_{0.50}MnO_3$ --- the Curie temperature (T_C=130K) is decreased by 20K and >100K, respectively
- Layered manganites - brownmillerites with intermediate/mixed Mn valence, fluorination
- New hexagonal manganites $Sr_{4/3}(Mn,Cu)O_3$ (collab. with Antipov et al)

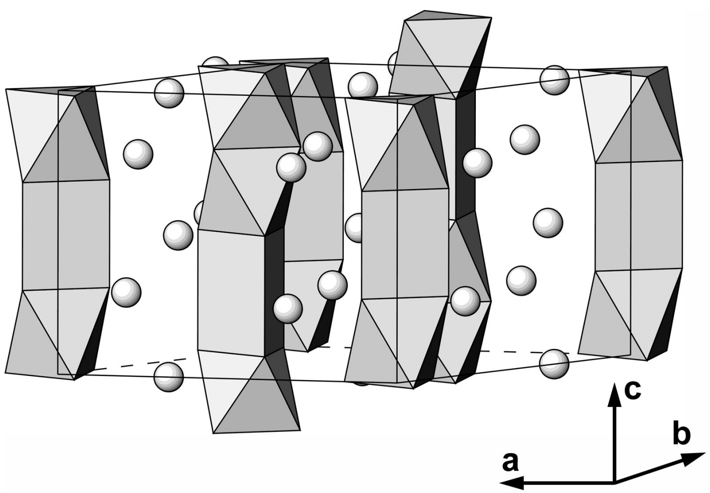

M-I transition in $(La_{1-y}Pr_y)_{0.7}Ca_{0.3}MnO_3$

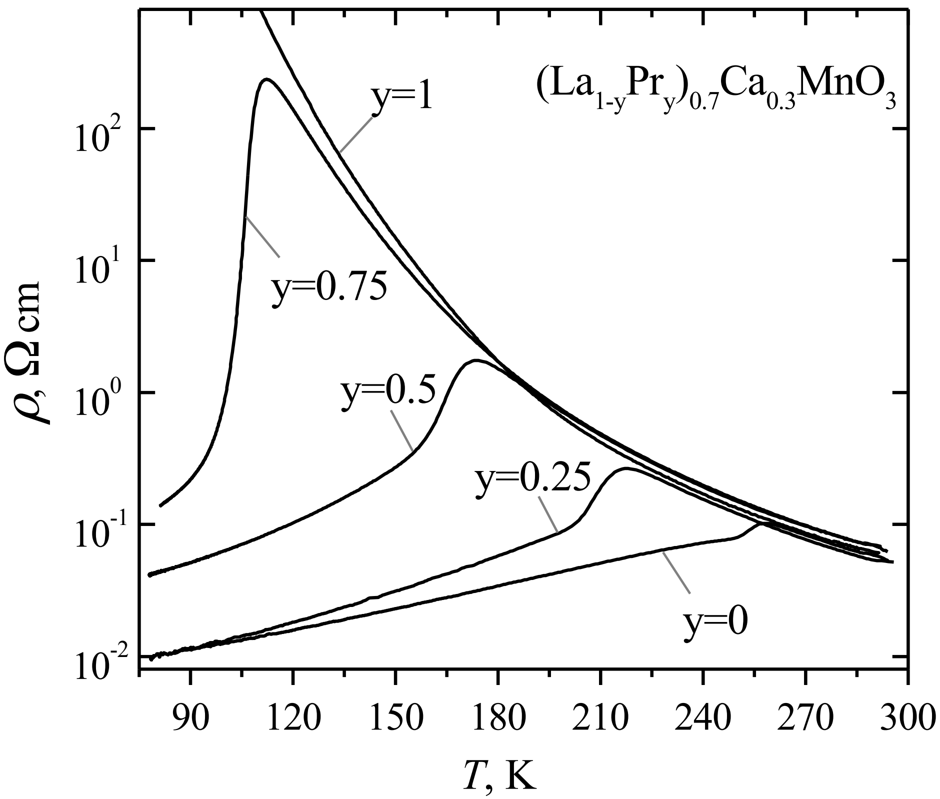

Low temperature magnetic moments

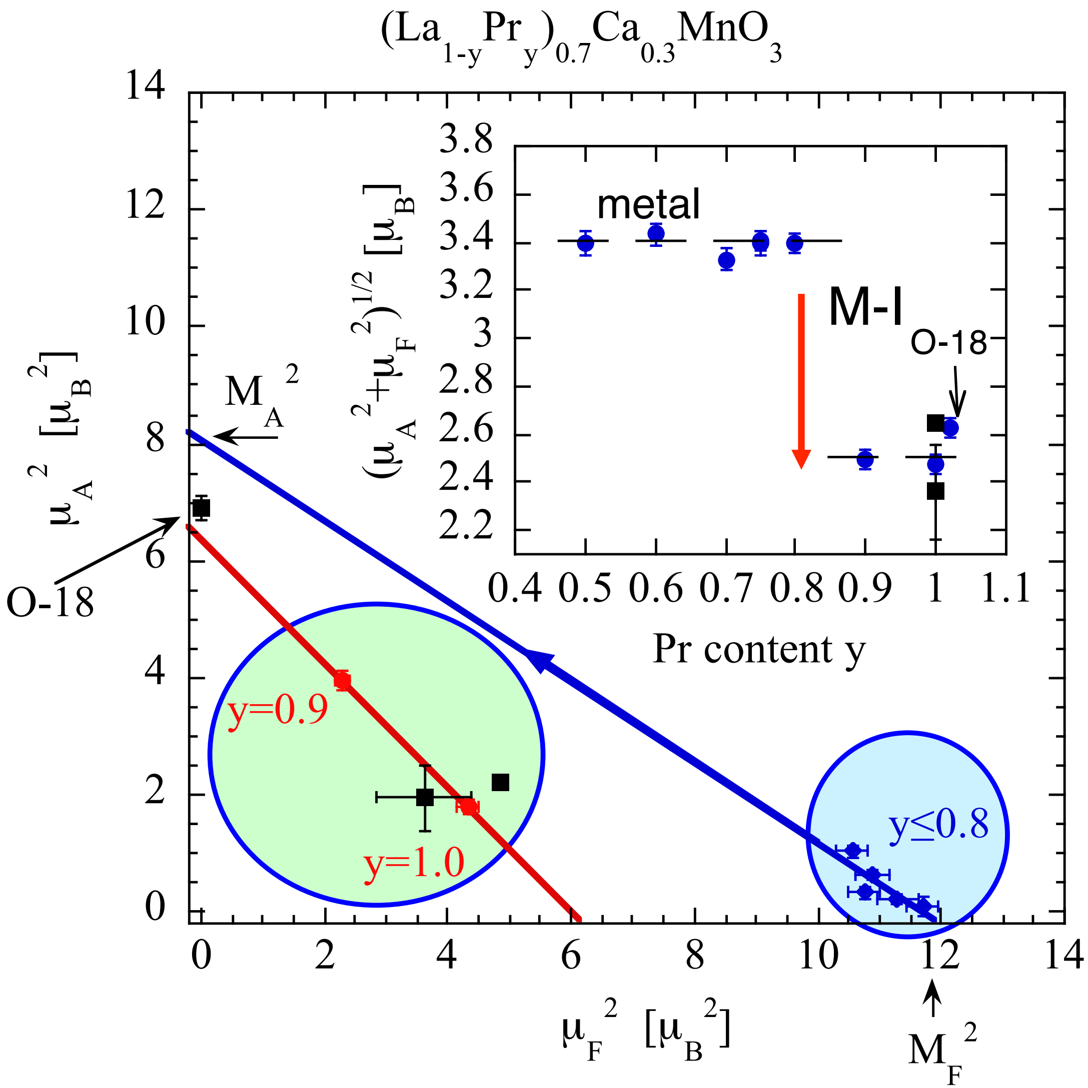

uSR in LPCM-O18/O16

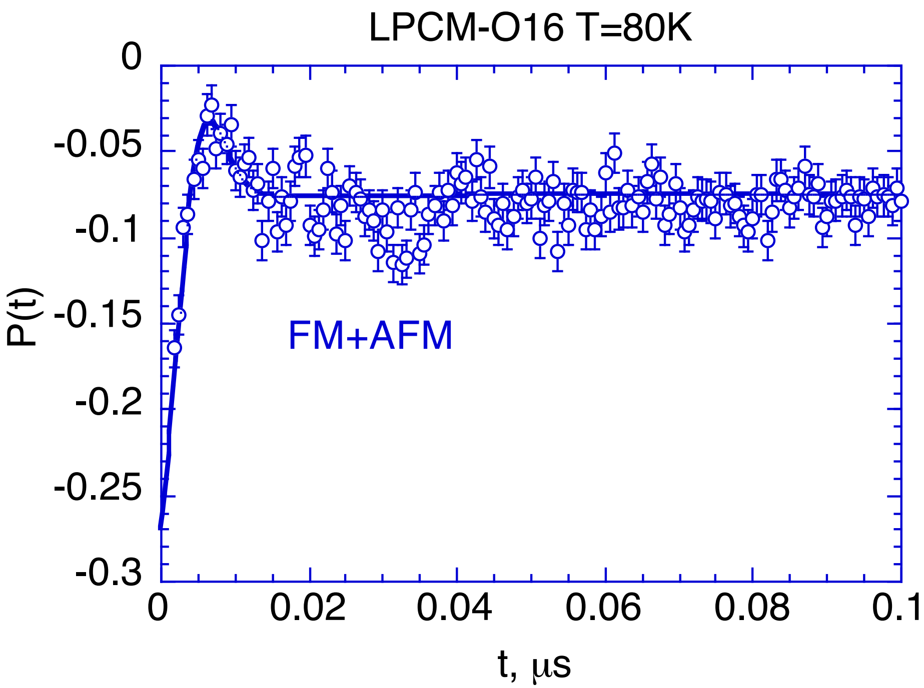

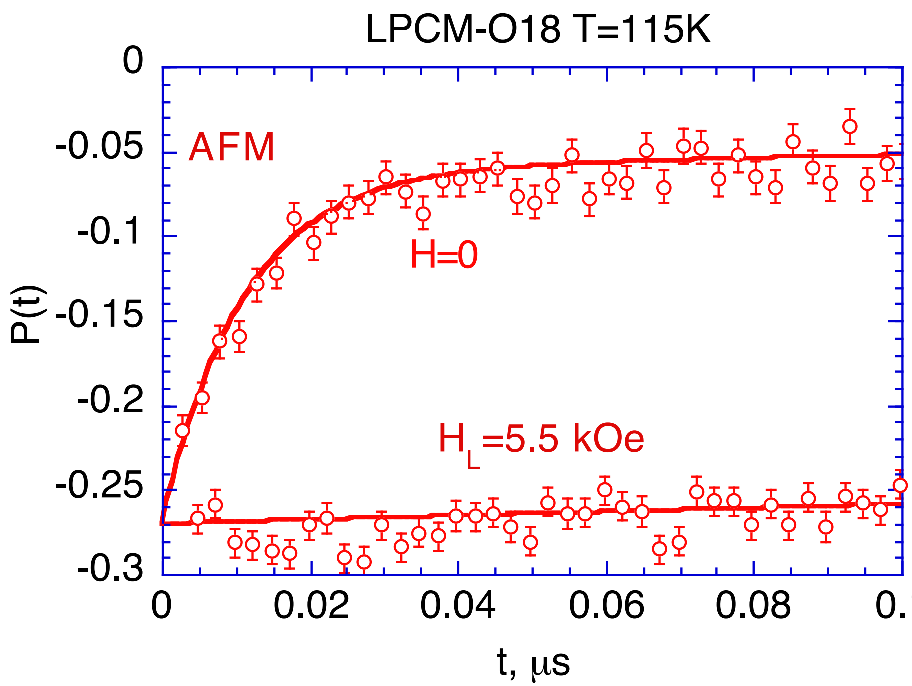

Why A_2MnGaO_{5+x} (A=Sr, Ca)? Manganese oxides with possible CMR

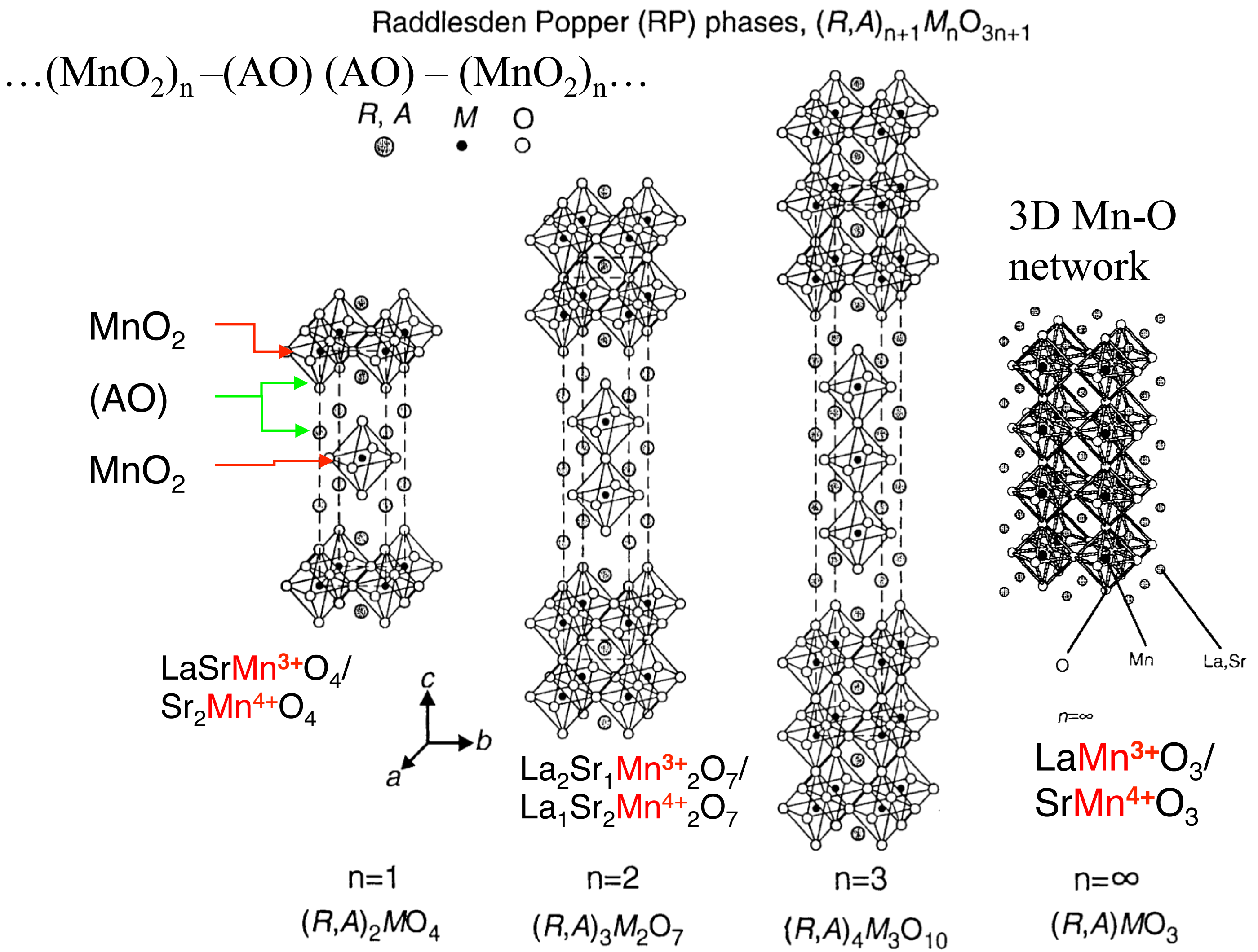

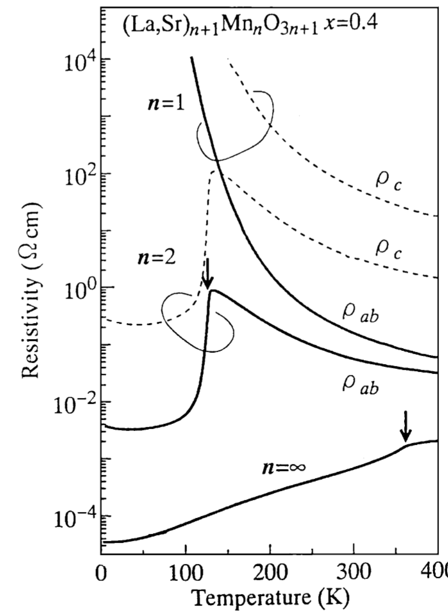

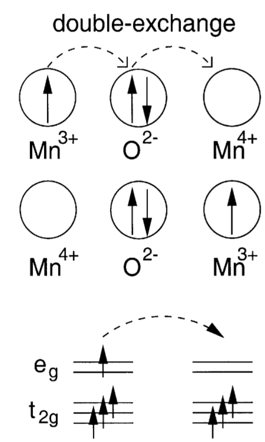

Three buffer (AO) layers: brownmillerite structures of A_2MnGaO_{5+x} (A=Sr, Ca)

x=0, Mn^{3+} — *Pnma, Ima2, Imcm*

x=0.5, Mn^{4+} — *P4/mmm, …*

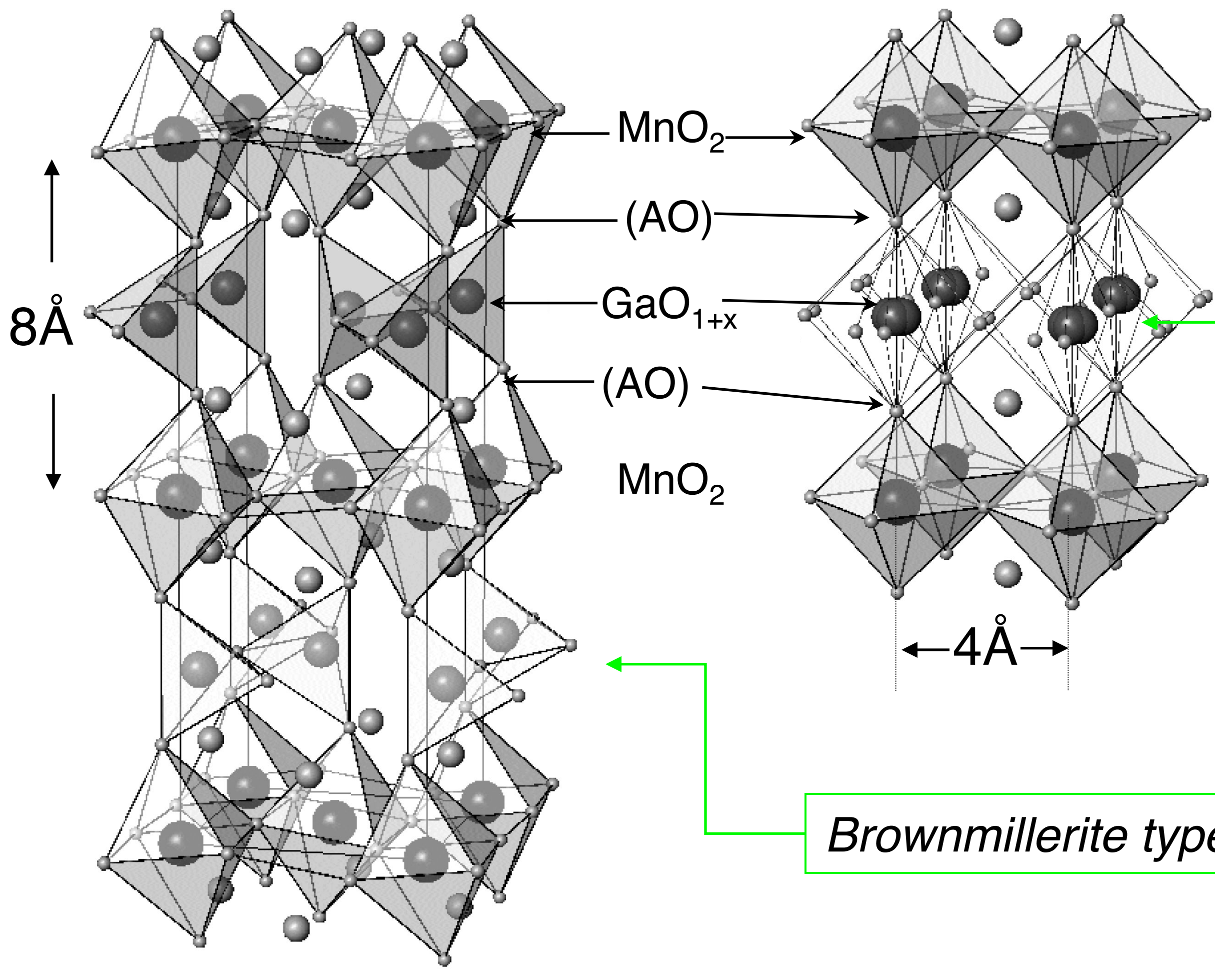

There is space for extra oxygen in GaO_{1+x}-layers

Brownmillerite type of crystal structure

Classification of magnetic structures in manganites

pseudo-perovskite (cubic) crystal structure

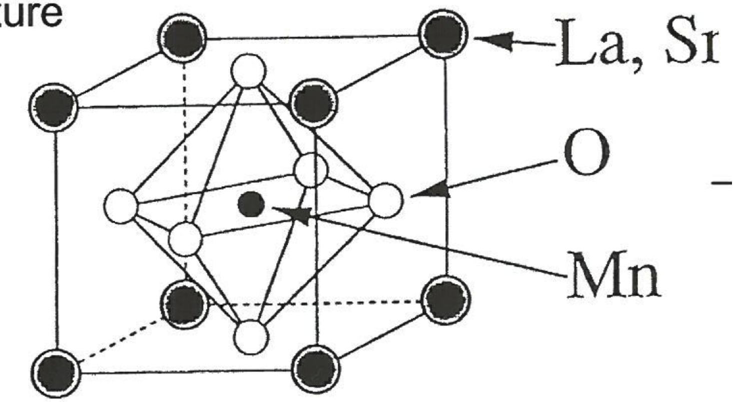

(a)

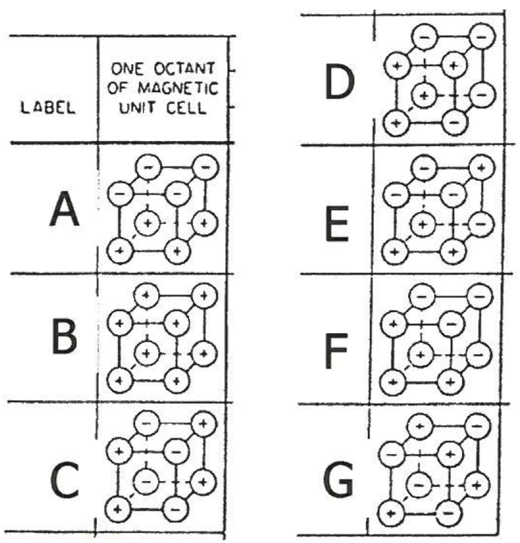

(b)

distortion/tilting of MnO_6 octahedra

- Orthorhombic (e.g Pnma)
- Rombohedral (R-3c)
- Monoclinic P21/m

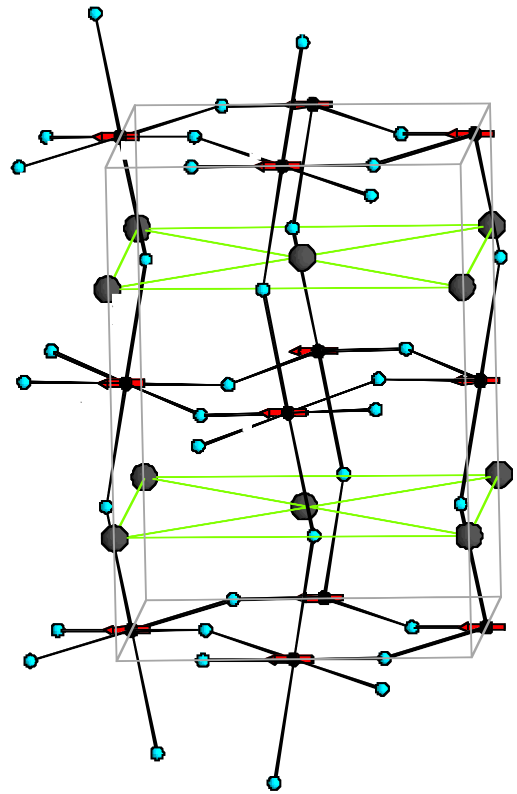

Cation disorder effects in CMR perovskites

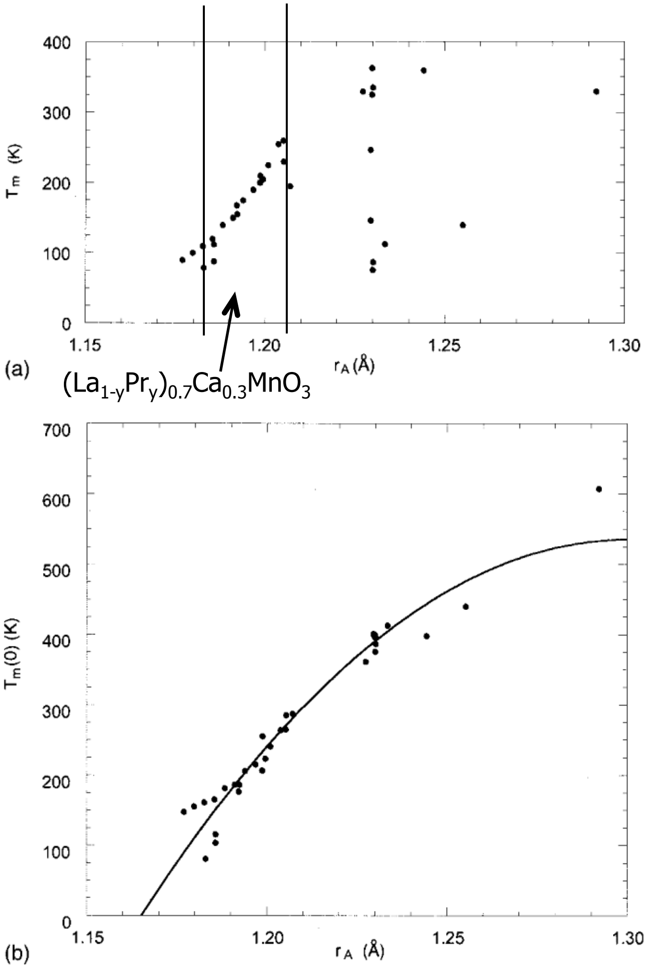

Effect of disorder due to size differences between A-cations in $A_{0.7}A'_{0.3}MnO_3$ (A=La,Pr,Nd,Sm;A'=Ca,Sr,Ba):

- for $\langle r_A \rangle < 1.22$Å T_C does not depend on σ
- for $\langle r_A \rangle > 1.22$Å $\Delta T_c \sim \sigma^2$ K/ ΔS_m. Disorder acts as preformed JT distortion promoting localization of e_g-electron

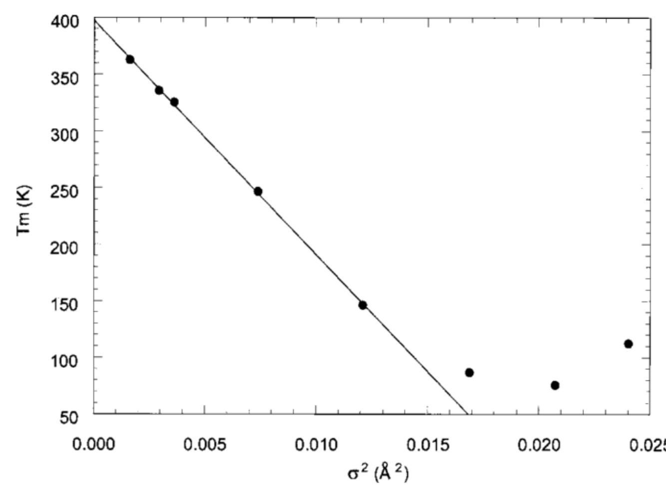

From L.Rodrigez-Martinez and P.Attfield, PRB 1996

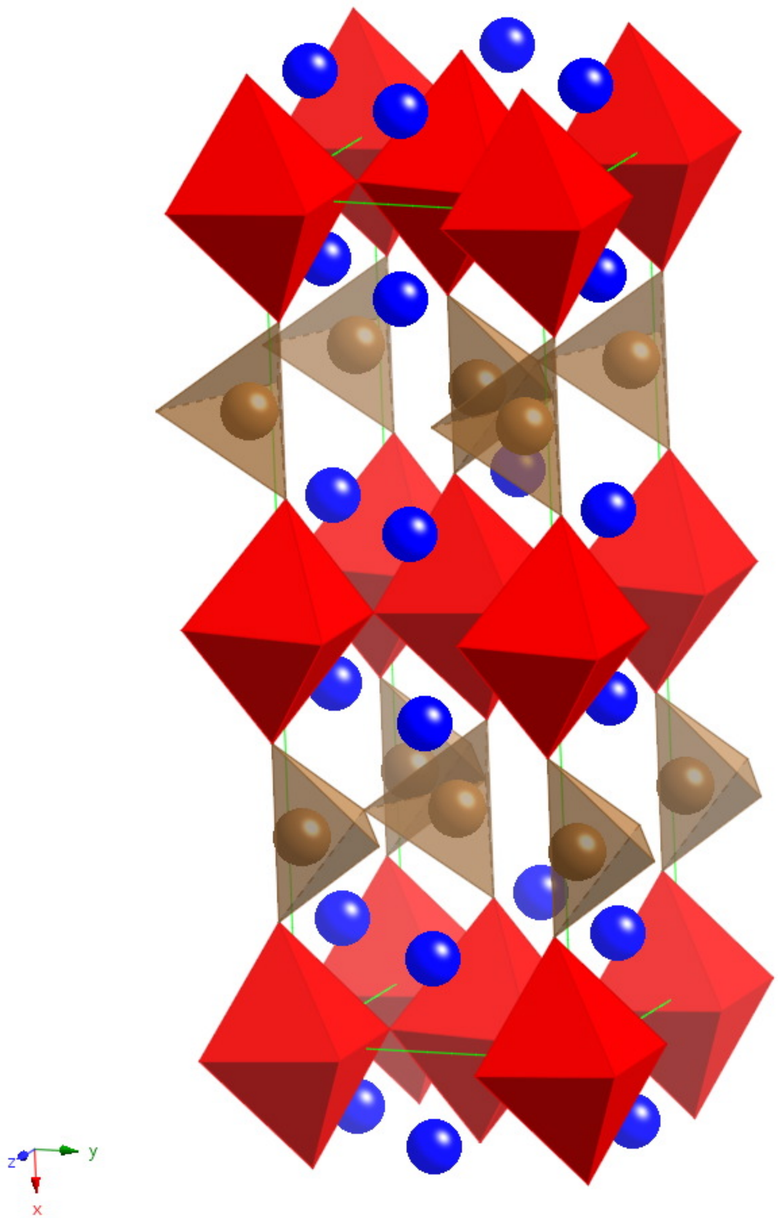
z
y
x

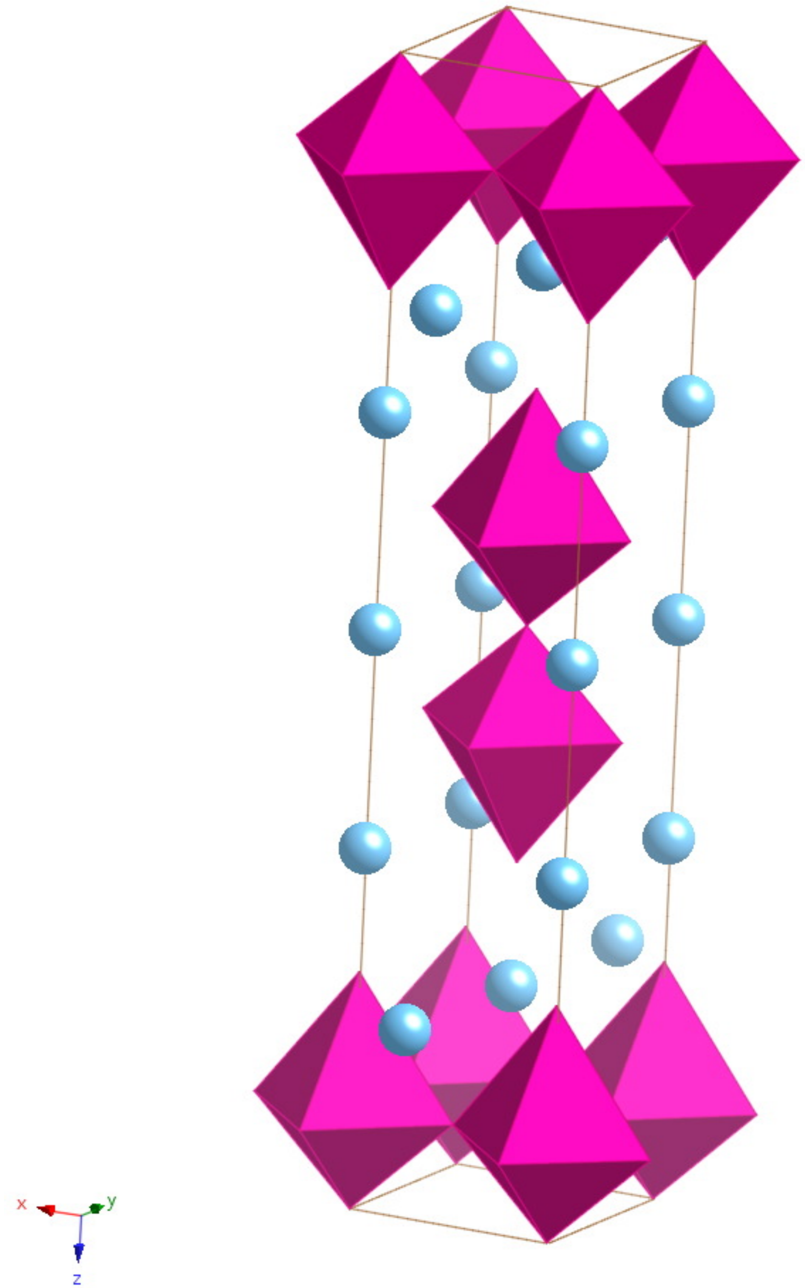
x
y
z

Energy scales in manganites

1. On site Coulomb U_0=3.5eV, 5.2eV in (La,Ca)MnO_3. Δ=3eV ($CaMnO_3$)
2. J_H=2 eV
3. 10Dq=1-2 eV
4. t=0.2-0.5 eV
5. E_{JT}=0.25 eV
6. J_{AF}=0.1t; $J_{AF}\sim t_\pi^2/U$
7. Intersite Coulomb U_1=0.3eV

r_A dispersion in $(La_{1-y}Pr_y)_{0.7}Ca_{0.3}MnO_3$

Reduced variance $\sigma/\delta r_A$ vs. Pr concentration y

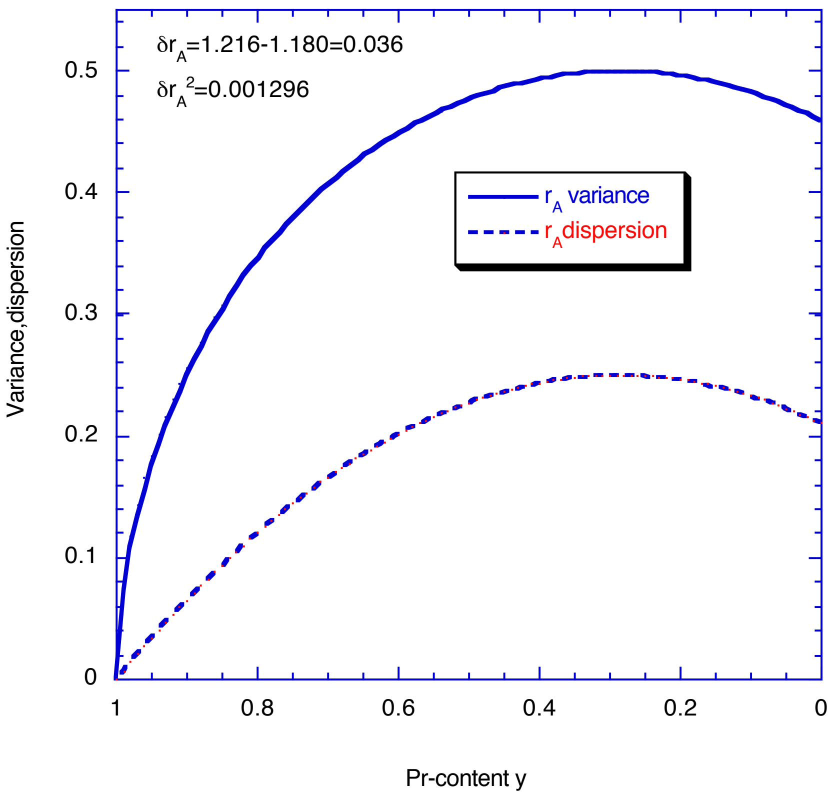

$\sigma = \delta r_A [0.7(1-y)(0.3+0.7y)]^{1/2}$

$\delta r_A = r(Pr) - r(La)$, $r(Ca) = r(Pr)$

Maximal $\sigma^2 = 0.00032 Å^2$

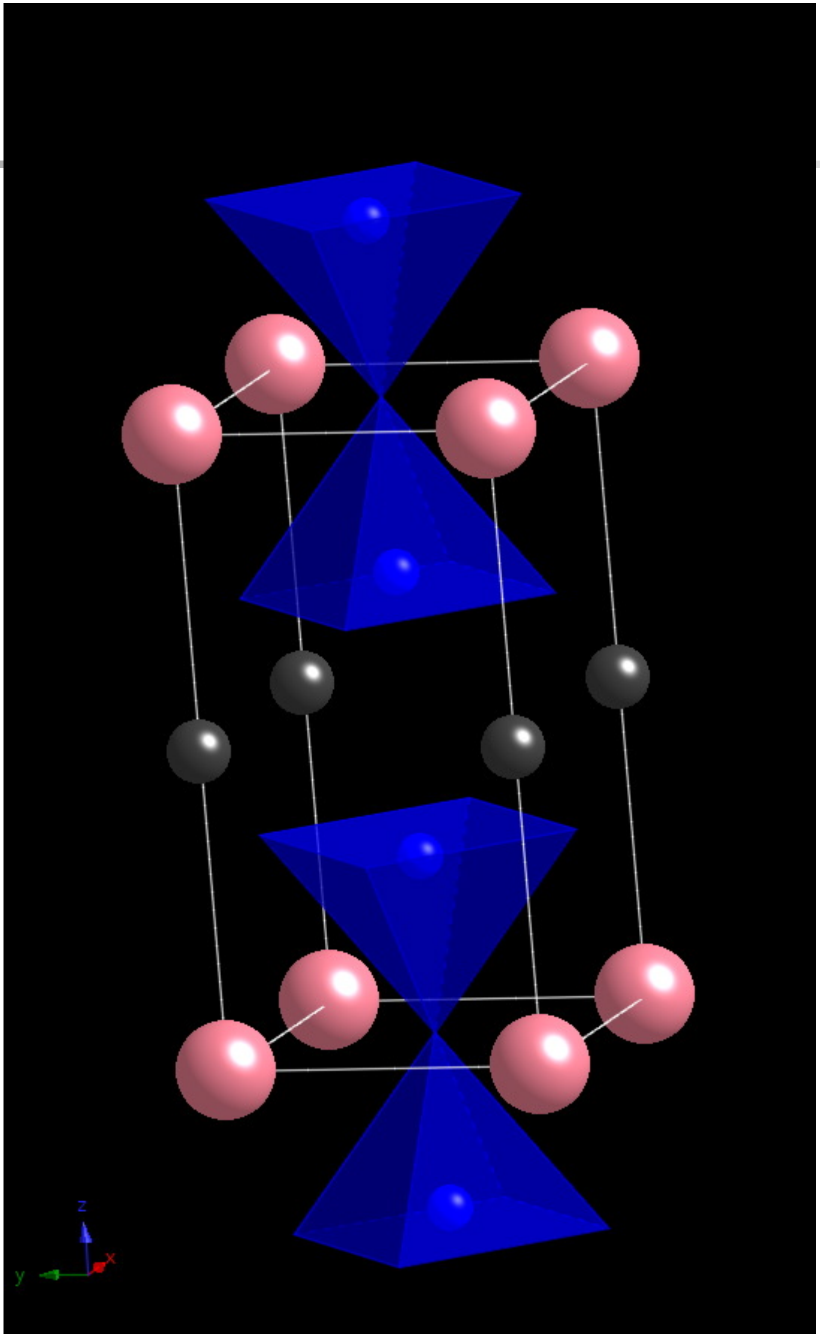
z
y
x

I(T) in LPCM

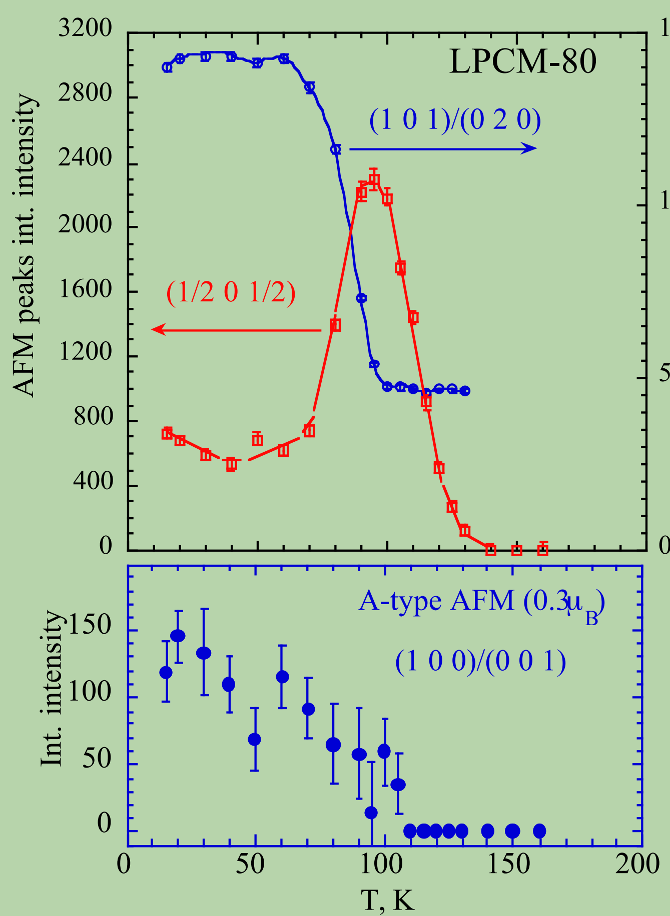
LPCM-80
3200
2800
2400
2000
1600
1200
800
400
0
1.5 10^4
1 10^4
5000
0
AFM peaks int. intensity
FM peaks intensity
(1 0 1)/(0 2 0)
(1/2 0 1/2)
A-type AFM (0.3μB)
(1 0 0)/(0 0 1)
Int. intensity
150
100
50
0
0
50
100
150
200
T, K

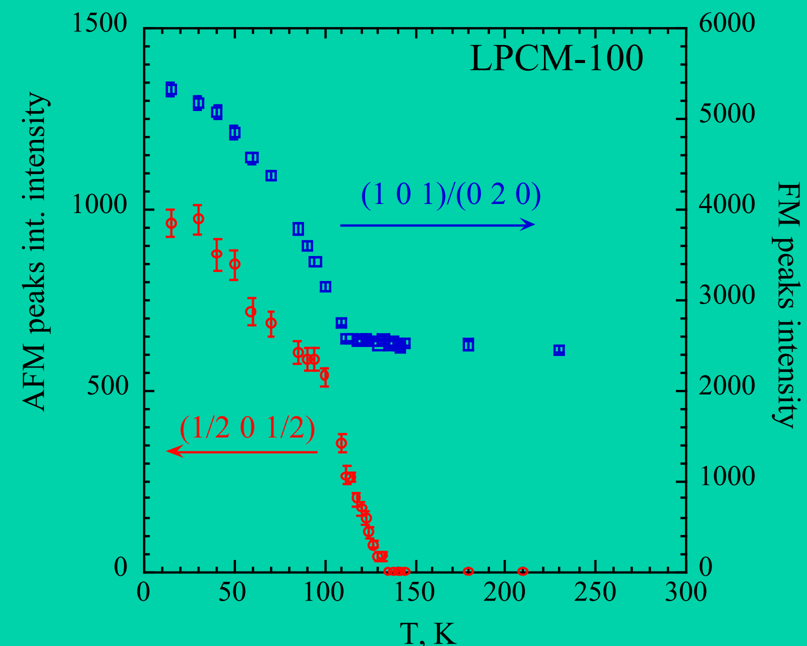
LPCM-100
1500
1000
500
0
6000
5000
4000
3000
2000
1000
0
AFM peaks int. intensity
FM peaks intensity
(1 0 1)/(0 2 0)
(1/2 0 1/2)
0
50
100
150
200
250
300
T, K

Essential physics of manganites

1. Octahedral coordination. Crystal field splitting scheme
2. Spin state is from balance between 10Dq and on atom exchange
3. J/T distortion of $Mn^{3+}O_6$. e_g-level splitting.
4. CO Mn^{3+}/Mn^{4+} state
5. AFM SE Mn-O-Mn:
6. FMM delocalized state for Mn^{3+x}. Double exchange.
7. Strong electron-lattice coupling due to (anti)J/T polarons
8. Competition between FMM and AFMI/CO gives macroscopic phase separation, metastable states.

muSR

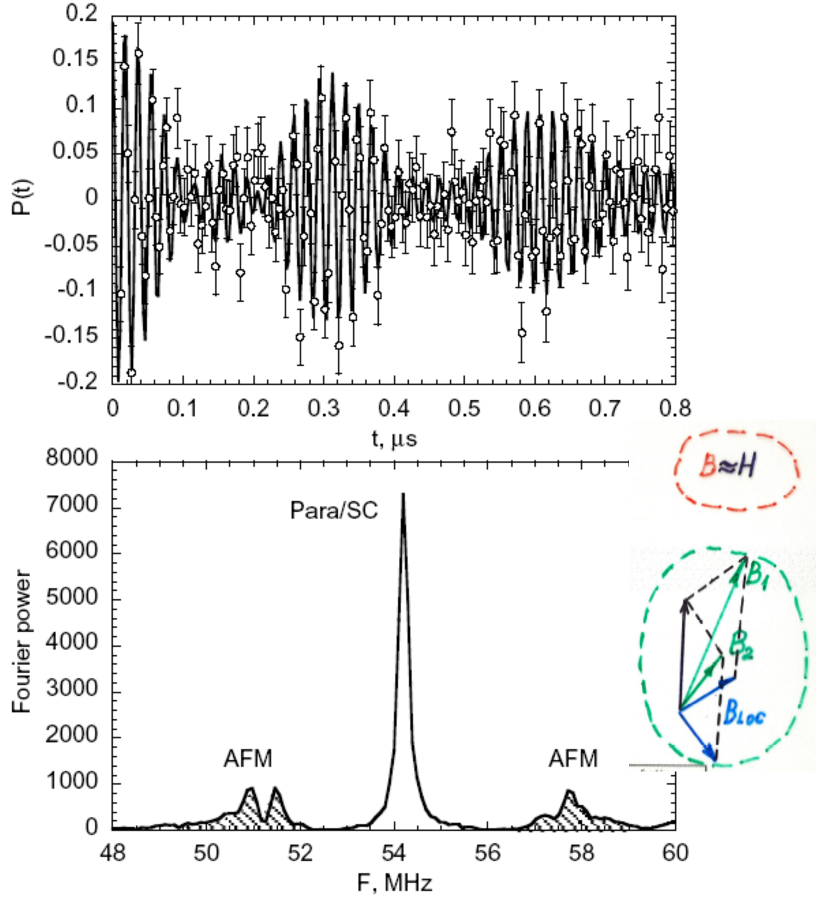

P(t)
t, µs
Fourier power
Para/SC
AFM
AFM
F, MHz
B≈H
B_1
B_2
B_{Loc}

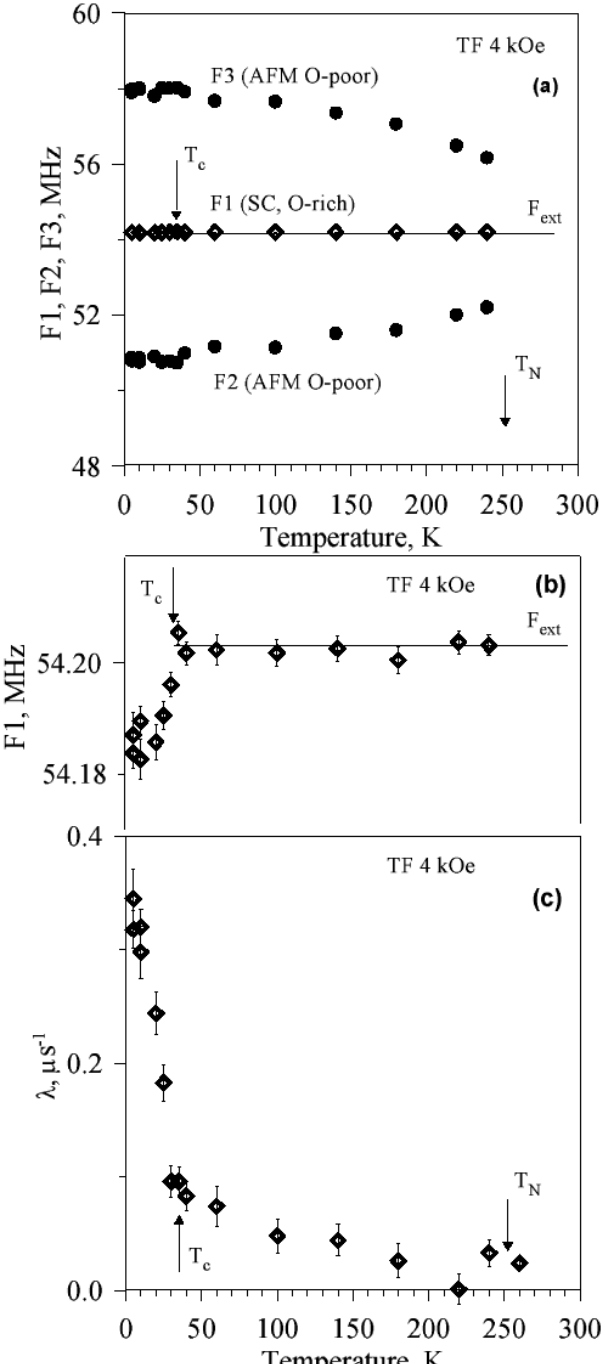

TF 4 kOe
(a)
F3 (AFM O-poor)
T_c
F1 (SC, O-rich)
F_{ext}
F2 (AFM O-poor)
T_N
F1, F2, F3, MHz
Temperature, K
TF 4 kOe
(b)
T_c
F_{ext}
F1, MHz
TF 4 kOe
(c)
λ, μs^{-1}
T_N
T_c
Temperature, K

Absence of AFM in LOM LCO.

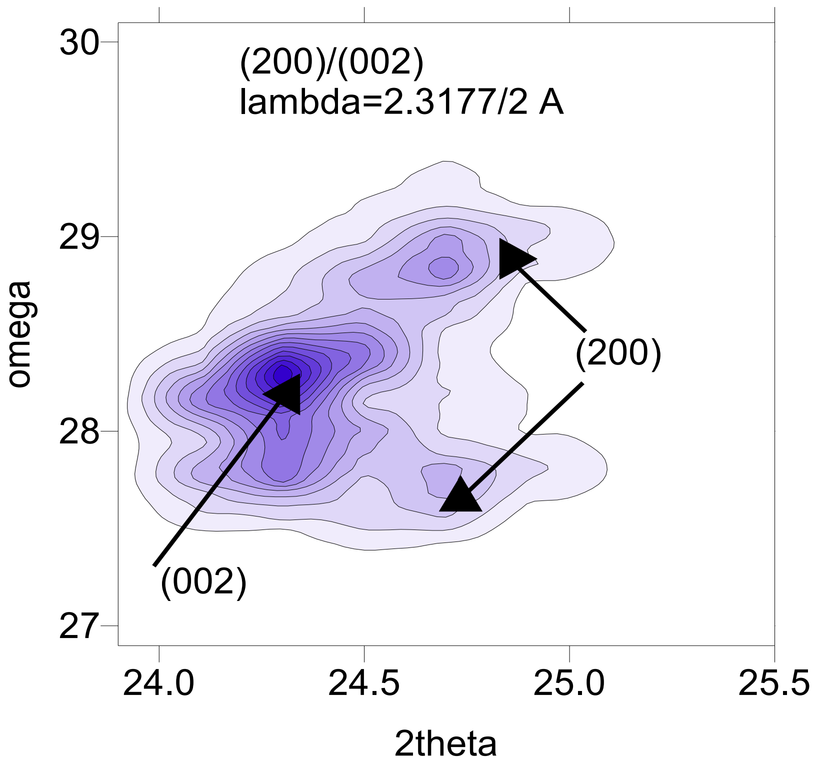

Fig. 1: 2θ-ω scan in (ac) plane around (200) at T=1.5K making use λ/2 contamination. The twin domain structure is in excellent accordance with our previous X-ray and neutron diffraction data [6].

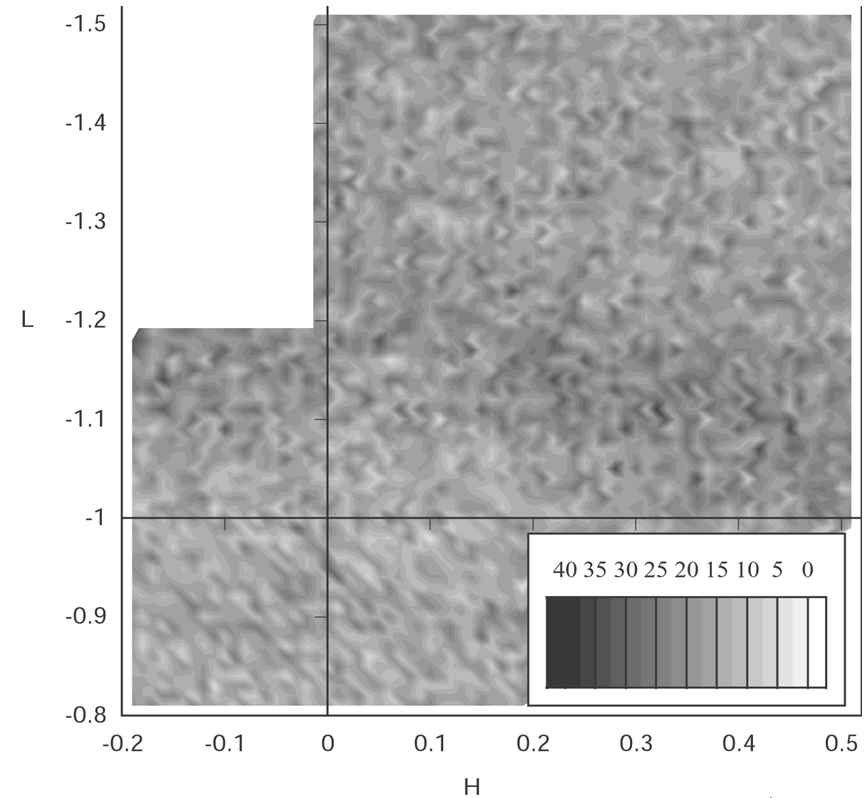

Fig. 3: *Two-dimensional scan of the reciprocal lattice plane (a*c) around (0,0,-1) measured with λ=2.3177Å,* Δh=Δk=0.01. Neutron monitor 100’000/point.